ABSTRACT

LONG, NICOLE JOYCE. Isotopic Applications in North Carolina: Taphonomic Effects on Stable Isotopes, Dual-Isotopic Modeling for Human Identification, and a Multidisciplinary Approach to Forensic Casework (Under the direction of Dr. Ann H. Ross).

Stable isotope analysis has emerged as a valuable complementary tool to forensic investigations involving unidentified skeletal remains. Traditional anthropological techniques can be limited by taphonomic alteration or challenges in estimating population affinity, particularly when skeletal completeness and preservation are compromised. Isotope analysis can provide a chemically grounded approach using the isotopic composition of skeletal tissues to estimate region of origin, recent movement, and dietary history. Used alongside anthropological techniques, the effective application of isotope analysis to North Carolina forensic anthropological casework depends on the integrity of isotopic signatures, the availability of a valid regional model for geographic provenancing, and its integration into a multidisciplinary approach.

The interpretation of these signatures, particularly in individual forensic cases rather than population-level studies, depends on bone preservation and the integrity of isotopic values. Understanding when these signatures may be compromised by early diagenetic processes is essential. This dissertation begins with an investigation into how depositional conditions affect isotope signatures in bone collagen, with implications in the analysis of subadult remains in North Carolina temperate environments. Additionally, effective interpretation of these signatures as they relate to geographic areas requires regional isoscapes for comparison. This dissertation contributes to the development and validation of isotopic models across North Carolina. The models are validated using individuals of known origin from forensic casework, demonstrating improved accuracy for isotopic assignment. Finally, stable isotope analysis is applied to forensic

casework in North Carolina. Stable isotope analysis is now formally integrated into the Standard Operating Procedures at the North Carolina State University Human Identification and Forensic Analysis Laboratory, based in part on the effectiveness of these methods demonstrated here. Given the large number of unresolved unidentified remains in North Carolina, this research applies stable isotope analysis to a multidisciplinary approach to strategically prioritize resource allocation. By integrating taphonomic research, geospatial analysis, and real-world case applications, this dissertation advances the forensic use of stable isotopes as a complementary tool in human identification. It underscores the importance of multidisciplinary approaches and region-specific models in improving the accuracy, effectiveness and impact of forensic investigations.

Isotopic Applications in North Carolina: Taphonomic Effects on Stable Isotopes, Dual-Isotopic Modeling for Human Identification, and a Multidisciplinary Approach to Forensic Casework

by
Nicole Joyce Long

A dissertation submitted to the Graduate Faculty of
North Carolina State University
in partial fulfillment of the
requirements for the degree of
Doctor of Philosophy

Biology

Raleigh, North Carolina
2025

APPROVED BY:

_____	_____
Dr. Ann H. Ross Committee Chair	Dr. Ethan Hyland
_____	_____
Dr. Julie Wesp	Dr. Lisa Paciulli

DEDICATION

This dissertation is dedicated to my family & friends, whose unwavering belief in me has been my constant source of strength.

And to those whose names and stories remain unknown. May the pursuit of knowledge, guided by compassion and curiosity, never cease in its pursuit to bring you recognition and peace.

BIOGRAPHY

Nicole Long earned dual undergraduate degrees in Biological Anthropology and Archaeology, with a minor in Spanish, from Boston University. She competed for the Cross County, Indoor Track & Field, and Outdoor Track and Field varsity teams at BU and served as team captain her senior year. Her first hands-on experience with human skeletal remains came during a summer field school at the Blackfriary Archaeology Field School in Trim, Ireland, the site of a medieval monastery. This experience sparked her interest in bioarchaeology and shaped the direction of her academic and professional career. Ms. Long remained at Boston University to complete a Master of Science in Criminal Justice, working under the mentorship of Dr. Danielle Rousseau. During her undergraduate and graduate studies, she also worked at the Peabody Museum of Archaeology and Ethnography, eventually transitioning to a full-time role in the Osteology Department after graduation. She returned to the Blackfriary Archaeology Field School for nine summer seasons as a Bioarchaeology Site supervisor, where she instructed students in skeletal excavation, recording, and post-excavation processes and handling of human skeletal remains under the direction of Dr. Rachel Scott. For the remainder of the year, Ms. Long worked for several cultural resource management (CRM) firms in the western United States as an assistant crew chief, and as a collections manager at the Fort Collins Museum of Discovery, further expanding her experience in archaeological collections and public engagement.

Ms. Long's training and background in archaeology, skeletal analysis, and criminal justice led her to the North Carolina State University Human Identification and Forensic Analysis Laboratory (NCSU-HIFAL), directed by Dr. Ann H. Ross. She began her doctoral studies in 2019 in the Department of Biological Sciences, with a concentration in forensic sciences. For her first seven semesters, she served as a Teaching Assistant for the Principles of

Human Anatomy & Physiology courses, helping to transition laboratory instruction to a virtual format during the COVID-19 pandemic, and later supporting the return to in-person coursework. Ms. Long moved into a research assistant role in the NCSU-HIFAL and served as the laboratory manager through the end of her studies. In 2023, Ms. Long began working under a Department of Justice grant under Dr. Ross, focused on the identification of missing and unidentified human remains in North Carolina. Her role involved expanding the lab's standard operating procedures for to include selecting skeletal elements for molecular analyses and stable isotope analysis, as well as interpreting the isotopic data. This work aligned closely with her growing research interest in the application of biogeochemical methods in forensic contexts.

Ms. Long has worked in the NCSU-HIFAL for a total of six years of training in forensic casework. Laboratory procedures provided training in traditional biological profile analysis, trauma analysis, taphonomic assessment, radiographic comparison, and isotopic analysis. Nicole is a member of the American Academy of Forensic Sciences (student), where she has presented some of her dissertation work in recent years. She has also presented this research at the GSAB Symposium (2024, 2025), the Graduate School Symposium (2025, 2nd place Life Sciences), the Southeastern Biological Anthropology Interest Group (SEBIG 2025), and the Southeastern Biogeochemistry Symposium (SBS 2025).

ACKNOWLEDGMENTS

I wish to express the deepest gratitude to my family. Mom, you are my role model, for better or for worse, and I admire you in more ways than I can count. Thank you for every piece of unsolicited advice, every phone call, and for always, always, always believing in me. Thank you, Dad and Linda, being constant sources of support through all the highs and lows of this journey. Neil and Morgan, I could not ask for a cooler brother and sister-in-law. Neil - top this! To Rahree and Pop-Pop, thank you for first introducing me to archaeology and for being endlessly supportive grandparents. To the rest of my family: thank you for your encouragement, love, and belief in me from near and far.

I would like to extend my heartfelt thanks to my doctoral advisor, Dr. Ann H. Ross, first, for taking a chance on an archaeologist, and next, for embracing my research interests and providing opportunities to explore them fully. Thank you for sharing your expertise and knowledge – genuine gifts in my training. I am also deeply grateful to my committee members for bridging disciplinary boundaries and meeting me in the middle. Dr. Ethan Hyland, thank you for your patience, kindness, and openness as I navigated the world of geochemistry. I probably owe you rent for how often I've occupied your email inbox, your calendar, your office, and your lab. To Dr. Julie Wesp, thank you for being a steady and sincere source of belief, hope, and encouragement. Your mentorship is a rare and generous gift. To Dr. Lisa Paciulli, I appreciate your thoughtfulness and your seamless support for students. I feel incredibly lucky to have had you all by my side.

To my colleague and friend, Devin Williams, thank you for sharing in a sense of dedication, initiative, and vision. It has been a privilege to grow alongside you. I am also grateful for the support I've received from the NC State Community. Thank you to Freha Legoas, Dr.

John Godwin, Dr. Brian Reich, and many others, for your guidance, encouragement, and contributions to my academic journey. To my fellow graduate students, thank you for inspiring new curiosities and for generously sharing your ideas, research, and camaraderie along the way. I would also like to thank our collaborators across the country who have made this work possible.

I have been fortunate to receive incredible support throughout my academic and professional journey. My deepest thanks go to the staff at Blackfriary Archaeology Field School: Finola O'Carrol, Laura Corrway, Mark McConnan, Dr. Rachel Scott, Erika McMullin, Dr. Melissa Clarke, Dr. Charisse Vesterby, and the many other bioarchaeology supervisors and interns I've worked alongside. I am profoundly grateful for the knowledge and experiences that we share. Thank you to the town of Trim, and to the wonderful friends and families that I have come know for nearly a decade. These relationships transformed my twenties and thirties in unforgettable ways and I carry them with me always. Thank you to my previous supervisors, each an inspiring and impactful woman, for their guidance and example: Dr. Michele Morgan at the Peabody Museum of Archaeology & Ethnology at Harvard University, Dr. Danielle Rousseau at the Metropolitan College at Boston University, and Linda Moore at the Fort Collins Museum of Discovery. I wish to thank those who encouraged and helped to launch this dream six years ago. Tenny, your consistency and curiosity as a friend is irreplaceable.

I would like to thank the Raleigh Distance Project, for supporting my athletic pursuits surrounding me with the unwavering love and encouragement from the incredible RDP women when I moved to Raleigh. I am also deeply grateful to my friends and roommates throughout my time here, who made coming home from school something I always looked forward to: Dr. Xin Dong and Dr. Alison Waldman, with whom I survived the COVID-19 pandemic, and to

Cameron Masiello, thank you for caring for me and Oliver, and making our house a home. Your steady friendship and kindness carried me through some of the most difficult seasons.

I also wish to thank those who have come into my life during this journey and offered steady love, acceptance, and encouragement. I've shared countless miles, both literal and metaphorical, with extraordinary people, and those moments have been invaluable to my well-being and the perseverance this project demanded. These connections have not only sustained me but also reminded me of the deep strength found in community, friendship, and shared purpose.

And to my soul dog, Oliver, thank you for your endless love. You are and always will be my inspiration, my pride, and my joy.

TABLE OF CONTENTS

LIST OF TABLES

Chapter 3

Chapter 4

Chapter 5

LIST OF FIGURES

Chapter 3

Chapter 4

Chapter 5

CHAPTER 1

INTRODUCTION

Forensic anthropologists analyze human skeletal remains to aid in identification by estimating biological characteristics such as sex, age at death, population affinity, and stature, as well as identifying trauma or pathological conditions that serve as individuating characteristics. These analyses provide information on the health, lifestyle, and life history of an individual. An individual's identity is one of the most important pieces of evidence to provide investigators in criminal investigations, disaster victim identification, and missing persons cases. Traditional methods rely on the completeness of the remains and assume that taphonomic alteration will not interfere with the analysis; however, this is not always the case. Furthermore, an individual's identity may not fit into prescribed categories that are typically used in investigative techniques. For example, law enforcement often relies on social race as an identifying characteristic, which oversimplifies genetic histories. Race is a social construct and does not hold biological meaning, and its use in forensic anthropology is scientifically inaccurate and potentially harmful.

The field has moved away from the outdated and oversimplified concepts of social race and the ancestry trifecta, and adopted the term population affinity, a more inclusive and scientifically based approach (*Standard for Population Affinity Estimation in Forensic Anthropology*, 2023). Outdated terms can perpetuate harmful and racist ideologies and should be avoided when discussing human variation and population history (Buikstra et al., 2022). Population affinity estimation reflects shared genetic similarity within populations and acknowledges the influence of microevolutionary processes such as gene flow, drift, selection, and historical events like colonization and forced migration (Ross & Pilloud, 2021). A statistical estimation of genetic similarity to broader groups avoids typological classifications based on race

or ancestry, and evolutionary population structure approach allows for meaningful analyses grounded in human biological variation (Ross & Williams, 2021). The same factors that have shaped genetic histories have also affected geographic histories of populations over time due to migration and movement. Stable isotope analysis offers a way to clarify human biological variation as it relates to geographic origin. When used alongside population affinity estimates, isotopic analyses can provide more details in an individual's life history.

In order to offer additional details when remains are sparse or affected by taphonomic alteration, and to simplify individual migration histories as they pertain to forensic applications, stable isotope analysis can provide information on a region of origin estimation through chemical analysis that is also unrelated to social identity. This helps to guide investigators in developing leads where they may not have previously turned their attention. Ultimately, stable isotope analysis can be used to supplement and validate traditional methods of identification. While still relatively new to the field of forensics, developments have been made as guidelines for the use of stable isotope analysis within the field of forensic anthropology (Chesson, 2014). A practical application of these methods to casework is the next step in the implementation of isotope analysis in the identification of human remains.

This dissertation is structured as three interrelated studies that advance forensic applications of isotope analysis to forensic anthropological casework in North Carolina. The following research questions are addressed in each of the studies:

1. *Taphonomic Effects on Bone Collagen C:N Ratio and $\delta^{13}C$ and $\delta^{15}N$ Values in a Temperate Zone Using a Sus scrofa domesticus Model:* How does decomposition impact isotope integrity in bone collagen in a temperate region?

2. *Enhancing Isotopic Models for the Identification of Human Remains in North Carolina: A Dual-Isotopic Approach:* Do theoretical strontium and oxygen isotopic trends exist within the state of North Carolina, and how well does refining these models improve geographic provenancing methods?
3. *Applying Multidisciplinary Methods to Forensic Casework in North Carolina:* How does isotope analysis integrate with current forensic techniques and contribute to human identification efforts?

CHAPTER 2

LITERATURE REVIEW

Elements, Isotopic Variation, and Human Tissues

Isotopes are fundamental to a wide range of scientific applications, with their natural variation and fractionation providing valuable insights into biological, geological, and environmental processes (Allègre et al., 1995; Boecklen et al., 2011; Dawson et al., 2002; Eagle et al., 2015; Hood-Nowotny & Knols, 2007). Isotopes were first discovered in 1912 by Fredrick Soddy, and techniques developed for analyzing elements and the different kinetic and thermodynamic behaviors began in the 1950's (Klein & Klein, 1997). Isotopic studies concerning diet and migration were explored in the 1970s and applied to paleoenvironmental and archaeological studies (Ambrose, 1986; Katzenberg, 2008; Koch, 1998; Merwe, 1982; Richards & Trinkaus, 2009). Today, isotope analysis is an essential tool in forensic anthropology, aiding in the identification of human remains and tracking movement and residency history (Bartelink et al., 2016; Beard & Johnson, 2000; Benson et al., 2006; Chesson et al., 2018; Ehleringer et al., 2010; Meier-Augenstein, 2017).

Basic Principles of Isotopes

An isotope is a variation of an element that has the same number of protons and electrons, but a different number of neutrons. This results in elements existing as atoms with the same atomic number, but different atomic masses. Although isotopes of an element share the same chemical properties due to their identical electron configurations, their differing atomic masses influence their kinetic behavior and thermodynamic properties (Fry, 2006). These variations play a crucial role in fields such as geochemistry, forensics, and medicine, where isotope analysis helps in tracing origins, dating materials, and studying biochemical processes.

Isotopes exist in two forms, stable, or non-radioactive and unstable, or radioactive. Radioisotopes are unstable isotopes that decay over time, releasing energy in the form of radiation. This predictable decay rate makes them useful as chronological tools in dating organic and inorganic materials. Commonly applied in anthropology and archaeology, radiocarbon dating (^{14}C) is used on material that contains organic carbon and was once part of a living organism (Bowman, 1990). In contrast, stable isotopes do not decay over time, but their natural variations as a result of chemical reactions can provide valuable information about environmental conditions, dietary sources, and physiological processes (Hoefs, 2015).

Stable isotope values are reflected as a ratio of the heavy to its corresponding light isotope, measured relative to a known international standard (Brand et al., 2014; Fry, 2006; Hoefs, 2015). Because these differences in mass can be extremely small, isotope ratios are reported using delta notation (δ) and expressed in parts per thousand (‰):

$$\delta=(R_{sample}-R_{standard})/(R_{standard}) \text{ X } 1000 \text{ (‰)}$$

Where R represents the ratio of the heavy to light isotope, with R_{sample} is the ratio from the sample and $R_{standard}$ is the reference standard. For light isotopes, hydrogen (H), carbon (C), nitrogen (N), and oxygen (O), delta notation is essential because the absolute differences in isotope ratios are too small to be meaningfully expressed as raw values (Bartelink & Chesson, 2019). Heavy isotopes have larger atomic masses, and the difference in mass between isotopes is substantial enough that their values can often be expressed as a simple ratio rather than using delta notation.

The relative abundance of isotopes in a given material is influenced by several processes. One process is radioactive decay, as mentioned previously, where unstable isotopes transform into more stable forms over time altering isotopic ratios. Another process is isotope fractionation,

which is the preferential partitioning of isotopes due to physical, chemical, or biological processes (Hoefs, 2015). Fractionation occurs because isotopes of the same element have different masses, which influence their behavior in phase changes, diffusion, reaction rates, and equilibrium states. The two main types of fractionation are kinetic and equilibrium. Kinetic fractionation occurs in unidirectional or incomplete reactions, where lighter isotopes react or diffuse more quickly than heavier isotopes due to differences in reaction rates. This type of fractionation is prevalent in biological and atmospheric processes such as photosynthesis, evaporation, and microbial metabolism (Sharp, 2017). In contrast, equilibrium fractionation occurs in exchange reactions when isotopes are redistributed between substances at thermodynamic equilibrium (Sharp, 2017). Heavier isotopes form stronger bonds and concentrate in the phase or compound where bonds are more stable. This is commonly observed in processes such as mineral formation and water-carbonate interactions (Hoefs, 2015).

Fractionation effects are particularly significant for light elements, such as hydrogen (H), carbon (C), nitrogen (N), and oxygen (O), because the relative mass differences between their isotopes are large, and their bonds are weaker. This makes them more susceptible to kinetic and thermodynamic effects, leading to measurable variations in their isotopic composition (Sharp, 2017). These reactions, along with metabolic and physiological processes, influence the isotopic composition of tissues as elements move from the environment and through the body. For example, when a light isotope moves between different mediums (for example, from water to body tissue) it undergoes fractionation, meaning the isotopic composition changes rather than being directly retained in its original form (Hoefs, 2015). In contrast, heavy isotopes such as strontium (Sr) and lead (Pb) are much less affected by fractionation due to their greater atomic mass and stronger bonds (Sharp, 2017). Because the relative mass differences between their

isotopes are small, fractionation effects are negligible and their isotope ratios remain relatively unchanged as they move through the food chain and into biological tissues (Beard & Johnson, 2000).

Isotope ratios within a sample are measured using mass spectrometry techniques. For stable isotopes, the most common method is isotope ratio mass spectrometry (IRMS), which measures the relative proportions of isotopes in a sample with high precision (Meier-Augenstein, 2017; Sharp, 2017). The sample preparation process varies depending on the material type and the element being analyzed. Solid samples are typically finely powdered and then chemically treated to remove contaminants or to isolate the specific component of interest, such as collagen or carbonate from skeletal tissue (Ambrose & Norr, 1993; Koch, 1998; Schwarcz & Schoeninger, 1991; Sealy et al., 2014). After sample preparation, the samples are weighed and enclosed in a tin or silver capsule before being introduced into the instrument. Liquid and gas samples may undergo filtration, chemical separation, or direct injection, depending on the analytical requirements (Sharp, 2017).

Within the IRMS system, the sample is combusted or otherwise converted into simple gases (for example, CO_2 for carbon, N_2 for nitrogen) to facilitate isotopic measurement. These gases are then ionized in a vacuum chamber, where they lose electrons and become charged particles. The ionized sample enters the mass spectrometer, where different isotopes are separated based on their mass to charge ratio (m/z). A magnetic field deflects the ion beams, with lighter isotopes being deflected more than heavier ones, causing them to follow distinct paths. These separated ion streams are then detected by Faraday cups, which measure their relative intensities and generates an isotope ratio (Sharp, 2017).

There are two primary IRMS configurations that differ in sample introduction and analytical precision. Dual inlet IRMS introduces purified gases directly into the mass spectrometer from two separate reservoirs: a sample gas and a reference gas. This allows for repeated measurements of the same sample and increased precision. However, because dual inlet IRMS requires precise gas handling and multiple measurements, it is more time intensive and requires longer analysis time for each sample (Muccio & Jackson, 2009). Continuous Flow IRMS (CF-IRMS) analyzes sample generated gases that are carried on a helium stream directly into the machine, streamlining the analytical process. This method enables faster throughput and higher sample efficiency, which is useful with large data sets. The tradeoff, however, is lower precision compared to dual inlet IRMS due to the continuous flow of the sample gas (Muccio & Jackson, 2009). In contrast, gas chromatography IRMS (GC-IRMS) is ideal for analyzing the isotopic composition of individual compounds within complex mixtures because it first separates components in a mixture or sample based on chemical properties (Sharp, 2017). This separation process allows GC-IRMS to provide high precision for identifying the isotopic signatures of specific compounds, making it particularly useful for studies requiring detailed isotope analysis of individual substances.

Other mass spectrometry techniques such as elemental analysis IRMS (EA-IRMS) and thermal ionization mass spectrometry (TIMS) provide additional analytical capabilities (Hoefs, 2015). EA-IRMS relies on an elemental analyzer to combust a sample, converting it into a gaseous product, which is then introduced into the IRMS system for isotope analysis. TIMS directly ionizes a sample by applying heat to a metal filament, causing atoms to evaporate and become ionized. The ionized atoms are separated and measured based on their mass to charge ratio, similar to IRMS (Becker, 2005; Heumann et al., 1995). Unlike IRMS, which relies on

chemical conversion or combustion to generate gases or analysis, TIMS uses thermal energy to ionize samples directly. This method is particularly useful for radiogenic isotope systems such as Sr and Pb, which are less affected by fractionation (Becker, 2005)

Biogeochemistry in Human Tissues

The environment influences isotopic values in human tissues. In forensic casework, commonly sampled tissues include hair, nails, teeth, and bone. Hair and nails reflect an individual's more recent environments, as these tissues continuously grow throughout a person's lifetime (Fauberteau et al., 2021; Lehn et al., 2011; Meier-Augenstein & Kemp, 2012). Both hair and nails grow at a predictable and measurable rate, making them reliable indicators of an individual's recent environmental conditions and diet. Teeth and bone, however, record environmental information from earlier periods in life. Tooth enamel forms during childhood and does not undergo changes once it has formed, making it a permanent record of the environment at that time (Hillson, 2014; J. Lee-Thorp & Sponheimer, 2003; Regan, 2006). Bone, on the other hand, remodels continuously throughout life, meaning it reflects changes in the environment over the past 10-20 years, depending on the skeletal element and individual growth pattern (J. A. Lee-Thorp, 2008; Quinn, 2024b, 2024a). Therefore, tooth and bone isotope analysis provides insights into longer periods of an individual's past, making them the primary focus of the studies present in this dissertation.

Bone serves both mechanical and functional roles within the human body. Mechanically, it provides the framework for muscular attachment and serves as protection for internal organs. Metabolically, bone acts as a reservoir for essential minerals, playing a crucial role in maintaining mineral homeostasis (Ortner & Turner-walker, 2003). To fulfill these roles, living bone constantly changes and adapts to mechanical stresses and chemical influences from the

environment (Hill, 1998). The structure of bone consists of an organic (proteinaceous) matrix, an inorganic (mineral) phase, and water (Hill, 1998; Weiner & Wagner, 1998). The organic component consists primarily of Type I collagen, a triple-helix protein that provides tensile strength and flexibility. The inorganic component known as bioapatite has the chemical formula ($Ca_5(PO_4CO_3)_3(OH)$) and contributes to bone's rigidity. The composite structure of bone provides protection against degradative processes during diagenesis. Although the small size of the bioapatite crystals makes them susceptible to dissolution, their association with the framework of collagen offers structural protection. Similarly, collagen, which would otherwise degrade rapidly, is stabilized by the mineral phase. The close association of these two components creates a mutual dependence for protection from degradative processes (Trueman & Martill, 2002). The third component of bone is water, which fills the porous network of cortical bone and fluctuates in response to pressure gradients (Granke et al., 2015). It contributes to the mechanical properties of bone and the ability to respond to environmental changes.

Bones are formed through intramembranous ossification and endochondral ossification (T. D. White et al., 2011). Skeletal development begins in utero and continues throughout childhood and adolescence, with different bones maturing at varying rates (Scheuer et al., 2010). The maturation of skeletal elements results in epiphyseal fusion, which occurs at different times depending on the bone. This process is generally complete in the 20's, marking full skeletal maturity. However, bones continue to remodel throughout life through the coordinated activity of osteoclasts, which resorb old bone tissue, and osteoblasts, which generate new bone. This remodeling occurs as part of metabolic processes or in response to injury or mechanical stress (T. D. White et al., 2011). As new bone is formed, it incorporates the isotopic composition of an

individual's environment, diet, and drinking water, providing a record of their geographic and dietary history over time (Fahy et al., 2017; Hedges et al., 2007).

Teeth serve masticatory and digestive roles in the human body facilitating the mechanical breakdown of food to aid in digestion (Scott & Irish, 2017; T. D. White et al., 2012). Structurally, a tooth is composed of four primary tissues: enamel, dentin, cementum, and pulp. Tooth enamel is the outermost layer covering the crown, or the masticatory surface of the tooth. It is the hardest and most mineralized tissue in the human body, consisting of a tightly packed, and dense structure of apatite crystals (T. D. White et al., 2012). Despite its high mineral content, enamel contains water (~2%) and a small organic component (~1%), primarily composed of amelogenin, a protein that provides a framework for mineral deposition, much like collagen does in bone. Dentin is beneath the enamel and encapsulates the pulp cavity. It is a calcified tissue with microscopic tubules allowing for communication between the outer enamel and the inner pulp. Dentin is softer than enamel, but still highly mineralized, contributing to the tooth's structure and resilience. Cementum is the bone-like tissue that covers the tooth root. It attaches the tooth to the socket through connections with periodontal ligament fibers. The pulp is the innermost part of the tooth and contains nerves, blood vessels, and connective tissue. Housed within the pulp cavity, the pulp provides nutrients and sensation to the tooth facilitating repair and maintenance of dentin.

The pulp is protected by the exterior hard surfaces in the dentin and most notably enamel, protecting it from diagenetic changes in postmortem environments. Additionally, enamel itself is highly resistant to diagenetic change, making it one of the most stable biological tissues (Kamenov et al., 2018). Because of this resistance, and the fact that dental enamel remains chemically unchanged throughout an individual's lifetime, it is often used in chemical and

molecular studies. Its resistance to remodeling makes it particularly valuable for isotopic analyses, which provide insights into childhood diet and mobility by preserving geochemical signals from early life environments (Kamenov et al., 2018; J. A. Lee-Thorp & van der Merwe, 1991; J. Lee-Thorp & Sponheimer, 2003).

Tooth development in humans occurs in two stages: the deciduous dentition, and the permanent dentition. The first set of teeth begin forming in utero with eruption occurring from infancy through early childhood (AlQahtani et al., 2010). The second set, or permanent teeth, begin forming before birth with crown development continuing through childhood and root formation typically reaching completion around 18-25 years of age (AlQahtani et al., 2010; Hillson, 1996, 2014). Third molars, commonly referred to as wisdom teeth, do not fully develop until late adolescence or early adulthood. The formation and eruption of teeth are strongly correlated to an individual's age, making dental development a key indicator in age estimation studies (AlQahtani et al., 2010; Hillson, 2014; Ubelaker & Khosrowshahi, 2019). Unlike bone, once enamel is fully formed, it does not remodel or regenerate. This means that the mineralogical and elemental composition present at the time of enamel formation is permanently preserved. The specific tooth sampled in isotopic studies can provide valuable insights, since different teeth develop at different stages of life and reflect the environmental, dietary, and geographic histories of the time of formation. This makes tooth enamel particularly useful for isotope analysis (Curtis et al., 2022; Hemer & Evans, 2018; Shepherd et al., 2016).

Isotopes play a crucial role in understanding biological and environmental processes, offering a snapshot of an individual's dietary patterns, migration, and physiological history. The incorporation of isotopes into human tissues is primarily through the consumption of food and water, and from environmental influences. Isotopic values in hair, nails, bone, and teeth reflect

these influences. Hair and nails offer insights into more recent activities, while bone and teeth provide a longer history of activities related to past environments, diets, and geographic histories. The resistance of teeth and bone to diagenetic change makes them especially valuable in forensic analyses, as they can preserve geochemical signatures over extended periods and in cases of dismemberment or environments that are damaging to skeletal material such as bioerosion or scavenging activities. Diagenetic alteration is a concern when selecting samples for isotopic analyses, and these processes will be discussed as they pertain to geochemical and molecular studies.

Diagenesis

The preservation of human remains is influenced by diagenetic processes, which affect different human tissues in varying ways. Diagenesis refers to the chemical, physical, and biological changes that occur in tissues after death driven by environmental factors such as temperature, moisture, microbial activity, and soil composition (Hedges, 2002; Kendall et al., 2018; Nielsen-Marsh & Hedges, 2000). These processes can lead to the breakdown or alteration of tissues over time, and as discussed previously, some human tissues are more resistant to these changes due to their composition. Taphonomy is the study of postmortem processes that affect a body from the time of death until its discovery (Haglund & Sorg, 1997; Pokines et al., 2013). It examines how intrinsic and extrinsic factors influence the rate and nature of decomposition, skeletal preservation, and potential postmortem alterations. Intrinsic factors include an individual's health, age, body mass, and microbiome (Manifold, 2012; Ross & Hale, 2018). Extrinsic factors include environmental conditions such as temperature, humidity, soil composition, scavenger activity, and exposure to water or fire (Hale & Ross, 2023; Wescott,

2018). Human intervention, such as dismemberment or burial practices, can also impact taphonomic processes (Symes et al., 2002).

Water flow around bone is a major contributor to its dissolution (Turner-Walker, 2007). Initial degradation of the organic content of bone is driven by microbial attack, perpetuated by a moist environment. Microbes eventually create tunnels and borings, which have been characterized by Hackett (Hackett, 1981) and Hedges et al. (Hedges et al., 1995). Bone that has been affected by bacterial alteration results in spaces for additional water fluctuation to move within the tunnels and bores. During the movement of water, ions from the environment may be transported within the network and interact with the crystallinity of the bone (Turner-Walker, 2007). Bone apatite has been observed to be susceptible to diagenetic processes because of its similarity with compounds in the burial environment, notably calcium carbonate (Ambrose, 1990). This compound, which is present in surrounding sediments in the environment, can be substituted within the mineral matrix of bone, potentially replacing isotopic values of the original material.

Water plays a crucial role in maintaining the structure and stability of the collagen matrix within the mineral phase of bone. The mechanical function and integrity of bone is dependent on the balance between its three major components, discussed previously - collagen, hydroxyapatite, and water. Changes in water content introduce extraneous ions and contaminants into bone while also facilitating the leaching of mineral components (Smith et al., 2007; Turner-Walker, 2007). Due to its porous nature, bone absorbs and releases water through its canal system that, during life, serves as a passage for blood vessels, nerves, and nutrient transport (Kendall et al., 2018). These postmortem alterations can significantly impact the preservation and chemical integrity of bone.

In an acidic environment, the mineral structure of bone begins to break down and recrystallization from the surrounding soil or groundwater can alter its chemical composition (Lambert et al., 1985). The breakdown of collagen, driven by microbial activity or enzymes from the decomposing organism further accelerates diagenetic changes. Once collagen breaks down the crystalline structure of bone is susceptible to dissolution, accelerating diagenetic changes (Hedges, 2002; Jans, 2008).

Bioerosion is the physical and chemical breakdown of skeletal remains caused by biological organisms such as bacteria or fungi. Histological analysis is used to investigate the bone microstructure and identify the presence and causes of bioerosion. For example, fungal and cyanobacterial alteration in bone can be recognized through the observation of Wedl tunnels in bone histology (Hackett, 1981). Other types of microscopical focal destruction (MFD) are attributed to bacterial invasion (Child, 1995).

Bone preservation is strongly linked to bioerosion (Trueman & Martill, 2002). In a study that compared thin sections of fossil bones using the Oxford Histology Index and Hackett's (1981) tunneling categories, the authors found that bioerosion significantly contributes to bone preservation, where fossil bone showed little or none (Hackett, 1981; Trueman & Martill, 2002). They concluded that bioerosion is a major factor in the degradation of collagen in bone, which, as previously noted, is essential in maintaining bone structure and integrity (Turner-Walker, 2007). According to Turner-Walker (2007), the degradation of collagen during bioerosion can negatively impact the protective role collagen plays in the bone matrix. Jans (2008) further emphasized the importance of bacterial alteration, noting that it is associated with early postmortem history rather than burial environment factors. This suggests that the transport of gut microbes during decomposition plays a significant role in bacterial degradation of bone (Jans,

2008). In contrast, Jans (2008) also highlighted the role of fungi and cyanobacteria in bone bioerosion as a method for reconstructing the past burial environment. For example, cyanobacteria require photosynthesis and therefore would not survive if the remains are rapidly buried in sediment. Therefore, the presence or absence of cyanobacteria activity can provide valuable insights into the timing and conditions of burial. Overall, bioerosion is caused by various factors of the burial environment, which can lead to significant diagenetic processes affecting the remains.

The causes and mechanisms of diagenetic changes are vast and highly variable, and their impact on the isotopic composition of human tissues is not yet fully understood. Research on the preservation of isotopic composition in hair through a variety of taphonomic processes suggests caution when using it for forensic purposes due to its susceptibility to environmental alterations (Gordon et al., 2018; Kootker et al., 2024; Kootker, von Holstein, et al., 2020; Saul et al., 2021). Additionally, the isotopic composition of Sr and Pb can be altered by environmental factors such as soil chemistry and moisture levels (Bentley, 2006; Kamenov et al., 2018; Lambert et al., 1985; Nelson et al., 1986; Tuross et al., 1989). Acid leaching techniques aimed at removing diagenetic strontium are not always effective, as strong acids may dissolve biogenic strontium, while weaker acids may fail to remove all diagenetic contamination (Bentley, 2006). Studies have shown that isotopic values of bone carbonate, particularly with oxygen ($\delta^{18}O$), can be altered due to diagenetic processes affecting the carbonate in bone(Koch et al., 1997; Pellegrini & Snoeck, 2016; Reid et al., 2024; Snoeck & Pellegrini, 2015). The C-O bond in the carbonate ion is vulnerable to changes in the surrounding environment, leading to shifts in isotopic values. However, carbonate from tooth enamel is generally more resistant to these diagenetic changes (Meier-Augenstein, 2017). Additionally, the preservation of $\delta^{18}O$ values measured from the

phosphate group is much better, with little to no alteration observed (J. Lee-Thorp & Sponheimer, 2003; Sharp, 2017). However, as discussed previously, the analytical procedure is more intensive and therefore, it is preferable to measure the carbonate component. Conditions when diagenesis affects isotopic composition need to be investigated further (Meier-Augenstein, 2017).

Bone collagen, when used for carbon and nitrogen isotope analysis, can be susceptible to diagenetic alteration, impacting the accuracy of isotopic measurements. While collagen has been shown to be preserved for thousands of years in archaeological and paleontological settings, its presence does not guarantee that its isotopic composition remains unaltered. Environmental factors such as microbial activity, soil chemistry, and water fluctuations can influence the breakdown or contamination of collagen, potentially skewing isotopic results. Assessing the preservation quality of collagen typically involves evaluating the carbon to nitrogen ratio (C:N), which measures the relative mass of these elements. A well-preserved collagen sample falls within an established acceptable range, between 2.9 and 3.6 for modern human and animal bone (Ambrose, 1990; DeNiro, 1985; Hedges, 2000). Values exceeding this range suggest background alteration from exogenous carbon rich materials, such as humic acids from the soil, whereas values below the range may indicate collagen degradation, selective loss of carbon, or artificial enrichment of nitrogen (E. Guiry, 2019; E. J. Guiry & Szpak, 2020; van Klinken, 1999).

Recent research has suggested that the acceptable C:N ratio for human bone may be more narrowly defined around 3.2 (Schwarcz & Nahal, 2021; van Klinken, 1999). Furthermore, studies on other taxa, such as fish, have proposed alternative preservation thresholds recognizing that collagen stability can vary across species due to differences in physiology and bone composition (Szpak, 2011). In addition to the C:N ratio, it is suggested to analyze the amino acid

profile, as well as the %C and %N values to understand the bigger picture of diagenetic effects on collagen (Meier-Augenstein, 2017). These refinements in collagen preservation criteria are crucial for ensuring the reliability of isotopic data.

Relevant Isotopes

Strontium isotopes

Strontium is an alkaline earth metal with four naturally occurring isotopes, ^{84}Sr, ^{86}Sr, ^{87}Sr, and ^{88}Sr. Of these, ^{87}Sr is radiogenic, produced by the decay of $^{87}Rubidium$ (^{87}Rb), which has a half-life of 48 billion years (Faure & Powell, 1972). The abundance of ^{87}Sr varies across geological materials including igneous, metamorphic, and sedimentary formations (Faure & Hurley, 1963). Strontium is present in the environment across geological, hydrological, and biological systems, where the $^{87/86}Sr$ ratio is characterized by the underlying geology (Bataille & Bowen, 2012; Beard & Johnson, 2000; Faure, 1977). This ratio is influenced by the age and elemental composition of geological materials and varies spatially in relation to bedrock composition (Beard & Johnson, 2000; Bentley, 2006; Faure & Powell, 1972). Over geologic time, the $^{87/86}Sr$ ratio is controlled by the radioactive decay of ^{87}Rb and is reflected in the local environment including the geology, soils, water, and plants.

Due to its high atomic mass, strontium is thought to undergo minimal mass-dependent fractionation through biological, chemical, or physical processes (Capo et al., 1998). As a result, $^{87/86}Sr$ values can be directly compared to primary intake sources of strontium. Given the strong relationship between $^{87/86}Sr$ and bedrock composition, models of strontium variation across a region were primarily based on geological substrates (Beard & Johnson, 2000). More recent models have incorporated additional factors such as weathering processes, water transport, and bioavailable strontium sources to improve accuracy and applicability (Bataille et al., 2018, 2020;

Bataille & Bowen, 2012; Beard & Johnson, 2000; Chesson et al., 2012). $^{87/86}$Sr ratios are expressed as raw ratios between the quantity of ^{87}Sr and ^{86}Sr, as they are meaningful to several decimal places. Because the ratio ^{87}Sr and ^{86}Sr is closely linked to bedrock geology, comparisons can be made between measured $^{87/86}$Sr values in biological tissues and geographic locations where these ratios are present in the environment. This relationship allows for inferences about geographic origin based on strontium isotope analysis.

In the human body, strontium is absorbed primarily through dietary intake and the consumption of water, although environmental factors also play a role. In skeletal tissues, strontium behaves similarly to calcium (Ca) and incorporates into the inorganic fraction due to their elemental similarity (Åberg, 1995; Faure & Powell, 1972). Because strontium undergoes minimal fractionation through biological processes, $^{87/86}$Sr ratios measured in tissues can be directly compared to values from comparative models, such as water (Åberg, 1995; Beard & Johnson, 2000; Capo et al., 1998). The $^{87/86}$Sr ratios in skeletal tissue reflect the sources of strontium intake over different periods of an individual's life. Isotopic values measured from tooth enamel correspond to the time of its formation during childhood, while bone tissue continues to change and remodel throughout life, reflecting more recent sources of strontium intake. Since strontium does not undergo significant fractionation, direct comparisons can be made between strontium values in skeletal tissues and those from isotopic models or isoscapes, allowing for the determination of geographic origins or movement patterns.

Measured isotopic values from skeletal material can be used to determine geographic origins or movement patterns, a method applied in both archaeological and modern forensic contexts (C. Chenery et al., 2010; C. A. Juarez, 2008; Knudson et al., 2004; Kramer & Bartelink, 2022). The development of spatial isotope models, or isoscapes, relies on baseline data on which

to construct these models. Isoscapes based on drinking water have been shown to successfully model the $^{87/86}Sr$ ratios as they correspond to human tissues (Brennan et al., 2015; de Oliveira Mascarenhas et al., 2022; Kramer et al., 2022; Laffoon et al., 2017; Wright, 2005). However, the use of $^{87/86}Sr$ ratios alone should be used with caution, as, for example, within the US values can vary more within a state than between states (Keller et al., 2016). Therefore, a multi-isotope approach can help to further clarify in determining a region of origin (Bartelink & Chesson, 2019).

Oxygen isotopes

Oxygen is a light element that has three naturally-occurring isotopes: ^{16}O, ^{17}O, and ^{18}O (Sharp, 2017). Ratios of ^{18}O to ^{16}O isotopes are expressed using delta notation ($\delta^{18}O$) in parts per thousand (‰). In water, these values are calculated using the following formula, where the standard is either Vienna Standard Mean Ocean Water (VSMOW), Vienna Standard Light Antarctic Precipitation (VSLAP), or Vienna Pee Dee Belemnite (VPDB) depending on the sample and analysis:

$$\delta^{18}O = [((^{18}O/^{16}O)sample / (^{18}O/^{16}O)standard) - 1] * 1000$$

The water cycle plays a crucial role in determining oxygen ratios in the environment (Fry, 2006). These ratios are influenced by processes in the water cycle like precipitation, condensation, temperature, and evaporation, which vary based on geography and topographic features (Craig, 1961; Dansgaard, 1964). For example, precipitation at higher elevations tends to have lower $\delta^{18}O$ values than at lower elevations because, during cooling, heavier ^{18}O isotopes preferentially condense and fall out, leaving the remaining vapor increasingly depleted in ^{18}O and enriched in lighter ^{16}O (Bowen & Wilkinson, 2002; Dansgaard, 1964). This connection to geographic and topographic features allows for the comparison of $\delta^{18}O$ from an organism to that of ingested

water. Precipitation and groundwater are the major sources of ingested water, so the $\delta^{18}O$ values influence the isotopic composition of an organism's tissues. As a result, there is a strong relationship between the oxygen isotopic composition of ingested water, and that of biological tissues, allowing for the identification of geographic regions based on isotopic analysis.

$\delta^{18}O$ values can be measured from skeletal material, reflecting different time periods from tooth or bone samples. Tooth enamel remains unchanged after formation, preserving the isotopic signature from childhood. In contrast, bone continuously remodels throughout life with different skeletal elements reflecting oxygen intake over the past 5–30 years, depending on the turnover rate of the skeletal element. There are two sample preparation and extraction methods for oxygen from skeletal material: from either phosphate (PO_4) or carbonate (CO_3). Phosphate is more resistant to diagenetic alteration than carbonate because of the stronger chemical bonds in the phosphate group and its stability in bioapatite. However, the preparation and analysis methods for phosphate oxygen are labor intensive, and thus, measuring carbonate is preferred (Chesson et al., 2018; Meier-Augenstein, 2017). Regression equations have been developed and are applied to convert between phosphate and carbonate oxygen (C. A. Chenery et al., 2012; Iacumin et al., 2022).

The standards used for oxygen isotope analysis are VSMOW and VPDB, with the former used for phosphates and water, and the latter with carbonates. Coplen et al. (1983) provided a conversion equation to adjust $\delta^{18}O$ values measured in either scale, allowing for direct comparisons between different types of oxygen measurements (Coplen et al., 1983). Conversion equations are also needed because tooth enamel and bone bioapatite do not directly reflect the $\delta^{18}O$ values of consumed water (Hoefs, 2015). This is due to physiological processes, dietary inputs, and isotopic fractionation that occur during metabolism and mineralization (Daux et al.,

2008; Dotsika, 2020; Longinelli, 1984; Ueda & Bell, 2021). These empirically derived conversion equations help estimate an individual's geographic origin, and, in some cases, contribute to the development of human tissue oxygen isoscapes (de Oliveira Mascarenhas et al., 2022; Ehleringer et al., 2010; Laffoon et al., 2017).

Carbon Isotopes

The three most abundant isotopes of carbon are the stable isotopes ^{12}C and ^{13}C, and the radioactive isotope ^{14}C (Hoefs, 2015; Merwe, 1982). While ^{12}C and ^{13}C are stable, ^{14}C is radioactive and decays over time at a known rate, with a half-life of 5,730 years (Johnstone-Belford & Blau, 2020). Once an organism dies, the amount of ^{14}C in an organism begins to decrease through radioactive decay. This decay rate allows for the calculation of time elapsed since death, making ^{14}C dating a powerful tool for determining the age of archaeological samples. In forensic science, ^{14}C dating has been extended to differentiate between archaeological and forensic cases. The atmospheric levels of ^{14}C were significantly increased during nuclear testing in the 1950's and 1960's, which doubled the amount of ^{14}C in the environment. As a result, individuals who lived during or after this period have elevated ^{14}C in their tissues, a factor that can be used to help date remains and distinguish between modern and ancient cases (Fournier & Ross, 2013; Johnstone-Belford & Blau, 2020; Milani et al., 2025; Stenhouse & Baxter, 2020). This unique isotope shift in ^{14}C levels provides an important tool in forensics, where it can help differentiate between modern and older remains, especially in cases where the time of death is uncertain (Bertrand et al., 2024). In archaeological studies, ^{14}C dating allows for the precise determination of ancient human activities, environmental conditions, and dietary patterns, providing a deeper understanding of past human behavior and migration patterns.

Stable carbon ratios are expressed using delta notation ($\delta^{13}C$), with values compared to the international standard VPDB (Hoefs, 2015). These values are particularly useful in dietary reconstruction when measured in bone bioapatite and bone collagen. Plants utilize one of three photosynthetic pathways –C_3, C_4, or CAM– which discriminate differently between ^{13}C and ^{12}C (Chesson et al., 2018; Fry, 2006). The difference in carbon fixation and discrimination between these pathways in ^{13}C and ^{12}C results in distinct $\delta^{13}C$ values in plants. C_3 photosynthesis, the most common, is found in plants like wheat, rice, fruits, vegetables, and most trees, particularly in temperate and cooler regions. C_4 photosynthesis is typically found in hot, sunny grasslands, and used by plants like corn, sugarcane, and certain grasses. The CAM (Crassulacean Acid Metabolism) is the least common photosynthetic for dietary input, but it is used by drought-adapted plants such as cacti and succulents. The differences in photosynthetic pathways contribute to varying $\delta^{13}C$ values, which can be used to differentiate plant types based on their environmental and metabolic conditions. C_4 plants generally have more enriched $\delta^{13}C$ values compared to C_3 plants due to differences in carbon fixation processes during photosynthesis (Cerling et al., 1997; Tipple & Pagani, 2007). The differences in $\delta^{13}C$ values between C_3 and C_4 plants are not only useful for dietary reconstruction but have also been instrumental in paleoclimatic studies. By examining the isotopic signatures in plant and animal remains, researchers can infer past climate conditions and the types of ecosystems that existed in various regions during different periods, aiding in the understanding of historical climate shifts (Koch, 1998; van Klinken et al., 2002). The influence of aquatic environments on $\delta^{13}C$ values is context dependent. Marine sources in the diet can influence $\delta^{13}C$ values, as marine plants obtain their carbon from dissolved bicarbonate in the ocean, resulting in less enriched $\delta^{13}C$ values (Corr et al., 2005; Hobson et al., 2004; O'Brien, 2015). In freshwater systems, the carbon source is more

varied, and therefore organisms in this environment reflect more enriched $\delta^{13}C$ values (Chisholm et al., 1982; E. Guiry, 2019).

$\delta^{13}C$ values measured in human tissues reflect dietary input, including both direct consumption of plants and the consumption of animals that feed on plants, thereby capturing the isotopic signature of the food chain. Carbon isotope values are measured in both bone collagen and bone apatite, as these components provide different insights into diet. $\delta^{13}C$ values measured in bone collagen primarily reflect the dietary consumption of proteins in the diet. In contrast, $\delta^{13}C$ values measured in bone apatite represent a broader range of dietary inputs, including proteins, carbohydrates, and lipids, as these macronutrients are incorporated into the bone mineral matrix during metabolism and mineralization (Ambrose & Norr, 1993; J. A. Lee-Thorp et al., 1989). Carbon isotope values in bone and teeth are subject to fractionation during both metabolic processes and mineralization. Fractionation refers to the preferential incorporation of lighter or heavier isotopes during biological processes. In bone collagen, fractionation typically occurs during the synthesis of proteins, where ^{12}C is preferentially incorporated over ^{13}C. This results in bone collagen generally being depleted in ^{13}C relative to the source diet (Ambrose & Norr, 1993; Krueger & Sullivan, 1984; J. A. Lee-Thorp et al., 1989). Similarly, in bone apatite, fractionation occurs during the process of mineralization, where carbon from dietary sources is incorporated into the mineralized bone matrix, and this fractionation tends to be smaller compared to collagen.

Nitrogen isotopes

The two stable isotopes of nitrogen are ^{14}N and ^{15}N, expressed using delta notation ($\delta^{15}N$) and measured relative to the international standard, atmospheric N_2 (Hoefs, 2015; Sharp, 2017). The primary nitrogen reservoir is in the atmosphere, but biological processes such as nitrogen

fixation, assimilation, and decomposition cycle nitrogen through ecosystems (Sharp, 2017). Most nitrogen isotope fractionation occurs during metabolic processes, leading to an enrichment of ^{15}N in consumer tissues relative to their diet (Sharp, 2017). This is known as the trophic level fractionation shift, which directly relates to the trophic level of an organism. The higher an organism is on the food chain, the higher the $\delta^{15}N$, and vice-versa (Ambrose, 1991; Deniro & Epstein, 1981). Marine ecosystems also display distinct $\delta^{15}N$ patterns due to nitrogen cycling in oceanic food webs, often leading to higher $\delta^{15}N$ values in marine organisms compared to their terrestrial counterparts (Chikaraishi et al., 2014; Schoeninger & DeNiro, 1984).

Beyond trophic level relationships, $\delta^{15}N$ can also reflect physiological stress and health status. During periods of nutritional or metabolic stress, such as prolonged illness or starvation, the body preferentially recycles nitrogen, leading to increased $\delta^{15}N$ values in tissues (B. T. Fuller et al., 2005; Reitsema, 2013; Tea et al., 2021). Additionally, $\delta^{15}N$ values have been widely used in archaeological and anthropological studies on weaning and early childhood diet (B. t. Fuller et al., 2006; Herring et al., 1998; Richards et al., 2002). Breastfeeding infants exhibit elevated $\delta^{15}N$ values compared to their mothers, as they function at a trophic level above them. However, as solid foods are introduced and breastfeeding ceases, $\delta^{15}N$ values gradually decrease, neutralizing the trophic enrichment effect.

Application of Isotope Analysis in Forensic Anthropology

While still relatively new to forensic anthropology, much of the research in the field has been on adapting archaeological isotope methods for forensic applications. Strontium and oxygen isotope analyses have been used to estimate the region of origin and assess recent migration patterns, aiding in the identification of unknown individuals (Bartelink et al., 2014, 2016; Chesson, 2014; Kramer et al., 2020; Kramer & Bartelink, 2022). Carbon and nitrogen

isotopes provide insight into dietary habits, which can be linked to geographic affinity and used to differentiate commingled remains (Ammer et al., 2020; Berg et al., 2022; Singh Sehrawat & Rai, 2023). To ensure the reliability of results from isotope analysis, the interpretation of isotope values must remain consistent across laboratories, research studies, and casework. When properly applied, stable isotope analysis is a valuable tool for forensic investigations. While isotope analysis can provide valuable geographic and dietary information, it cannot confirm identity on its own. Instead, it should be integrated with other forensic evidence to help direct investigations and optimize the use of resources for more definitive and costly methods, such as forensic genetic genealogy (Long et al., 2024). The development of best practices for isotope analysis is guided by organizations such as the Forensic Isotope Ratio Mass Spectrometry (FIRMS) Network, which promotes standardization and methodological advancements in the field (P. Dunn & Carter, 2018).

This dissertation encompasses three projects that apply methods of isotope analysis to taphonomic research, isotopic modeling, and forensic casework, with a specific focus on anthropological casework in North Carolina. This region is particularly relevant due to its diverse environmental and climatic conditions, which influence isotopic variation in human remains. The taphonomic study examines postmortem alterations in bone chemistry. The isotope modeling project aims to refine geographic origin predictions by constructing regional isotope maps. The forensic casework component integrates isotopic data to aid in unidentified human remains investigations. Collectively, these studies contribute to the advancement of forensic anthropology and enhance the applicability of isotopic analysis in forensic and bioarchaeological contexts.

CHAPTER 3

TAPHONOMIC EFFECTS ON BONE COLLAGEN C:N RATIO AND $\delta^{13}C$ AND $\delta^{15}N$ VALUES IN A TEMPERATE ZONE USING A *SUS SCROFA DOMESTICUS* MODEL

Abstract

Understanding bone collagen preservation, often assessed via the C:N ratio, is critical for interpreting isotopic data. The depositional environment influences $\delta^{13}C$ and $\delta^{15}N$ values in bone collagen, and the examination of these conditions offers valuable insights into the factors influencing bone preservation and isotopic reliability. The purpose of this study is twofold: to explore collagen preservation in subadult *Sus scrofa domesticus* bone as a human proxy using the C:N ratio and its variation according to seasonal and depositional environments in a temperate zone; and to examine individual $\delta^{13}C$ and $\delta^{15}N$ variations within these environments. The current research drew samples from a decomposition study by Ross & Hale [2018] using *Sus scrofa domesticus* (fetal *n*=16 and juvenile *n*=13). A one-way analysis of variance (ANOVA) was performed to compare the effect between seasons (summer, spring, winter, fall) and depositions (fetal bag, fetal blanket, fetal control, juvenile buried, juvenile surface) separately on isotopic composition. Results indicated seasonal effects on C:N ratios and $\delta^{13}C$ values, but not $\delta^{15}N$ values (p=<0.05). These effects varied among the fetal and juvenile *Sus scrofa domesticus* samples, with the greatest alterations observed during the hottest and wettest seasons (summer, fall), suggesting early taphonomic changes. Deposition was not a significant factor in isotopic composition, but elevated C:N ratios and altered isotopic signatures in surface-exposed fetal controls suggest environmental factors contribute to contamination or degradation. These results highlight the complexity of taphonomic alteration in subadult remains, indicating that collagen

preservation and isotopic reliability are influenced more by seasonal rather than depositional factors.

Keywords: forensic anthropology, taphonomy, pig model, bone collagen, diagenesis, stable isotopes

Highlights

- The C:N ratio, and $\delta^{13}C$ and $\delta^{15}N$ values in bone collagen are variably affected by seasonality.
- Seasonal conditions affecting $\delta^{13}C$ values imply taphonomic changes occur soon after deposition.
- $\delta^{13}C$ and $\delta^{15}N$ values remain unchanged across various depositional treatments.
- Taphonomic processes affect isotopic signatures in fetal and juvenile bone collagen differently.

Introduction

Diagenetic alteration of skeletal material occurs early in the depositional timeline and thus is important to understand in a forensic context (Bell et al., 1996; Hedges et al., 1995). At the macroscopic level, diagenesis is measured using methods focused on determining the postmortem interval (PMI) through the observation of soft tissue decomposition and macro- and microscopic skeletal evidence (Megyesi et al., 2005; Simmons, 2017; Jaggers & Rogers, 2009; Koch et al., 2000; Ross & Hale, 2018; Hale & Ross, 2023). Underlying microscopic and molecular processes drive these macroscopic changes (Damann & Jans, 2017; Emmons et al., n.d.). Microscopic degradation of bone is measured with the Oxford histological (OHI) and Tunneling indices, which are scored using methods described by Hedges et al., Hackett, and White & Booth (Hackett, 1981; Hedges et al., 1995; L. White & Booth, 2014). At the molecular level, stable isotopic signatures of carbon and nitrogen indicate the preservation quality of the organic material (Ambrose, 1990). Changes can occur in the first months and years, jeopardizing DNA and isotopic analyses and influencing the ability to rely on standard forensic analyses in the identification process (Bell et al., 1996; DeNiro, 1985; Latham & Miller, 2018; Pérez-Martínez et al., 2017; Yoshino et al., 1991).

The microscopic and molecular structure of bone provides the framework and load-bearing design of skeletal tissue, composed of organic and inorganic components and water (Hill, 1998; Turner-Walker, 2007). This composition offers a foundation for structure and function that resists bioerosion. The protein collagen makes up most of the organic component, and less than 10% of the organic component of bone is non-collagenous proteins that have not yet shown a mechanical function (Weiner & Wagner, 1998). Tightly packed collagen fibrils create the flexible support on which the inorganic component, the mineral hydroxyapatite, is arranged

(Weiner & Wagner, 1998). These mineralized structures, with the chemical formula ($Ca_5(PO_4CO_3)_3(OH)$), are extremely small and are therefore susceptible to dissolution. However, when packed between collagen fibrils the mineral structure is protected and provides a dense substructure (Trueman & Martill, 2002). Therefore, the skeletal structure is heavily dependent on this relationship between hydroxyapatite and collagen fibrils. Given this dependence, any disruption to the integrity of these structures can make bone more susceptible to diagenetic alteration, driven by both chemical and microbial processes at the microscopic level (Child, 1995; Hedges, 2002; Jans, 2008, 2021; Turner-Walker, 2007). The effects of these processes on skeletal preservation are dependent on the duration and the conditions of the depositional environment (Hedges, 2002). Extrinsic factors including duration of exposure, characteristics of the depositional environment, and seasonal climate stimulate taphonomic processes resulting in contamination or degradation of the organic content (Hopkins et al., 2000; Nielsen-Marsh et al., 2007; Turner-Walker et al., 2023; van Klinken, 1999).

The C:N ratio, and $\delta^{13}C$ and $\delta^{15}N$ values from collagen are used in anthropology to determine the suitability of collagen for radiocarbon dating, reconstruct past diets, and segregate commingled human remains (Ambrose & Norr, 1993; Berg et al., 2022; Boutton et al., 1991; Brock et al., 2012; Chesson et al., 2024; DeNiro, 1985, 1987; DeNiro & Epstein, 1978; Deniro & Epstein, 1981; Tykot, 2016; Vogel & Merwe, 1977). Within the field of forensic anthropology, carbon and nitrogen isotopes in collagen aid in the identification of human remains (Bartelink & Chesson, 2019; Berg et al., 2022; Chesson et al., 2024; Singh Sehrawat & Rai, 2023; Tarrant et al., 2025). Taphonomic alteration of collagen can affect the interpretation of the isotopic composition in these studies. The C:N ratio is used as a preservation quality indicator of the organic structure of bone, where C:N ratios between 2.9 – 3.6 are accepted as good preservation

in both modern human and animal bones (16,29,30–36). The isotopic composition of collagen measured via the $\delta^{13}C$ and $\delta^{15}N$ values is unreliable when the C:N ratio falls outside of this range (DeNiro, 1985; Schwarcz & Nahal, 2021). Diagenetic alteration and quality indicators of collagen preservation have primarily been studied in adults (Harbeck & Grupe, 2009; Reid et al., 2024). Per contra, weaning studies focus on health and diet between infants and mothers (Herring et al., 1998; Katzenberg et al., 1996; Miller et al., 2020; Richards et al., 2002; Wright & Schwarcz, 1998). Subadult bones are disproportionately altered by taphonomic processes in archaeological contexts, partly due to differences in size and organic-to-mineral skeletal composition (Caruso et al., 2021; Guy et al., 1997; Manifold, 2012). In a forensic context, it is important to identify conditions that may lead to taphonomic alteration to ensure reliable interpretations of isotopic composition in subadult populations.

Previous taphonomic studies on fetal and juvenile remains using *Sus scrofa domesticus* models have examined how seasonal and depositional variables affect decomposition and bone bioerosion, as well as the use of total body score and histological analyses to measure the progression, rate, and timing of this process (Hale & Ross, 2023; Ross & Hale, 2018). The results support the finding that fetal and juvenile remains decompose more quickly than adult remains likely due to their lower body mass and intrinsic bone mineral density. Decomposition rates of fetal and juvenile *Sus scrofa domesticus* remains varied across seasons, correlating with temperature and moisture fluctuations. Additionally, the type of deposition influenced decomposition rates and affected microbial activity in different ways. Early postmortem microbial activity, particularly, plays a crucial role in bone degradation. Microbial activity and bone bioerosion are primary mechanisms of collagen loss, which has been observed

histologically in these *Sus scrofa domesticus* studies (Hale & Ross, 2023; Kendall et al., 2018; Ross & Hale, 2018).

To expand on these findings, the purpose of this study is to explore collagen preservation in fetal and juvenile *Sus scrofa domesticus* via C:N ratios and its variation according to seasonal and depositional environments in a temperate zone. Additionally, the individual $\delta^{13}C$ and $\delta^{15}N$ variations in fetal and juvenile *Sus scrofa domesticus* bone across different seasonal and depositional environments were examined to identify patterns of C:N ratio degradation. Raleigh, North Carolina is in the Piedmont region, which is defined by the Köppen-Geiger climate classification system as a Cfa climate: temperate, without a dry season, and with a hot summer (Peel et al., 2007). By examining collagen preservation and isotopic shifts in fetal and juvenile *Sus scrofa domesticus* remains exposed to these variables, and in samples that show that these factors affect bioerosion, we hypothesize that the effects of season and deposition type will align with those observed in previous studies, while also highlighting the unique taphonomic processes influencing fetal and juvenile *sus scrofa domesticus* bone degradation (Hale & Ross, 2023; Ross & Hale, 2018).

Materials and Methods

Materials

Samples were collected from a larger decomposition study on *Sus scrofa domesticus* remains conducted from 2013—2015, where pigs obtained from the North Carolina University Swine Farm were used as proxies for human remains due to compositional similarities (Hale & Ross, 2023; Ross & Hale, 2018; Stokes et al., 2009). The use of animal proxies as a model for humans in a forensic context allows for greater control over variables such as diet, lifestyle, and health status that can influence isotopic values in bone collagen, and processes of decomposition.

Immediately following euthanization, all pigs were deposited seasonally for the two-year research period. Deposition occurred in the first month of each season defined as summer (May-July), fall (August-October), winter (November-January), and spring (February-April). For each season, 16 juvenile pigs were split evenly between placement on the surface or buried, and 16 fetal pigs were split evenly between placement inside a plastic bag or wrapped in a cotton blanket. Six control fetal pigs were placed on the surface beginning in the winter of 2013. Twenty-nine samples were selected for the current study, as additional samples were lost to carnivore consumption during deposition (Table 1, Table 2).

Table 1 Summary statistics of isotopic analysis for each group by season.

	N	C:N Mean (St. Dev)	$\delta^{13}C$ (‰) Mean (St. Dev)	$\delta^{15}N$ (‰) Mean (St. Dev)
Combined Spring	9	3.76 (0.53)		
Combined Summer	6	4.13 (0.50)		
Combined Fall	7	3.67 (0.32)		
Combined Winter	7	3.56 (0.26)		
Fetal Spring	5		-10.57 (0.88)	1.48 (0.65)
Fetal Summer	3		-10.60 (0.81)	1.40 (1.59)
Fetal Fall	4		-8.99 (0.76)	0.80 (0.76)
Fetal Winter	4		-9.74 (0.89)	1.68 (0.59)
Juvenile Spring	4		-14.04 (0.41)	2.40 (0.94)
Juvenile Summer	3		-16.18 (0.95)	3.40 (0.46)
Juvenile Fall	3		-14.87 (0.52)	2.80 (0.56)
Juvenile Winter	3		-14.52 (0.64)	3.27 (0.15)

Table 2 Summary statistics of isotopic analysis for each group by deposition treatment.

	N	C:N Mean (St. Dev)	$\delta^{13}C$ (‰) Mean (St. Dev)	$\delta^{15}N$ (‰) Mean (St. Dev)
Fetal Bag	4	3.60 (0.16)	-10.34 (0.65)	1.78 (0.59)
Fetal Blanket	8	3.64 (0.56)	-9.87 (0.84)	1.35 (0.77)

Table 2 (continued).

Fetal Control	4	4.00 (0.22)	-9.80 (1.69)	0.90 (1.22)
Juvenile Buried	7	3.67 (0.41)	-14.92 (1.16)	3.00 (0.42)
Juvenile Surface	6	4.00 (0.55)	-14.74 (0.86)	2.83 (0.98)

The left ulna was chosen for analysis based on its availability from each sample and its distance from the gut to limit effects from microbiome activity during decomposition (Jans et al., 2004). The diet and lifestyle within each the fetal and juvenile groups are presumed to be nearly identical, as all samples from each group were obtained from a singular locale.

Sample Preparation and Analysis

Sample preparation was performed at the North Carolina State University's Paleo^3 Preparation Laboratory. Bone samples were surface cleaned with deionized water and brushed to remove exterior contaminants. Whole bone samples were air-dried at room temperature in a fume hood. A Dremel tool was used to collect powdered bone in an antistatic polystyrene weigh boat. Samples were subjected to a dilute solution of 1 M hydrochloric acid (HCl) at room temperature to remove all carbonate material (~24 hours) and rinsed with deionized water until cleaned, following the standard procedure of Sealy et al. 2014 (Sealy et al., 2014). Collagen bone samples were centrifuged and dried at 50°C before being loaded into tin capsules for isotopic analysis using a Costech elemental analyzer attached to a Thermo Delta V+ isotope ratio mass spectrometer at North Carolina State University's Paleo^3 Isotope Laboratory. Carbon isotope measurements are reported in units per mil (‰) relative to the Vienna Pee Dee Belemnite and used IAEA sucrose (-10.45‰) and caffeine (-27.77‰) standards for calibration. Analytical uncertainty is maintained at < 0.1‰, and replicate analyses had a mean standard deviation of 0.25‰.

Statistical Analysis

Data quality was assessed by examining the C:N ratio and comparing the relative isotopic compositions of samples with C:N ratios within the well-preserved range for modern animal and human bone (2.9—3.6) to those outside of the range (3.6 <) using the F-test to compare variances between the two groups. A two-sample t-test was applied to compare means of isotopic composition (C:N ratio, $\delta^{13}C$, and $\delta^{15}N$ values) between fetal and juvenile samples as dietary differences are expected between these groups. Juveniles undergo nursing, which influences their isotopic composition (Fogel et al., 1989; B. t. Fuller et al., 2006). If no statistically significant difference was found between the two groups ($p > 0.05$), the fetal and juvenile samples were combined to increase statistical power, and a one-way analysis of variance (ANOVA) was used to compare the effects of season and deposition treatments on isotopic composition. ANOVA was chosen because it allows for the comparison of means across multiple groups, which is more appropriate than multiple t-tests when assessing variation due to season and deposition treatments. If a significant difference was found between fetal and juvenile samples ($p < 0.05$), ANOVA was performed separately to evaluate the effects of season and deposition treatments within each group. For ANOVAs with some evidence of a difference in means between groups, pairwise comparisons were conducted using two-sample t-tests. Reported p-values are nominal; no adjustment for multiplicity was made. All analyses were conducted in JMP 17.0 (*JMP®, Version 17.0. SAS Institute Inc., Cary, NC, 1989–2021.*, n.d.).

Results

Data Quality

The F-test results indicate a significant difference in variances between well-preserved and altered C:N ratios in fetal $\delta^{13}C$ ($F(4, 9) = 5.22$, *p=0.037*), juvenile $\delta^{13}C$ ($F(4,7) = 6.93$, *p=0.028*), and fetal $\delta^{15}N$ ($F(4, 9) = 10.51$, *p=0.004*) (Figure 1, Table 3).

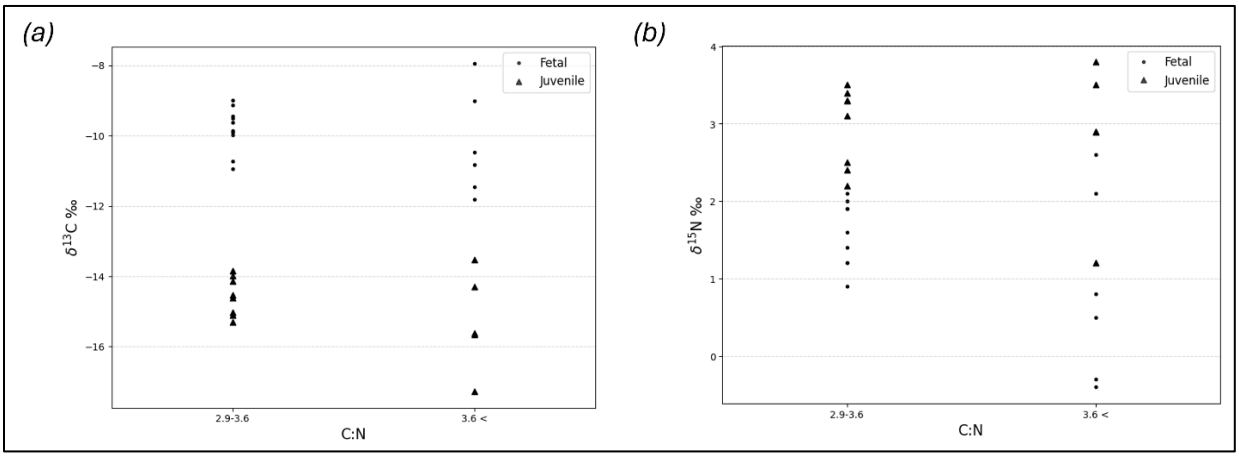

Figure 1 Variation of $\delta^{13}C$ (a), and $\delta^{15}N$ (b) between samples with good and altered C:N values. Note the spread of individual isotopic signatures for samples with C:N values above 3.6.

Table 3 Results of F-Test analysis of isotopic analysis for each group.

Group	df	Analysis	F Ratio	p-Value
Fetal	4, 9	$\delta^{13}C$	5.22	**0.037**
		$\delta^{15}N$	10.51	**0.004**
Juvenile	4, 7	$\delta^{13}C$	6.93	**0.028**
		$\delta^{15}N$	3.86	0.116

We also recognized values in the isotopic results, particularly in samples F1 and J15, which reflect a high C:N ratio (Supplementary File 1). Both samples (F1 and J15) also exhibited highly variable $\delta^{13}C$ and $\delta^{15}N$ values when compared to their respective groups (Figure 2). Removing these two values did not affect the results of the analysis below and this output is available upon request. Because we are specifically interested in outliers and the conditions in which these results are evident, all samples were included in subsequent analyses.

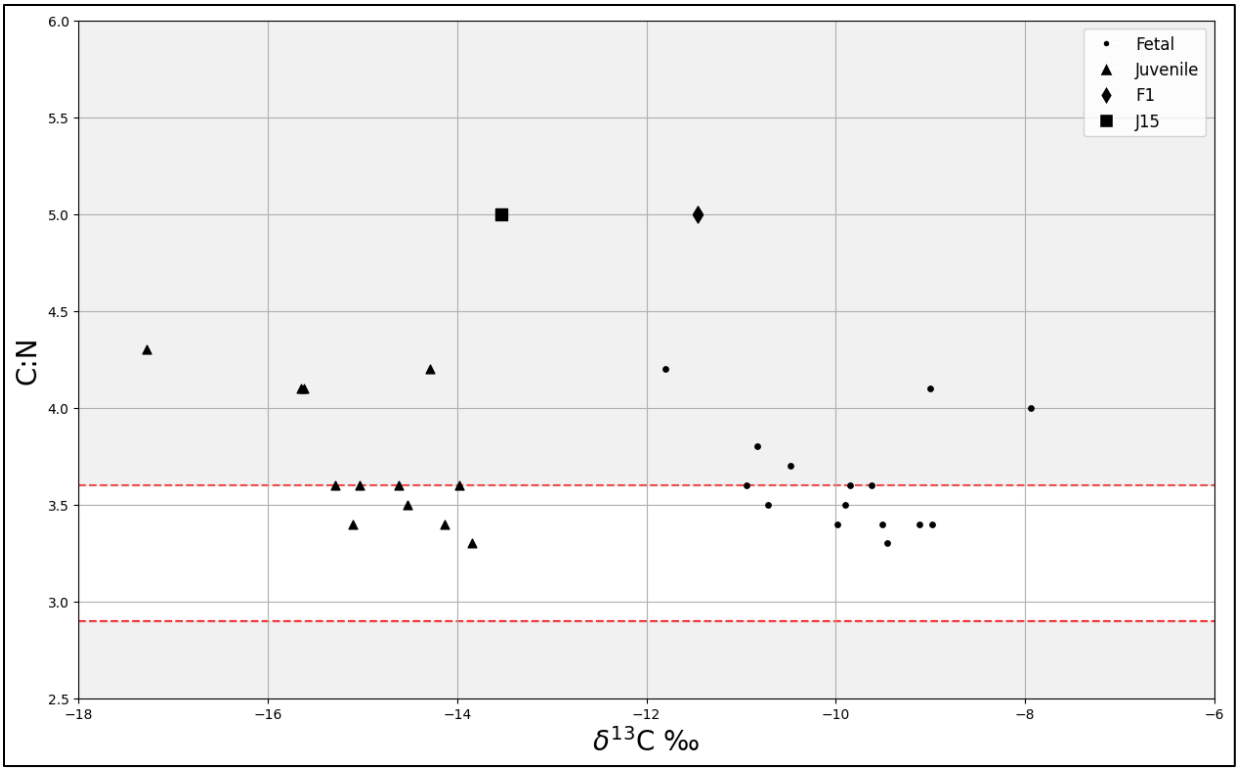

Figure 2 Crossplot of $\delta^{13}C$ and C:N values. Dashed line marks limits of good C:N values (2.9—3.6). Notably, samples F1 and J15 show altered values compared to their respective groups.

C:N Ratio Statistical Analyses

There was not a significant difference in the C:N ratio between fetal samples ($\bar{x}$ =3.72, SD=0.43) and juvenile samples ($\bar{x}$ =3.82, SD=0.49); t(degrees of freedom = 28)=0.610, *p=0.547* (Table 4). The ANOVA of C:N by season revealed there is not a significant difference between seasons (F(3, 25) = [2.15] *p = 0.119*) (Table 5). However, there is some evidence of a difference between summer ($\bar{x}$ =4.13, SD=0.50) and winter ($\bar{x}$ =3.56, SD=0.26); t(25) = -2.423, *p=0.023* (Table 1, Table 6). The ANOVA of C:N by deposition revealed there is not a significant difference between deposition treatments (F(4, 24) = [1.045], *p = 0.405*).

Table 4 Results of t-test analysis between fetal and juvenile groups for each isotopic analysis.

Comparison	n (Fetal, Juvenile)	Mean Difference	SE Difference	95% CI (Lower, Upper)	p-Value
C:N	16, 13	0.10	0.17	(-0.25, 0.46)	0.5471
$\delta^{13}C$	16, 13	-4.86	0.38	(-5.63, -4.09)	**<0.0001**
$\delta^{15}N$	16, 13	1.58	0.30	(0.97, 2.19)	**<0.0001**

Table 5 ANOVA results of isotopic analysis for each deposition and season, by group.

	df	SS	MS	F ratio	p-value
C:N Deposition	4, 24	0.852	0.213	1.05	0.405
C:N Season	3, 25	1.179	0.393	2.15	**0.119**
Fetal $\delta^{13}C$ Deposition	2, 13	0.741	0.37	0.33	0.727
Fetal $\delta^{13}C$ Season	3, 12	6.953	2.318	3.26	**0.059**
Fetal $\delta^{15}N$ Deposition	2, 13	1.532	0.766	1.03	0.387
Fetal $\delta^{15}N$ Season	2, 13	1.724	0.575	0.72	0.557
Juvenile $\delta^{13}C$ Deposition	1, 11	0.111	0.111	0.10	0.753
Juvenile $\delta^{13}C$ Season	3, 9	8.251	2.75	6.77	**0.011**
Juvenile $\delta^{15}N$ Deposition	1, 11	0.090	0.09	0.17	0.689
Juvenile $\delta^{15}N$ Season	1, 9	2.176	0.725	1.74	0.228

Table 6 Student t-test pairwise comparison for ANOVA results where *p<0.05*.

C:N Season (combined)				
Comparison	Mean Difference	SE Difference	95% CI (Lower, Upper)	p-Value
Summer - Winter	0.58	0.24	(0.09, 1.07)	**0.023**
Summer - Fall	0.46	0.24	(-0.03, 0.95)	0.063
Summer - Spring	0.38	0.23	(-0.09, 0.84)	0.106
Spring - Winter	0.2	0.22	(-0.25, 0.64)	0.366
Fall - Winter	0.11	0.23	(-0.36, 0.59)	0.621
Spring - Fall	0.08	0.22	(-0.36, 0.53)	0.699
Fetal δ13C Season				
Fall - Summer	1.6	0.64	(0.20, 3.00)	**0.029**
Fall - Spring	1.57	0.57	(0.34, 2.80)	**0.017**
Winter - Summer	0.85	0.64	(-0.55, 2.26)	0.210
Winter - Spring	0.82	0.57	(-0.41, 2.06)	0.171

Table 6 (continued).

Fall - Winter	0.75	0.6	(-0.55, 2.05)	0.234
Spring - Summer	0.03	0.62	(-1.31, 1.37)	0.964
Juvenile δ13C Season				
Spring - Summer	2.1	0.49	(1.0, 3.2)	**0.002**
Winter - Summer	1.7	0.52	(0.49, 2.8)	**0.011**
Fall - Summer	1.3	0.52	(0.14, 2.5)	**0.033**
Spring - Fall	0.83	0.49	(-0.28, 1.93)	0.124
Spring - Winter	0.48	0.49	(-0.63, 1.58)	0.353
Winter - Fall	0.35	0.52	(-0.83, 1.53)	0.518

$\delta^{13}C$ and $\delta^{15}N$ Values Statistical Analyses

There was a significant difference in the $\delta^{13}C$ values between fetal samples ($\bar{x}$ =-9.97, SD=1.01) and juvenile samples ($\bar{x}$ =-14.84, SD=0.99); t(28)=-12.93, *p=<0.0001* (Table 4). There was also a significant difference in the $\delta^{15}N$ values between fetal samples ($\bar{x}$ =1.34, SD=0.87) and juvenile samples ($\bar{x}$ =-2.92, SD=0.70); t(28)=5.30, *p=<0.0001*. An ANOVA was conducted on $\delta^{13}C$ and $\delta^{15}N$ values for the fetal and juvenile samples separately between season and deposition treatments.

The ANOVA of $\delta^{13}C$ of juvenile samples by season revealed there is a significant difference between seasons (F(3, 9) = [6.77], *p=0.011*) (Table 5, Figure 3A). Seasonality did not have an effect on $\delta^{13}C$ of fetal samples (F(3, 12) = [3.26], *p = 0.059*). A significant difference was observed between fall ($\bar{x}$ =-8.99, SD = 0.76) and summer ($\bar{x}$ =-10.60, SD = 0.81); t(12) = -2.484, *p = 0.029*, and fall and spring ($\bar{x}$ =-10.57, SD = 0.88); t(12) = -2.778, *p = 0.017* (Table 6, Figure 3B). Season did not have an effect on $\delta^{15}N$ of fetal samples (F(2, 13) = [0.72], *p = 0.557*) or juvenile samples (F(1, 9) = [2.18], *p = 0.228*). Deposition did not have an effect on $\delta^{13}C$ of fetal samples (F(2, 13) = [0.33], *p = 0.727*), $\delta^{13}C$ of juvenile samples (F(1, 11) = [0.10], *p = 0.753*),

$\delta^{15}N$ of fetal samples (F(2, 13) = [1.03], *p = 0.387*), or the $\delta^{15}N$ of juvenile samples (F(1, 11) = [0.17], *p = 0.689*).

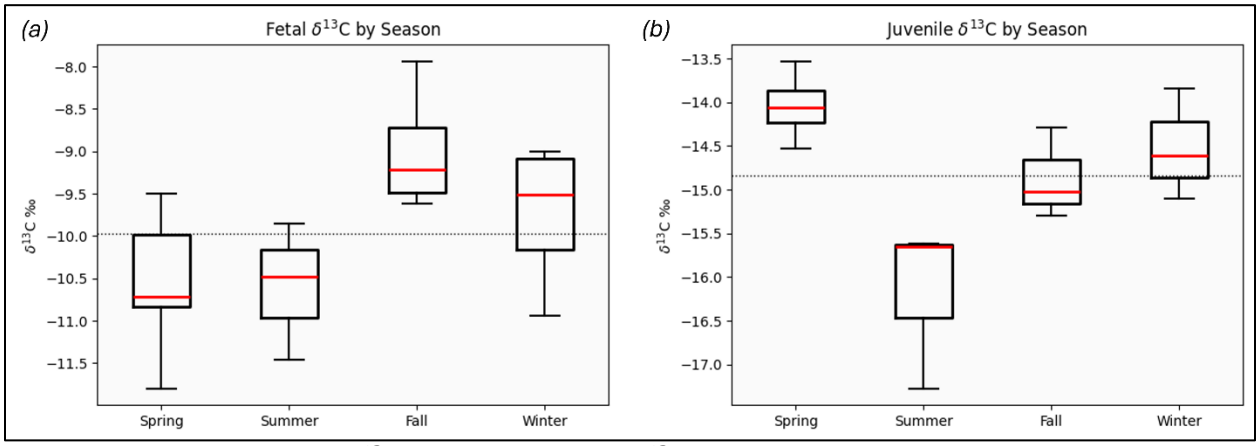

Figure 3 Boxplot of Fetal $\delta^{13}C$ (a), and Juvenile $\delta^{13}C$ (b) by season. Fetal remains were less enriched in the fall, while juvenile samples were more enriched in the summer, the wettest and hottest seasons in the study area.

Discussion

The results presented here indicate that season and deposition are not significant factors in collagen preservation variation in a temperate climate, as measured by the C:N ratio. Although there is some evidence of seasonal differences between summer and winter, this variation does not coincide with the changes observed in isotopic composition during the same seasons; that is, the C:N ratio and individual $\delta^{13}C$ and $\delta^{15}N$ values do not vary concurrently. This is surprising, as the C:N ratio is used as a quality control measure to assess the preservation of the organic structure of bone and to filter out diagenetically altered samples in isotopic studies. Seasonality is a significant factor affecting $\delta^{13}C$ values in both fetal and juvenile samples, particularly in the hottest and wettest seasons (fall and summer). However, seasonality did not have a significant effect on $\delta^{15}N$ values, suggesting that the isotopic values do not covary. The depositional environment was not a significant factor influencing the C:N ratio nor the isotopic composition, indicating that isotopic signatures in bone collagen are not preferentially affected by burial

treatment under the conditions presented here. Seasonality should be examined more closely as a potential driving factor in bone diagenesis and its potential effect on stable isotope analysis.

C:N Ratio

Samples with C:N ratios outside of the biological range (>3.6) exhibited more variation in $\delta^{13}C$ and $\delta^{15}N$ values than samples with well-preserved C:N ratios (2.9—3.6) (Figure 1). Elevated C:N ratios often result from contamination or degradation, which also explains the deviation of the $\delta^{13}C$ and $\delta^{15}N$ ratios (Ambrose, 1990; DeNiro, 1985; Schwarcz & Nahal, 2021; van Klinken, 1999). These samples were included in the analysis to explore trends in bone preservation. The results further validate the use of the C:N ratio as an indicator of poor preservation or contamination, as erratic $\delta^{13}C$ and $\delta^{15}N$ values can lead to inaccurate conclusions and are typically excluded in interpretive analyses (Ambrose & Norr, 1993; DeNiro, 1985). While neither season nor deposition were significant factors in the C:N ratio variation in this sample, the trends observed in values outside of the biological range suggest environmental conditions that affect bone preservation, warranting the exclusion of individual isotopic values.

All C:N ratios outside the acceptable range were above the threshold, suggesting that collagen degradation or contamination occurred in some samples (27) (Figure 2). Contamination with humic substances can elevate the C:N ratio by increasing carbon content, a process that can occur rapidly (van Klinken & Hedges, 1995). The sample preparation methods in this study included sub-sampling via drilling, which should theoretically minimize humic contamination. An additional NaOH treatment, proposed for further minimizing humic contamination, has also been shown to be effective (Deniro & Epstein, 1981; Szpak et al., 2017). Thus, some of the elevated C:N ratios in the data may be attributable to sample preparation methods. Collagen degradation, particularly the breakdown of individual amino acids, lowers the nitrogen content in

bone, which also increases the C:N ratio (van Klinken, 1999). Both contamination and degradation may contribute to the heightened C:N ratios observed in the present samples. Conversely, a selective loss of amino acids in collagen due to bacterial or fungal activity typically decreases the C:N ratio, as more resistant amino acids tend to have lower C:N ratios (Schwarcz & Nahal, 2021). This process is concerning because the differential loss of amino acids can also affect the isotopic composition, particularly $\delta^{13}C$ values (Schwarcz & Nahal, 2021). Using a combination of additional quality indicators, such as collagen yield, carbon yield, and nitrogen yield, can provide better insights into whether elevated C:N ratios result from contamination or degradation. Comparisons of low yields have been used to differentiate between these mechanisms and offer a clearer explanation for variations in C:N ratios (Ambrose, 1990; Sealy et al., 2014; van Klinken, 1999).

Trends were observed in some samples that fall outside the biological range of C:N ratios, indicating degradation or contamination of collagen. While deposition was not a significant factor in isotopic variation measured in this study, all the fetal surface control samples exhibited C:N ratios above the biological range. This suggests that the conditions of the fetal surface control deposition contribute to the observed diagenetic changes in the bone. Hale & Ross (2023) did not include surface fetal remains, but histotaphonomic analysis showed that juvenile buried remains experienced the greatest degree of diagenesis, with surface juvenile remains intermediate to the bagged and blanketed fetal remains (Hale & Ross, 2023). Of the fetal remains, the surface control treatment was the only one exposed to the soil and surrounding environment. If this exposure allowed contamination from surrounding humic acids, we would expect other depositions exposed to similar environmental conditions and humic contaminants to follow the same pattern. However, the elevated C:N ratios observed in the surface control fetal

remains may not be solely due to humic contamination, but rather related to deposition, such as direct exposure to surface weathering, insects, or surface microorganisms (Koch et al., 2000; Turner-Walker et al., 2023). Additionally, differences between fetal and juvenile remains may contribute to this variation, as fetal remains have lower body mass and a higher collagen-to-mineral ratio, potentially accelerating decomposition (Ross & Hale, 2018). Therefore, conditions of deposition and inherent differences between types of samples may explain the elevated C:N ratios observed in fetal surface control samples.

Isotopic Composition: $\delta^{13}C$

$\delta^{13}C$ values vary in both fetal and juvenile samples when deposited during the hottest and wettest seasons, suggesting that taphonomic alteration occurs within the first few months after deposition. Seasonal conditions contribute to bone bioerosion, leading to alterations in the isotopic composition of bone collagen. This aligns with the observed rates of macroscopic decomposition and microbial degradation, observed in these samples, where the fastest decomposition occurred during the summer and fall (Hale & Ross, 2023; Ross & Hale, 2018). The present results do not indicate that deposition treatment influenced stable isotope values, unlike the effects seen in microscopic decomposition and microstructural degradation. While there is a variation of 2-3‰ within deposition treatments, this difference is not significant and does not suggest that deposition treatment affected individual $\delta^{13}C$ values. Humic contamination, which may explain variations in the C:N ratio, can also influence $\delta^{13}C$ by increasing carbon content and altering the isotopic signature accordingly. Therefore, seasonal conditions, such as humidity, temperature, and soil moisture are the primary drivers of taphonomic alteration of bone collagen isotopic values.

Less enriched $\delta^{13}C$ values were observed in fetal remains during the fall, while juvenile remains were more enriched in summer (Figure 3). This opposing enrichment difference between the two groups may be explained by body mass and intrinsic variation in bone composition. The observed shift in values is consistent with alterations in the amino acid profile driven by bioerosion (Balzer et al., 1997). As certain amino acids degrade selectively, they reflect varying $\delta^{13}C$ values, and the remaining bone protein will represent the isotopic profile of the surviving amino acids. Additionally, differences in bone crystallinity and composition between fetal and juvenile bone could account for the opposing isotopic enrichment observed between these two groups (Manifold, 2012) (Figure 4).

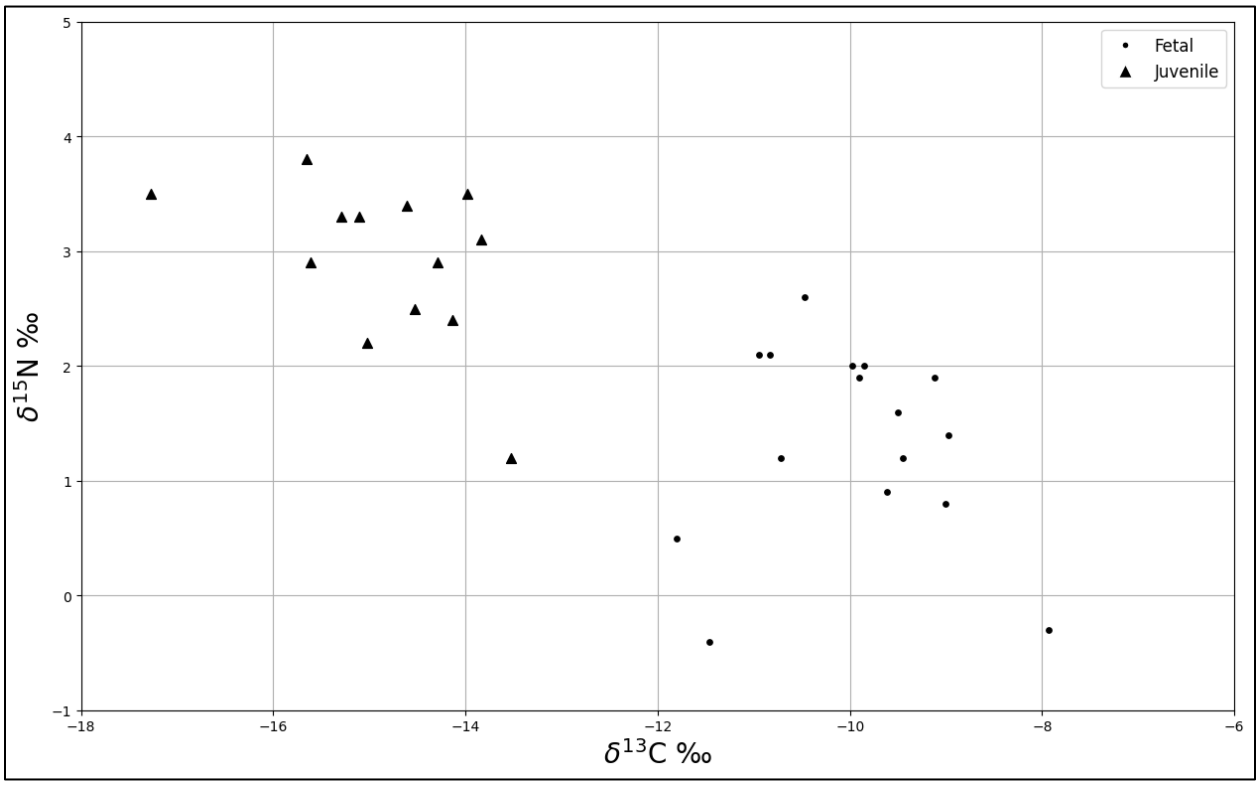

Figure 4 Crossplot of fetal and juvenile $\delta^{13}C$ and $\delta^{15}N$ values. Distinctive isotopic signatures are observed between the fetal and juvenile samples, likely a result of intrinsic variation in bone composition and body mass between the two groups.

Isotopic Composition: $\delta^{15}N$

The $\delta^{15}N$ value was not significantly affected by season or deposition in either group, but the data do show patterns of variation between groups. $\delta^{15}N$ values in bone collagen are commonly used to assess diet and the trophic level of an organism (Deniro & Epstein, 1981). We assume the same diet and lifestyle among the fetal and juvenile porcine groups as they were procured from the same facility. Juvenile individuals would have had the opportunity to breastfeed, while fetal individuals would not have. The elevated $\delta^{15}N$ values observed in the juvenile group support this explanation (Fogel et al., 1989; B. t. Fuller et al., 2006). Any other major differences in feeding, health, or stress between fetal and juvenile groups could explain the observed variation between these groups (Deniro & Epstein, 1981; B. T. Fuller et al., 2005; Katzenberg & Lovell, 1999). Therefore, the variation in $\delta^{15}N$ values between the fetal and juveniles observed in this study likely reflects physiological and developmental differences, rather than a result of taphonomic processes.

In the present study, deposition was not a significant factor in the $\delta^{15}N$ values in the fetal sample. Interestingly, the specimens with the lowest $\delta^{15}N$ values also exhibited high C:N ratios that fall outside the biological range (F1, F15, F18, F21). Notably, three of these samples, F15, F18, and F21, were fetal control samples deposited on the surface. Lower $\delta^{15}N$ values are unexpected, as decomposition processes typically yield enriched nitrogen products in surrounding soils and remaining organic matter, while the lighter nitrogen isotope is released during decomposition (Bateman & Kelly, 2007; Beasley et al., 2024; Hopkins et al., 2000; Stokes et al., 2009). A study on muscle decomposition and stable nitrogen isotope values in human tissue explained lowered $\delta^{15}N$ values in some samples due to perimortem blood loss and low body mass (Beasley et al., 2024). However, all donors in that study were covered with black

plastic, a deposition treatment also observed in the current study, which did not show a pattern of decreased $\delta^{15}N$ values. This further suggests that the surface control deposition is responsible for the observed shift. Juvenile surface remains did not follow the same pattern, indicating that intrinsic differences between the groups influence this deposition treatment. The less enriched $\delta^{15}N$ values unique to this deposition, correlated with high C:N ratios, further support the notion that environmental conditions significantly influence the fetal surface control sample.

Bone degradation and diagenesis remain significant concerns in the forensic timeline, as alterations can occur early in the postmortem period. In the present study, seasonality was identified as the only significant factor, with results indicating that variation in the C:N ratio did not preclude variation in $\delta^{13}C$ and $\delta^{15}N$ values under the same conditions. This result is unexpected, as the C:N ratio serves as a quality indicator of the preservation of bone collagen, and is used to filter out diagenetically altered samples before assessing $\delta^{13}C$ and $\delta^{15}N$ values. Additionally, previous studies on fetal and juvenile bone diagenesis using macro- and microscopic measures have shown both season and deposition to be a significant factor in bone preservation (Hale & Ross, 2023; Ross & Hale, 2018). However, these same trends are not observed at the molecular level. Differences were observed in isotopic composition between the fetal and juvenile groups, likely due to differences in development and bone composition. Seasonality had the greatest effect on isotopic composition during the hottest and wettest seasons, suggesting conditions of these seasons drive taphonomic alteration. Properties of seasonality should be further investigated to better understand the environmental conditions that pose the greatest risk for taphonomic alteration in bone.

The mechanisms involved in the alteration of isotopic composition are still poorly understood, and this alteration should be considered when validating results. Additional quality

control measures not considered in the present study could help clarify the factors influencing the isotopic composition of bone collagen, including collagen yield, amino acid composition, and additional sample preparation steps to control for humic acid contamination. Limitations in prior research design prevented isotopic sampling before deposition, which would have provided an isotopic baseline for measuring changes pre- and post-deposition. In place of pre-deposition values, incorporating the isotopic composition of other skeletal tissues that are more resistant to diagenetic alteration, such as tooth enamel or bone mineral, could enhance the discussion around patterns of alteration. Further research is needed to determine whether the variations observed in the present study are applicable in other contexts and how to better identify and control for this variation.

CHAPTER 4

A DUAL-ISOTOPE APPROACH TO ENHANCING ISOTOPIC MODELS FOR THE IDENTIFICATION OF HUMAN REMAINS IN NORTH CAROLINA

Introduction

Strontium ($^{87/86}Sr$) and oxygen ($\delta^{18}O$) isotopes have been widely applied across disciplines to study migration, geolocation, and provenance (Brennan et al., 2015; Hobson et al., 2004; Kramer & Bartelink, 2022; Scheeres et al., 2014; Wright, 2012). In forensic anthropology, these isotopes provide information to reconstruct past mobility and identify unknown individuals by linking their biological tissues to specific geographic regions. To interpret isotopic variation across geographic regions, predictive models known as isoscapes are developed using baseline datasets from biological, hydrological, and geological sources (Bataille et al., 2018, 2020; Bataille & Bowen, 2012; Bowen, 2010; Bowen et al., 2007, 2022; Bowen & Revenaugh, 2003; Holt et al., 2021; West et al., 2006). Isoscapes enable comparisons between measured sample values and expected isotopic distributions, aiding in the inference of geographic origin and migration patterns (Bartelink et al., 2020; Britton et al., 2022; Chesson et al., 2018; Laffoon et al., 2017; Warner et al., 2017).

Isotopic signatures measured from human tissues reflect different periods of life depending on the sampled material. Bone remodels throughout life, so its isotopic composition typically reflects inputs from the most recent decades of one's life (Hedges et al., 2007; Hill, 1998; Sealy et al., 1995). In contrast, tooth enamel does not remodel once formed and retains isotopic values from early childhood, providing insight into an individual's natal origin (Hillson, 1996). Strontium is absorbed in the body primarily through drinking water and is deposited in the mineral phase of bones and teeth by replacing calcium (Bentley, 2006). Strontium-87 (^{87}Sr) is a

radiogenic decay product of rubidium-87 (^{87}Rb). The $^{87/86}Sr$ value, therefore, reflects both the composition and age of underlying bedrock. This ratio varies across different rock types due to differences in initial strontium content and geological age. Like strontium, oxygen is incorporated into bone and teeth mainly through the ingestion of water (Keller et al., 2016). The oxygen isotope ratio ($\delta^{18}O$) is expressed as the ratio of the heavier, less abundant ^{18}O to the lighter, more abundant ^{16}O, relative to a standard. This ratio primarily reflects local water sources and condensation patterns, varying throughout the global water cycle. Predictable patterns of water oxygen isotope ratios emerge, with more positive $\delta^{18}O$ values found at coastal, lower-elevation regions and more negative values in inland, higher-elevation areas, reflecting patterns of precipitation and temperature across the water cycle (Dansgaard, 1964). As a result, $\delta^{18}O$ values typically decrease in distance from the oceanic coast moving inland, with increasing altitude, and decreasing temperature.

Together, $^{87/86}Sr$ and $\delta^{18}O$ values provide complementary spatial relationships between geology, and climatic and hydrological patterns, respectively. These predictable spatial patterns form the basis for geospatial modeling of isotopic data. Because of this spatial variability, isotopic values can be interpolated across a geographic region. Spatial interpolation relates data points based on their geographic proximity, with the idea that locations that are close to one another are more likely to have similar isotopic values (Bowen, 2010; West et al., 2006). Although the interpolation of individual isotopes can independently provide information, combining multiple isotopes enhances regional origin estimates by identifying areas where both values overlap (Keller et al., 2016; Laffoon et al., 2017). This is of particular concern with strontium, where geological boundaries can produce sudden shifts in $^{87/86}Sr$ values that do not perform well when applying spatial interpolation models. However, the combined use of

strontium and oxygen isotopes are particularly useful in this context, as they correspond to distinct geological and meteorological patterns, respectively, and are therefore linked to physiographic properties of a given region.

The combined use of multiple isotopes has become an invaluable tool in forensic anthropology for estimating geographic origin and reconstructing recent migration patterns of unidentified human remains (Aggarwal et al., 2008; Beard & Johnson, 2000; Chesson & Berg, 2022; Ehleringer et al., 2010). This is particularly relevant in high-traffic migrant regions, where isotope-based geolocation methods have proven effective (Ammer et al., 2020; Obertová et al., 2023). At a smaller scale, state-level isoscapes in the U.S. have demonstrated positive results (Warner et al., 2017). The application of these methods has gained traction in forensic casework both in the U.S. and internationally (Bartelink & Chesson, 2019; de Oliveira Mascarenhas et al., 2022; Eck et al., 2019; Kramer & Bartelink, 2022). Recently, dual-isotope analysis for geolocation has been adopted in North Carolina forensic casework, highlighting a need for a refined, regionally specific isoscape (Long et al., 2024).

The state of North Carolina spans approximately 500 miles from the Atlantic coastline in the east to the Appalachian Mountains in the west, exhibiting significant variation in both bedrock geology and elevation. $^{87/86}Sr$ values in water are expected to follow a predictable pattern across the state based on varying geology. The coastal plain reflects the strontium signature of lower $^{87/86}Sr$ marine sediments and past seawater influence, while the western region, composed of ancient crystalline rocks, displays older, higher $^{87/86}Sr$ values (Beard & Johnson, 2000; Peucker-Ehrenbrink & Fiske, 2019). The central region of the state is characterized by metamorphic terranes intersected by Triassic-age rift basins, and recent studies suggest that this area exhibits the lowest $^{87/86}Sr$ values due to the influence of diabase dikes

(Watts et al., 2019). Similarly, increasing altitude and distance from the Atlantic coastline is expected to create a predictable gradient of decreasing $\delta^{18}O$ water values from east to west.

Despite North Carolina's geological and climatic diversity, a comprehensive dual-isotope isoscape for forensic applications has not yet been fully developed. Existing regional isoscapes lack the resolution needed for fine-scale forensic casework (Bataille & Bowen, 2012; Bowen et al., 2007; Regan, 2006; Warner et al., 2017). The goal of this research is to develop a dual-isotope ($^{87/86}Sr$ and $\delta^{18}O$) isoscape specific to North Carolina, integrating strontium and oxygen isotope data from water sources across the state to enhance geolocation for forensic purposes. The relationship between isotopic variations in strontium and oxygen and the state's physiographic regions will also be explored to determine whether these regions can be defined as distinct regions of origin. Additionally, the model is tested against two individuals of known geographic origin to evaluate its predictive accuracy. The findings from this study contribute to forensic anthropology by enhancing the ability to estimate the geographic origins of unidentified remains, thereby improving casework applications.

Materials & Methods

Water Samples

Strontium isotope data ($^{87/86}Sr$) were obtained from Watts et al. 2019 and Crenshaw 2020. These sources provided 227 $^{87/86}Sr$ measurements from water samples collected across North Carolina (Figure 1A). The dataset included $^{87/86}Sr$ values associated with geographic coordinates. All samples were analyzed at the University of North Carolina – Chapel Hill using consistent preparation and analytical procedures. Oxygen isotope data ($\delta^{18}O$) were obtained from the Waterisotopes Database (*WaterIsotopes.Org*, n.d.). The database was accessed on March 1, 2025, by using the query tool with the following parameters: Country = US, State/Province =

NC, Type= Ground; River or Stream; Spring; Tap, and projects reporting $\delta^{18}O$ values (Figure 2A). This search yielded 456 data points from 10 projects (Supplementary File 1). The selected water sources represent the primary drinking water sources in North Carolina (Laughinghouse, 2024). The dataset included $\delta^{18}O$ values with corresponding latitude and longitude coordinates. The isotopic results obtained from these studies were then used to construct the isoscape.

Geographic Information Systems Procedures

Spatial patterns in the $^{87/86}Sr$ and $\delta^{18}O$ values were assessed using the Global Moran's I test in ArcGIS Pro (version 3.3, ESRI) (*ArcGIS Pro [Version 3.3]*, 2024). This tool quantifies spatial autocorrelation, determining the extent to which similar values cluster geographically. The analysis was performed on each of the point datasets containing sample locations with associated $^{87/86}Sr$ and $\delta^{18}O$ values. The dataset was projected using the North Carolina State Plane (NAD83) coordinate system to ensure alignment with the study area. The spatial weights matrix for Moran's I was defined using the Inverse Distance method, which calculates spatial relationships based on the inverse of the distance between sample locations. The results from the Moran's I test were used to evaluate the spatial distribution of both $^{87/86}Sr$ and $\delta^{18}O$ values, providing insights into the spatial dependence and clustering of isotopic signatures in the study area.

Geospatial analysis was conducted in ArcGIS 3.3 (version 3.3, ESRI) (*ArcGIS Pro [Version 3.3]*, 2024). Isotopic data, linked to geographic coordinates, was imported into the software for spatial interpolation and analysis. A contour mapping approach was applied, using geostatistical methods to interpolate values across a continuous spatial area. Empirical Bayesian Kriging (EBK) was selected for interpolation due to the high sample density and the well-defined spatial dependence of the isotopic data. Model optimization was performed using cross

validation to refine accuracy and uncertainty estimates. The exponential semivariogram model was used for $^{87/86}Sr$. To optimize interpolation performance, the maximum number of points in each local model was set to 150, while the maximum and minimum number of neighbors were adjusted to 18 and 8, respectively. Additionally, the number of simulated semivariograms was reduced to 40 to balance computational efficiency with predictive accuracy. For $\delta^{18}O$, the final model used an exponential semivariogram model with empirical data transformation. The maximum number of points per local model was set to 110, with minimum neighbors at 10 and maximum neighbors at 15. Both models were interpolated using Natural Jenks breaks to categorize the isoscapes.

Correlation with Geographic Variables and Physiographic Provinces

Additional statistical methods were employed to examine the relationship between isotopic values and physiographic features. To examine the relationship between isotopic values and physiographic provinces , an ANOVA was performed to assess significant differences between $^{87/86}Sr$ values across five physiographic provinces (Outer Coastal Plain, Inner Coastal Plain, Outer Piedmont, Inner Piedmont, and Blue Ridge) (Brown & Parker, 1985; Stewart & Roberson, 2007). Post-hoc comparisons were conducted using Tukey's HSD test to identify specific group differences when the ANOVA results indicated statistical significance. The analyses were performed using JMP 17.0 with a significance level set at $p<0.05$ (JMP®, Version 17.0. SAS Institute Inc., Cary, NC, 1989–2021., n.d.).

A Pearson correlation was applied to assess the strength and direction of linear relationships between $\delta^{18}O$ isotopic values and altitude. The correlations were tested for significance using a two-tailed hypothesis test with a significance level set at 0.05. The Pearson correlation coefficient was calculated to determine the magnitude and direction of this

relationship. The analysis was performed using JMP 17.0 with a significance level set at $p<0.05$ (JMP®, Version 17.0. SAS Institute Inc., Cary, NC, 1989–2021., n.d.).

Analyzing the Efficacy of the Dual-isotopic Approach

The isoscape was tested using $^{87/86}Sr$ and $\delta^{18}O$ values from tooth enamel carbonate of two identified decedents from North Carolina forensic casework. The individuals have been anonymized as MecklenburgID and GastonID. MecklenburgID was identified using multidisciplinary methods recently implemented at the Human Identification and Forensic Analysis Laboratory at North Carolina State University, and the family confirmed the geographic history of the decedent as being born, and living in Charlotte, NC throughout his life (Long et al., 2024). GastonID was identified through NamUS Project DNA in collaboration with local law enforcement. Records confirmed they were born in Gastonia, NC and spent their adult life in Gaston County and neighboring Cleveland County. All isotopic analyses for these decedents were performed at Washington State University. Standard sample preparation and analytical methods for modern human dental enamel were followed and are described elsewhere (Long et al., 2024).

Because the $\delta^{18}O$ value was measured from carbonate and reported relative to the VPDB scale, the measured carbonate value was first converted from the VPDB scale to the VSMOW scale using the Coplen (1988) equation (Coplen, 1988):

$$\delta^{18}O_{VSMOW}=1.03091 \times \delta^{18}O_{VPDB}+30.91$$

To account for oxygen isotope fractionation between drinking water and body tissues, the value was converted from dental enamel carbonate to drinking water using the Dotsika (2020) equation, allowing for direct comparison with the drinking water isoscape (Dotsika, 2020):

$$\delta^{18}O_{dw} = 1.020 \times \delta^{18}O_{c} – 32.941$$

The converted isotopic measurements from MecklenburgID and GastonID are listed in Table 1.

Table 1 Measured isotopic signatures from tooth enamel for both test cases. Oxygen values measured from carbonate have been converted to drinking water values for direct comparison to the oxygen water isoscape.

Case ID	Latitude	Longitude	$^{87/86}Sr$	$\delta^{18}O_{VPDB}$ (‰)	$\delta^{18}O_{dw}$ (‰)
MecklenburgID	35.22709	-80.8431	0.708905	-4.22	-5.85
GastonID	35.25528	-81.1803	0.709338	-3.93	-5.55

Bayesian Likelihood Approach

The dual-isotopic approach was tested using a Bayesian likelihood approach using the $^{87/86}Sr$ and $\delta^{18}O_{dw}$ values from the individuals of known origin in North Carolina to estimate the probability of the individuals' origin based on isotopic composition of dental enamel (Laffoon et al., 2017). First, the probability densities for both $^{87/86}Sr$ and $\delta^{18}O$ isotope values were calculated assuming normal distributions using the probability density equation:

$$f_{\mathcal{N}}(x \mid \mu, \sigma) = \frac{1}{\sqrt{2\pi\sigma^2}} \exp\left(-\frac{(x-\mu)^2}{2\sigma^2}\right)$$

The probability density values were determined by multiplying the normal density functions for $^{87/86}Sr$ and $\delta^{18}O$, using the predicted means (μ) and standard deviations (σ) for each isotope. The measured values of MecklenburgID and GastonID were used as the observed data points in these calculations:

$$f_{\mathcal{N}}\left({}^{87/86}Sr_{NCID} \mid \mu_{Sr}, \sigma_{Sr}\right) \cdot f_{\mathcal{N}}\left(\delta^{18}O_{NCID} \mid \mu_{\delta^{18}O}, \sigma_{\delta^{18}O}\right)$$

Where ${}^{87/86}Sr_{NCID}$ is the measured $^{87/86}Sr$ value from tooth enamel, and $\delta^{18}O_{NCID}$ is the converted $\delta^{18}O_{dw}$ value.

A 95% confidence interval was calculated by identifying the cumulative probability thresholds. The threshold was determined by finding the smallest cumulative sum closest to 0.95. Locations with probability density values above this threshold were assigned a value of 1,

indicating that they fell within the 95% confidence region. The predicted $^{87/86}Sr$ and $\delta^{18}O$ values, probability densities, and 95% confidence interval assignments were exported into a data frame with corresponding geographic coordinates. This approach allowed for spatial modeling of probabilities, helping to identify the most likely geographic origin of the known individual based on their $^{87/86}Sr$ and $\delta^{18}O$ isotopic signatures. To spatially represent the probabilities, the resulting data frame was imported into ArcGIS Pro 3.3 for visualization (ArcGIS Pro [Version 3.3], 2024). The geographic coordinates, along with the probability densities and confidence intervals, were displayed on a map providing insights into the most probable origin of the individual based on the dual-isotopic approach. Additionally, the true region of origin for each test case was mapped to visually compare the accuracy of the confidence interval assessment.

Results

Limitations of the dataset

The data obtained from previous studies and compiled in this study is variable in terms of sampling density, which is greater in the $\delta^{18}O$ data than the $^{87/86}Sr$ data. The $^{87/86}Sr$ data were obtained from two separate studies, however they were related in scope and direction (Crenshaw, 2020; Watts et al., 2019). The $\delta^{18}O$ data was compiled from a variety of studies with varying purposes and directions, reflected in Supplementary File 1. One limitation of the compiled $\delta^{18}O$ values is the type of water samples which may not accurately reflect the consumed water sources over time, as modern municipal water systems have been developed in North Carolina throughout the 20th century (McNeely, 2023). Overall, both $\delta^{18}O$ and $^{87/86}Sr$ data provide broad coverage of the study area with high sampling density (Figure 1, Figure 2). Additional sampling in less dense regions could further refine the model, particularly in the western part of the state

where the geology is more complex, but overall this compilation provides higher spatial resolution than most comparative studies (Bataille & Bowen, 2012; Bowen et al., 2007; Keller et al., 2016; Warner et al., 2017).

Figure 1 Strontium water data locations over 5 proposed physiographic provinces in the study area (a), the resulting strontium water isoscape (b), and a crossplot showing the relationship between strontium values, and longitude, characterized by physiographic province (c).

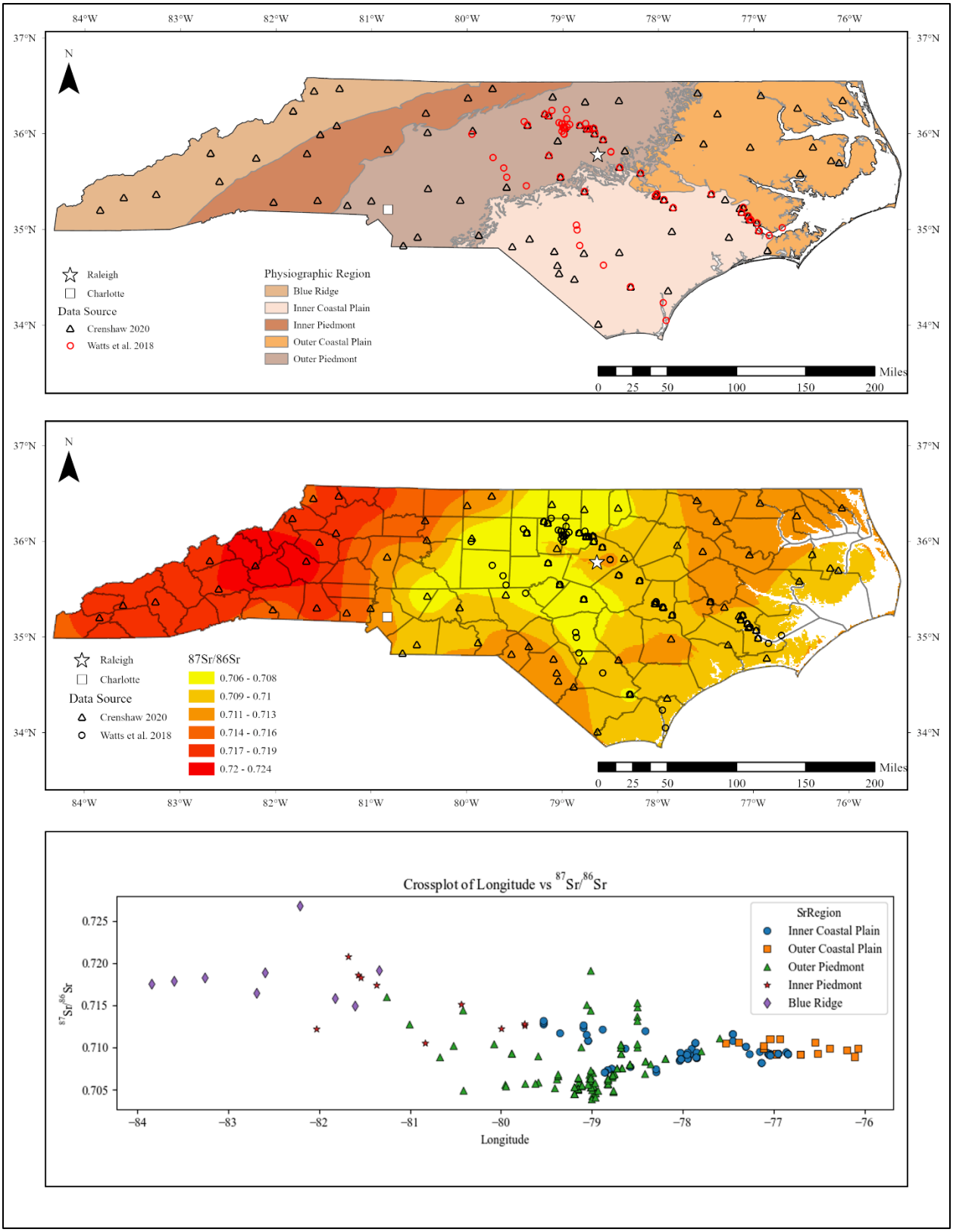
84°W
83°W
82°W
81°W
80°W
79°W
78°W
77°W
76°W
37°N
36°N
35°N
34°N
N
Raleigh
Charlotte
Data Source
Crenshaw 2020
Watts et al. 2018
Physiographic Region
Blue Ridge
Inner Coastal Plain
Inner Piedmont
Outer Coastal Plain
Outer Piedmont
Miles
0 25 50 100 150 200
87Sr/86Sr
0.706 - 0.708
0.709 - 0.71
0.711 - 0.713
0.714 - 0.716
0.717 - 0.719
0.72 - 0.724
Crossplot of Longitude vs 87Sr/86Sr
SrRegion
Inner Coastal Plain
Outer Coastal Plain
Outer Piedmont
Inner Piedmont
Blue Ridge
0.725
0.720
0.715
0.710
0.705
−84
−83
−82
−81
−80
−79
−78
−77
−76
Longitude

Figure 2 Oxygen water data locations over elevation profile of the study area (a), the resulting oxygen water isoscape (b), and a crossplot showing the relationship between oxygen values elevation (ft.) from east to west (c).

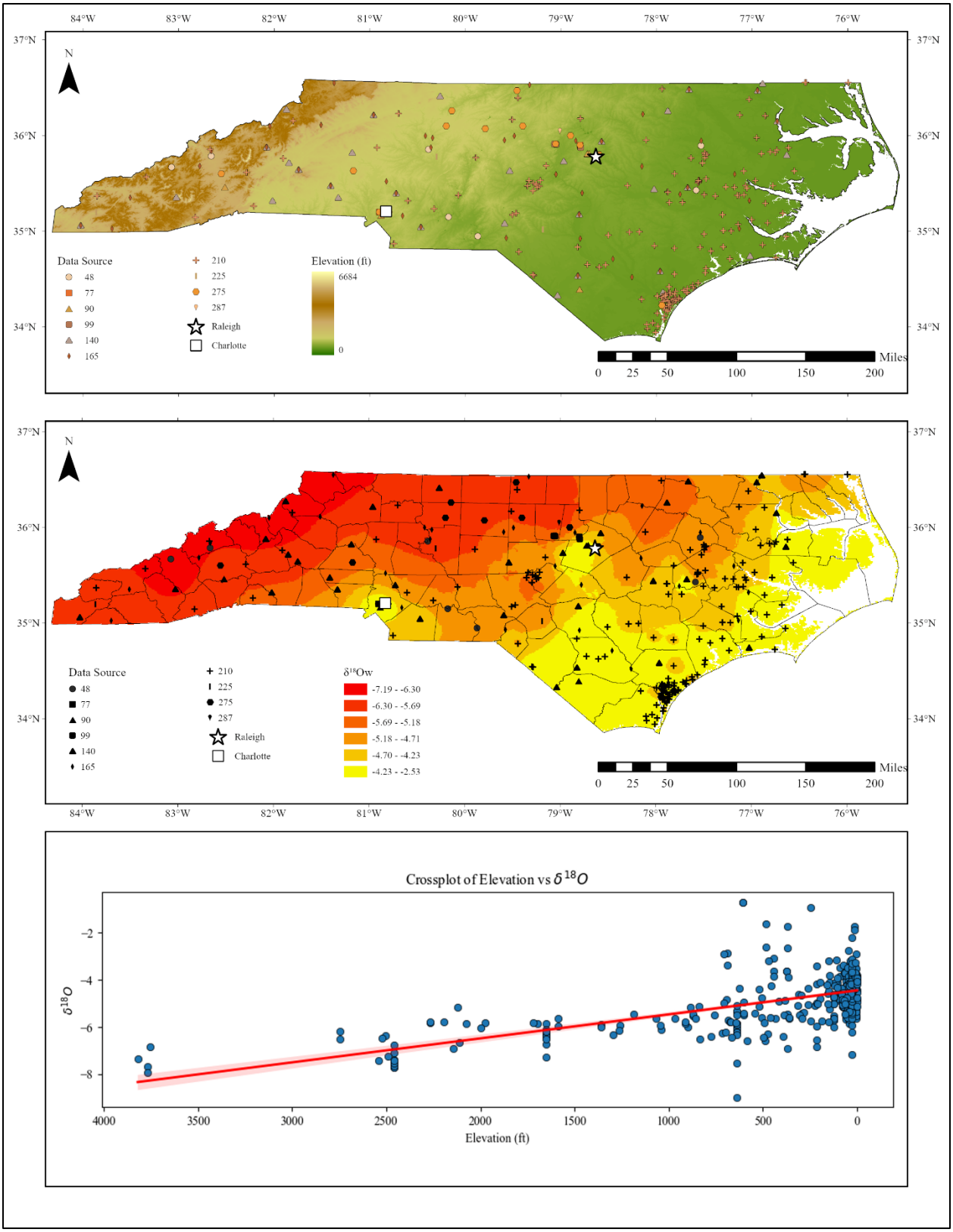
84°W
83°W
82°W
81°W
80°W
79°W
78°W
77°W
76°W
37°N
36°N
35°N
34°N
N
Data Source
48
77
90
99
140
165
210
225
275
287
Raleigh
Charlotte
Elevation (ft)
6684
0
Miles
0 25 50 100 150 200
δ¹⁸Ow
-7.19 - -6.30
-6.30 - -5.69
-5.69 - -5.18
-5.18 - -4.71
-4.70 - -4.23
-4.23 - -2.53
Crossplot of Elevation vs δ18O
δ18O
−2
−4
−6
−8
4000
3500
3000
2500
2000
1500
1000
500
0
Elevation (ft)

Strontium and Oxygen isoscapes

The isotope data from water sources in North Carolina show a wide range in both $^{87/86}Sr$ and $\delta^{18}O$ values. $^{87/86}Sr$ values ranges from 0.7038 to 0.7267 ($\bar{x}$ = 0.7089; σ = 0.003617) (Supplementary File 2), while $\delta^{18}O$ values range from -0.71‰ to -8.99‰ ($\bar{x}$= -4.87, σ = 1.14) (Supplementary File 3). The patterns observed in the $^{87/86}Sr$ data effectively align with the expected physiographic trends (Figure 1B). The lowest values are associated with water sources originating in the Piedmont region, the Coastal Plain exhibits moderately higher values consistent with underlying geological features, the highest values are from the Blue Ridge Mountains, and the transitional region of the upper Piedmont reflects values between the regions on either side. The $\delta^{18}O$ isoscape also follows the expected gradient related to elevation, with enriched values in the Coastal Plain, with decreasing values as altitude and distance from the oceanic coast increase (Figure 2B). However, two anomalous areas within the Piedmont region reflect unexpectedly enriched $\delta^{18}O$ values. Both Raleigh, NC and Charlotte, NC tap water have several enriched isotopic values (-2.64‰ to -1.64‰; -3.36‰ to -0.710‰, respectively) concentrated in these populous areas from municipal water sources, which contrast with the values in the surrounding areas.

An initial assessment of spatial autocorrelation using Moran's I indicates that both $^{87/86}Sr$ and $\delta^{18}O$ values have significant clustered spatial autocorrelation (Moran's I $^{87/86}Sr$ = 0.78, $p<0.05$; Moran's I $\delta^{18}O$ = 0.76, $p<0.05$). ANOVA revealed significant differences in $^{87}Sr/^{86}Sr$ values among the five physiographic provinces of North Carolina ($F(4, 218) = 61.76$, $p<0.05$) (Table 2, Figure 1C). Tukey's HSD post-hoc comparison revealed significant differences between all strontium region pairs except between the inner and outer coastal plain ($p<0.05$) (Table 3, Figure 3).

Table 2 ANOVA results of comparison between mean strontium values from five physiographic regions in North Carolina.

ANOVA					
Source	DF	Sum of Squares	Mean Square	F Ratio	Prob > F
Geologic Region	4	0.00151032	0.000378	61.762	**<.0001**
Error	218	0.00133274	6.11E-06		
C. Total	222	0.00284306			

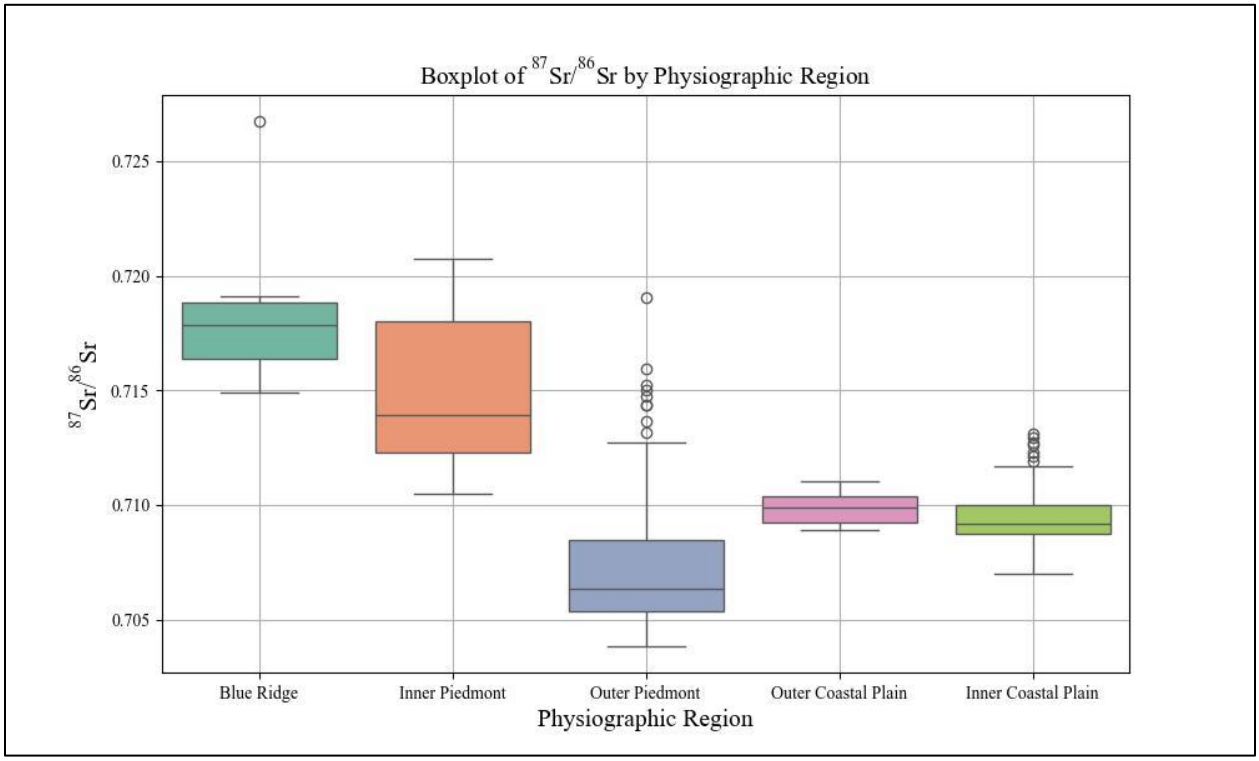

Figure 3 Visualizing the ANOVA results of strontium mean values from 5 proposed physiographic provinces through a box and whisker plot. Inner and Outer Coastal Plain show similarities, supported by results from post-hoc Tukey's HSD test showing no significant difference.

When examining the relationship between the $\delta^{18}O$ values and elevation using Pearson's correlation coefficient, there was a significant negative correlation between elevation and $\delta^{18}O$ ($r = -0.63$, $n=456$, $p<0.05$) (Figure 2C). These findings support the validity of the model, demonstrating expected relationships with geographic and physiographic variables.

Case Study Assignment

The result of the bivariate probability density function for both MecklenburgID and GastonID is presented in Figure 4. The 95% confidence threshold did reveal a clear spatial concentration of high-probability regions for each individual's origin in central North Carolina, with probability densities consistently high in these regions. This threshold, however, did not capture the true region of origin of Mecklenburg ID or Gaston ID (Charlotte, Mecklenburg County, NC; Gastonia, Gaston County, NC) (Figure 4). However, with the removal of the enriched tap water values from Charlotte, NC (see Discussion below), the true region of origin is within the 95% confidence interval for MecklenburgID. The removal of the enriched $\delta^{18}O$ tap water values did not correctly include GastonID within the confidence interval, and therefore the exclusion may be attributed to the $^{87/86}Sr$ values in the region (see Discussion below).

Table 3 Results of post-hoc Tukey's HSD for pairwise comparisons between each physiographic region. All comparisons were significant except for inner and outer coastal plains, suggesting these regions can be grouped.

Ordered Differences Report						
Region Comparison		Difference	Std Err Dif	Lower CL	Upper CL	p-Value
Blue Ridge	Outer Piedmont	0.011032	0.000855	0.00868	0.013383	**<.0001**
Blue Ridge	Inner Coastal Plain	0.008856	0.000879	0.006439	0.011272	**<.0001**
Blue Ridge	Outer Coastal Plain	0.008538	0.001001	0.005786	0.01129	**<.0001**
Inner Piedmont	Outer Piedmont	0.00767	0.000814	0.005431	0.009909	**<.0001**
Inner Piedmont	Inner Coastal Plain	0.005494	0.000839	0.003186	0.007802	**<.0001**
Inner Piedmont	Outer Coastal Plain	0.005177	0.000966	0.002519	0.007834	**<.0001**
Blue Ridge	Inner Piedmont	0.003362	0.001136	0.000237	0.006487	**0.028**
Outer Coastal Plain	Outer Piedmont	0.002494	0.000611	0.000813	0.004174	**0.0006**
Inner Coastal Plain	Outer Piedmont	0.002176	0.00038	0.001132	0.00322	**<.0001**
Outer Coastal Plain	Inner Coastal Plain	0.000317	0.000644	-0.00145	0.002088	0.988

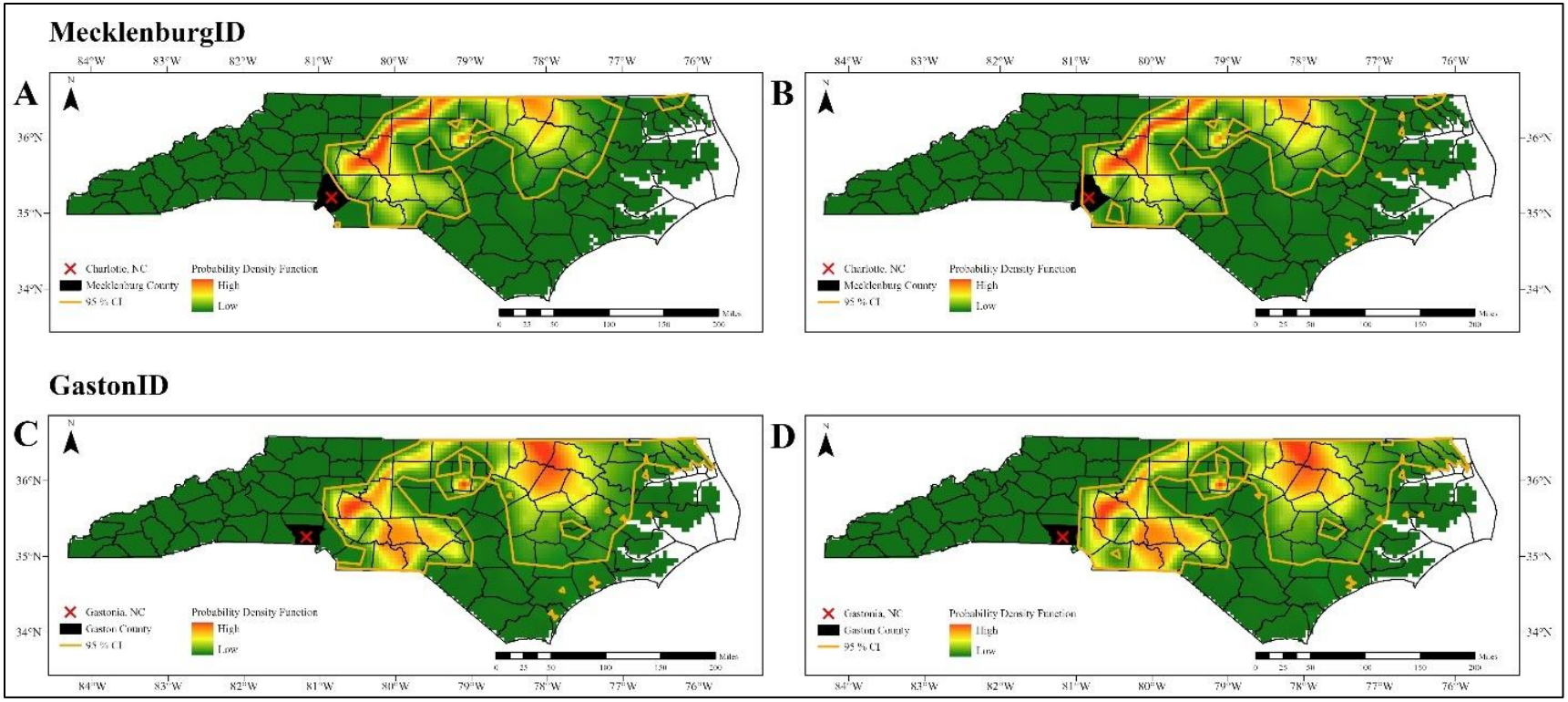

Figure 4 Results of the prediction density formula and 95% confidence interval for MecklenburgID when the model contains Charlotte tap water values (a), when Charlotte tap water values are removed (b), and Gaston ID when the model contains Charlotte tap water values (c), when Charlotte tap water values are removed (d).

Discussion

The state-level $^{87/86}Sr$ and $\delta^{18}O$ isoscapes of North Carolina accurately reflect expected isotopic trends based on the region's physiographic and topographic characteristics. General trends in $^{87/86}Sr$ values across the state align with major physiographic provinces, and results suggest that four distinct regions can be established for predicting region of origin based on $^{87/86}Sr$ values, with the combination of the Inner and Outer Coastal Plain regions due to their similar isotopic signatures and geology. The expected relationship between $\delta^{18}O$ values and elevation is broadly observed in the oxygen isoscape, with the exception of the regions surrounding Raleigh (Wake County) and Charlotte (Mecklenburg County). These are the two most populous areas in North Carolina, where municipal tap water is sourced from large surface reservoirs. In these systems, preferential evaporation of lighter isotopes leads to isotopic enrichment and higher $\delta^{18}O$ values. Previous $\delta^{18}O$ tap water isoscapes smoothed over the enriched values in these regions. However, the refined isoscape presented here incorporates more drinking water sources and reveals more enriched $\delta^{18}O$ values than previously published estimates, particularly when tap water values are included (Bowen et al., 2007).

Given that Wake and Mecklenburg counties are not only the most populous in the state, but also generate the majority of forensic casework, clarifying the relationship between $^{87/86}Sr$ or $\delta^{18}O$ baselines and isotopic signatures in human tissues is particularly important for forensic applications. When applying the Bayesian likelihood approach to test samples (MecklenburgID, GastonID), both were excluded from their respective regions of origin: Charlotte, Mecklenburg County, NC, and Gastonia, Gaston County, NC. The Bayesian likelihood approach offers a quantifiable, probabilistic method for region-of-origin estimation, offering a more objective alternative to visually comparing isotopic values and isoscapes. However, the exclusion of both

test samples from their respective 95% confidence intervals suggests the model may not fully account for local variation in $^{87/86}Sr$ or $\delta^{18}O$ values.

Looking more closely at the individual isoscapes, the exclusion of the Charlotte metropolitan area, including Gastonia, may be attributed to the $\delta^{18}O$ model, where the tap water samples have been identified as enriched. When these enriched values are excluded from the model, Charlotte and Mecklenburg County, NC are correctly included within the 95% CI for MecklenburgID (Figure 4B). However, even after removing these values, Gastonia and Gaston County still remain outside the predicted region for GastonID (Figure 4D). This discrepancy may be due to limited data coverage, as the $^{87/86}Sr$ model includes only one water sample from Gaston County and interpolation may smooth over differences in the local geology. Gastonia is on a granitic intrusion, which would be expected to yield lower $^{87/86}Sr$ values than the surrounding metamorphic terrain, and therefore lower than those from the model's water sample and closer to the decedent's measured value (Brown & Parker, 1985; Stewart & Roberson, 2007). Discrepancies between the $^{87/86}Sr$ or $\delta^{18}O$ values from the water samples and the dental enamel samples highlight the need to clarify the relationship between drinking water and human tissues, particularly in these populous areas where municipal water sources and local geology are influencing the model. Temporal and behavioral factors can influence individual histories that lead to the observed discrepancies. The exclusion of known-origin samples from their respective confidence intervals raises questions about how well the isoscapes reflect historical and lived experiences of water consumption, particularly in metropolitan areas where water sources have higher variability, and have changed over time.

The exclusion of the test samples from the original 95% confidence intervals suggest that the measured values do not reflect typical regional values. This could be due to differences in

water sources consumed during dental enamel formation in childhood. MecklenburgID was born in the mid-20th century, while GastonID was born in the latter half of the 20th century. Access to municipal water has changed in North Carolina over the past century, and therefore the isotopic signature in dental enamel values may reflect non-municipal water sources. The exclusion of tap water from the model resolved this discrepancy for MecklenburgID, however the exclusion of GastonID aligns more with the $^{87/86}Sr$ values, which may not accurately reflect the underlying geology in this region. Testing more known-origin samples would help clarify whether these mismatches result from individual outliers, or if it indicates broader model limitations. This would be particularly useful when testing samples from both rural and metropolitan areas, helping to identify whether the model performs poorly specifically in metropolitan areas. If so, incorporating additional municipal and non-municipal water samples from Wake and Mecklenburg counties, regions where most forensic casework originates, could improve local predictions and reduce future misclassifications. Additionally, testing the model against other biological tissues would be useful to determine how to better enhance the model. While tooth enamel retains the isotopic signature of early childhood, bone remodels throughout life and reflects more recent geographic residence. Identifying regional issues in the present dataset supports the inclusion of additional water samples or alternative human tissues in future models.

The enriched $\delta^{18}O$ values in Raleigh and Charlotte originate from Bowen et al.'s 2007 U.S. Tap Water isoscape dataset (Bowen et al., 2007). Given that the samples for the $\delta^{18}O$ isoscape come from a variety of sources, outlier removal is an option in an effort to standardize the data. However, dismissing these high values without further investigation may oversimplify the issue, particularly when only two test samples have been evaluated. Additionally, because the multiple water sources were collected across different seasons and time periods, the dataset

offers a wider range of $\delta^{18}O$ values than could be captured during a single sampling period. Rather than treating these enriched $\delta^{18}O$ values as anomalies and removing them, refining the isoscape with additional regional data (or supplemental sample data, like tissue type and histological age determination) would provide a more robust and reliable solution. Further validation using dental enamel samples could help determine the extent to which these values influence forensic applications.

Incorporating isotopic data directly derived from dental enamel from across the state would also help to bridge the gap between the tap water values and measured values from human tissues. This multi-layered approach could improve predictions by incorporating biological tissue data directly. Unlike a water isoscape, which reflects the isotopic signature of water mainly driven by geologic and topographic factors, an enamel isoscape directly reflects the isotopic signature of the individual during childhood, without the confounding effects of the complex relationship between $\delta^{18}O$ in drinking water and biological tissues (Ueda & Bell, 2021). Because it directly incorporates isotopic data from biological tissues, an enamel isoscape has the potential to provide more accurate predictions for forensic applications. Previous studies have shown the effectiveness of tissue-based models in other regions (Johnson et al., 2025; Kootker, Plomp, et al., 2020; Mascarenhas et al., 2022; Warner et al., 2017). While a variety of regression equations have been used to model the correlation between water and enamel $\delta^{18}O$ values, these conversion models have limitations. Ueda & Bell (2021) suggest that tissue-specific geographic reference maps could greatly improve region-of-origin assessment when using $\delta^{18}O$ (Ueda & Bell, 2021). The creation of such maps would require international standardization of isotopic analysis, but it would also create robust reference datasets that could help address the challenges presented in regions like Wake and Mecklenburg Counties.

Before implementing an enamel isoscape, however, preliminary data should be compared to the water isoscapes presented here. One major limitation when constructing enamel isoscapes is the logistical challenge of acquiring and analyzing human teeth from across the state. As an initial step, incorporating a preliminary set of enamel data as an additional component within the probability density function, alongside the $^{87/86}Sr$ and $\delta^{18}O$ water isoscapes, would be a more approachable strategy. This integrated approach could offer a more reliable and exclusionary method for region-of-origin estimation, ultimately improving the applicability of isotopic methods to forensic casework in North Carolina.

The strengths and limitations of using a dual-isotopic approach with $^{87/86}Sr$ and $\delta^{18}O$ isoscapes at the state level in North Carolina suggest that caution should be exercised when implementing this model in forensic casework. While the isoscapes reflect the predicted broad geologic and topographic patterns, the ability to accurately predict region-of-origin within the state is challenging in densely populated areas like Wake and Mecklenburg counties. Further testing of the Bayesian likelihood approach using a larger set of known-origin samples is required to assess the model's robustness. Incorporating enamel samples into the model could improve predictive accuracy by integrating isotopic data from biological tissues, but this approach requires extensive data collection and preliminary comparison to current water-based isoscapes. Alternatively, incorporating additional water samples from these populated areas could improve the local accuracy in the model. Considering the age of the case could help to inform how best to interpret the predictive output from the water sources. Future research should focus on testing the isotopic model with additional known samples and incorporating additional samples from multiple sources to enhance the $^{87/86}Sr$ and $\delta^{18}O$ dual-isotopic model for forensic applications in North Carolina. Despite current limitations, this study provides a foundation for

advancing isotopic methods in forensic casework in the state. By developing a regionally-specific isoscape and demonstrating the utility of probabilistic modeling, the results suggest that geographic provenance estimation is a tool suitable to be used alongside other investigative and identification techniques. The integration of isotopic methods can directly improve efforts to identify unknown individuals, and the dual-isotopic model has strong potential to become a valuable component of forensic investigations in North Carolina.

CHAPTER 5

APPLYING MULTIDISCIPLINARY METHODS TO FORENSIC CASEWORK IN NORTH CAROLINA

Abstract

A multidisciplinary approach in the investigation of unidentified decedents (UIDs) employs the use of a variety of scientific approaches. This approach is applied in casework in North Carolina, USA and has led to successful identifications using anthropological analysis and population affinity estimation using 3D-ID, investigative genetic genealogy, and isotopic analyses. Results from one scientific approach can help to inform the others, providing more information about the decedent, and thus enhancing the investigation. This case report outlines three cases from North Carolina that combine each of these scientific approaches and serve as examples of collaboration in a multidisciplinary approach.

Key Points

- Anthropological analyses including population affinity using 3D-ID can be used in conjunction with isotopic analyses in estimating geographic origin.
- Results from anthropological and isotopic analyses can help to narrow down or direct investigative genetic genealogy.
- Multidisciplinary collaboration in the investigation of unidentified decedents enhances the investigation.

Introduction

As of February 26, 2024, there are 158 unidentified persons cases listed in the National Missing and Unidentified Persons System (NamUs) in the state of North Carolina (Figure 1). A multidisciplinary approach has been adopted at the North Carolina State University Human Identification and Forensic Analysis Laboratory (NCSUHIFAL) (Ross & Passalacqua, 2024). Modern methods of skeletal analyses are employed including developing a biological profile (e.g., biological sex, age at death, stature, and population affinity) for unidentified decedents (UIDs), radiographic comparisons for identification, and trauma analysis, to assist Medical Examiner offices. Additional techniques are employed to develop standard operating procedures for North Carolina casework. An interinstitutional grant awarded in 2019 to North Carolina State University (NCSU) and Western Carolina University (WCU) funded a pilot project to implement a holistic approach to identification involving standard forensic anthropological analysis, investigative genetic genealogy (IGG), and isotopic signatures (Ross & Passalacqua, 2024). Further, NCSHIFAL partnered with the NC State Bureau of Investigation on a grant funded by a Bureau of Justice Assistance under their Missing and Unidentified Human Remains (MUHR) program to advance the multidisciplinary approach to reduce the backlog of unidentified cases in North Carolina. A more comprehensive overview of the multidisciplinary endeavor to cold case work within the state of North Carolina has been outlined by Ross and Passalacqua (Ross & Passalacqua, 2024). Recently, bone and tooth samples from nine decedents were sent to Washington State University (WSU) for isotopic analyses. Here, we present the results of isotopic investigations from three of those cases using geolocation and dietary isotopes,

anthropological analyses including population affinity estimation using 3D-ID (Slice & Ross, 2024), and investigative genetic genealogy. The purpose of this paper is to highlight the multidisciplinary approach and show the added value of using advanced testing in forensic anthropology casework in North Carolina.

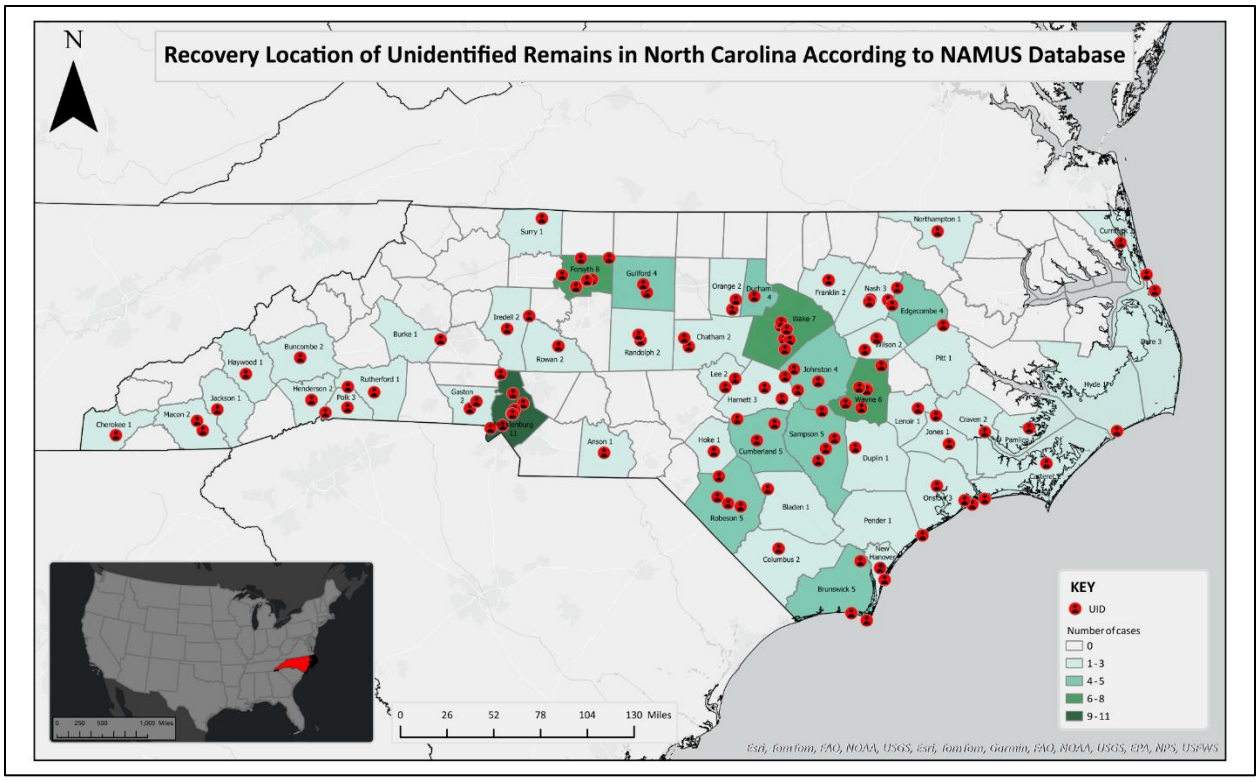

Figure 1 Map displaying recovery location of unidentified skeletonized human remains in North Carolina, USA by county.

Isotope Analysis – Background

Tissues Analyzed

Collagen is the main organic component and apatite is the mineralized component in bone structure and physiology (Weiner & Wagner, 1998). Different skeletal elements remodel throughout life at varying rates and therefore, isotopic signatures measured in bone are reflective of isotopic sources from the most recent decades of one's life (Hedges et al., 2007; Hill, 1998;

Sealy et al., 1995). Tooth enamel is a highly mineralized tissue that forms during childhood and does not remodel once formed (Hillson, 1996). Isotopic values in tooth enamel thus reflect childhood diet and place of residence. Due to the compact mineralized structure, tooth enamel is also resistant to the effects of diagenesis or taphonomic alteration (Turner-Walker, 2007).

$^{87/86}$Sr Analysis – Tooth Enamel and Bone: Geolocation

Analysis of $^{87/86}$Sr in human skeletal tissues is commonly used to reconstruct human mobility in archaeological and forensic contexts (Bartelink & Chesson, 2019; Bentley, 2006). $^{87/86}$Sr varies across the landscape based on the age, chemical composition, and weathering rates of the underlying geology (Bentley, 2006). As humans feed and drink, the $^{87/86}$Sr of consumed food and water is incorporated into their skeletal tissues (Bentley, 2006). Strontium isotopes are not significantly fractionated as they are passed up the food chain, so skeletal $^{87/86}$Sr reflects the local biologically available $^{87/86}$Sr in soil, plants, and water. $^{87/86}$Sr measured in tooth enamel corresponds to the location of origin during childhood, while bone represents an average of the past 5-25 years of location due to remodeling (Aggarwal et al., 2008).

δ^{18}O analysis – Tooth enamel: Geolocation

Stable oxygen isotope ratios (^{18}O:^{16}O) are similarly used as a proxy for human mobility. Oxygen isotope values are expressed using δ^{18}O notation in ‰ difference of the ratio of ^{18}O to ^{16}O compared to an international standard (Coplen, 2011; Meier-Augenstein, 2017; Sharp, 2017). δ^{18}O varies due to the fractionation of oxygen isotopes within the water cycle. Factors such as evaporation, condensation, precipitation, temperature, latitude, elevation, and distance from large bodies of water affect δ^{18}O (Craig, 1961; Dansgaard, 1954, 1964). Oxygen isotopes are incorporated into phosphate (PO_4^{3-}) and carbonate (CO_3^{2-}) groups in bones and teeth, which can be directly compared to measured values from individuals of known origin, or converted to

drinking water values, which have been modeled using isoscapes (C. A. Chenery et al., 2012; Iacumin et al., 2022). Direct comparison between measured tooth enamel from known populations is a simplified approach to utilizing $\delta^{18}O$ isotope as a geolocation tool and is useful when drinking water models are not yet available (Pollard et al., 2011).

$\delta^{13}C$ Analysis – Tooth Enamel and Bone Collagen

Carbon isotope ratios ($^{13}C/^{12}C$) are also expressed in ‰ using δ-notation (Craig, 1953). Carbon isotopes in plants vary according to their photosynthetic pathway (C3, C4, and CAM), which affects how they fractionate atmospheric carbon. C3 plants discriminate more against the heavier ^{13}C resulting in lower $\delta^{13}C$ in comparison to C4 plants. CAM plants have intermediate $\delta^{13}C$, which can be influenced by local environmental conditions (Cerling et al., 1997; Merwe, 1982; Schwarcz & Schoeninger, 1991). C3 plants comprise a majority of plants on the planet including fruits, vegetables, nuts, and grains such as wheat and rice. C4 plants consumed by humans include corn, sugarcane, amaranth, millet, and sorghum. CAM plants are not typically major components of the human diet and include succulents and cacti (Schoeninger & Moore, 1992; Tykot, 2016). Marine plants follow the same photosynthetic pathways as terrestrial plants, but plants in ocean water derive carbon from ocean bicarbonate, which is more enriched in ^{13}C than atmospheric carbon (Schoeninger et al., 1983). Bone and tooth enamel carbonate $\delta^{13}C$ reflects total dietary carbon including protein, lipids, and carbohydrates, while isotope values measured in bone or dentine collagen preferentially reflect carbon isotope ratios from dietary protein (Ambrose & Norr, 1993).

$\delta^{15}N$ Analysis – Bone Collagen

Nitrogen isotope ratios (^{15}N /^{14}N) are similarly expressed using δ-notation ($\delta^{15}N$) with atmospheric air (0‰) as the standard (Deniro & Epstein, 1981). In bone collagen, $\delta^{15}N$ reflects

dietary sources of animal protein. Metabolic fractionation of nitrogen corresponds to the trophic level of an organism: the higher the trophic level, the higher $\delta^{15}N$ (Post, 2002). Additionally, marine resources have higher $\delta^{15}N$ in comparison to terrestrial food resources since the source of nitrogen in marine systems is dissolved nitrogen, which is ~4‰ higher versus atmospheric air (0‰) (Schoeninger & DeNiro, 1984). Anthropogenic sources (e.g. fertilizer, sewage, and animal waste) can increase $\delta^{15}N$ in consumed foods (Kendall et al., 2007). A multi-isotope approach can help to minimize the impact of these inputs when interpreting values. Detailed isotopic laboratory methods are discussed in the supplementary material.

Identified Mecklenburg John Doe 2021

Case Background

Human remains in a state of advanced decomposition were discovered in a wooded area in Mecklenburg County, North Carolina in June of 2021. Based on anthropological analysis conducted at NCSU in June of 2022, the decedent was estimated to be a 30–50-year-old European-American male, with a mean stature of 5 feet 5 inches (Hartnett, 2010b, 2010a; Jantz & Ousley, 2005; Slice & Ross, 2024). The hair-on-end appearance or the perpendicular trabecular proliferation resulting from severe anemias was visible on the postmortem radiographic images (Figure 2) (Martin & Rackard, 2016). No perimortem trauma was observed on the remains available for analysis. Bone samples were selected for DNA extraction and sequencing, and isotopic analyses (87/86Sr, δ13C, δ15N) in 2022.

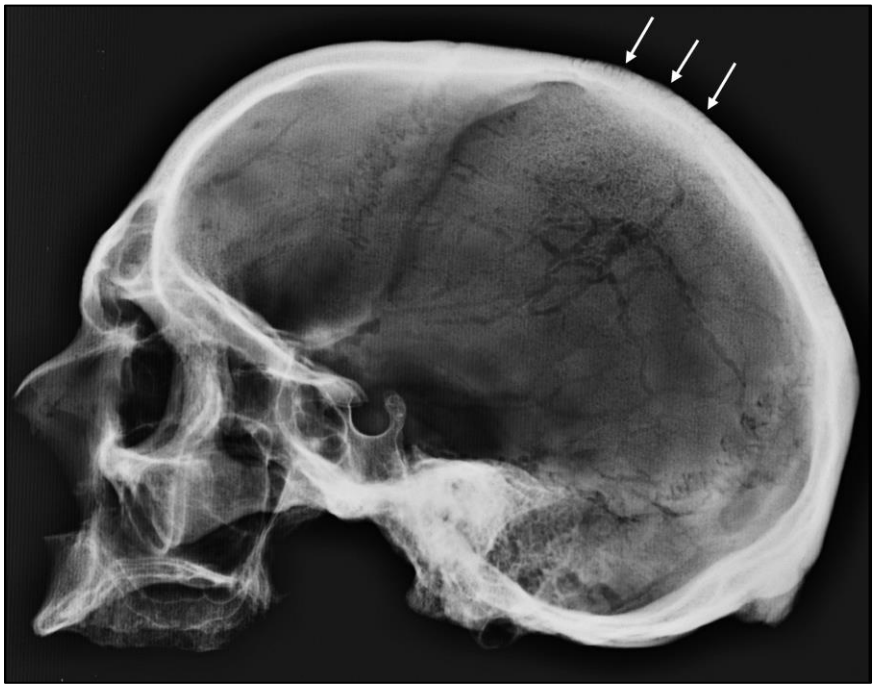

Figure 2 Lateral radiograph of the cranium of Identified Mecklenburg John Doe 2021 showing *hair-on-end* appearance (arrows) indicative of anemia.

Bone Apatite ($^{87/86}Sr$) for Recent Geographic Movement

Bone apatite cannot confirm natal origin but reflects recent movements. The strontium ($^{87/86}Sr$) isotope value of the bone sample (0.708307) is consistent with modern Americans (Table 1) (Keller et al., 2016; Lustig, 2013; Regan, 2006). Bioavailable strontium isoscapes indicate the strontium values are consistent with the southeast region of the US (Bataille et al., 2020; Chesson et al., 2012). Additionally, strontium isotopes have been shown to vary across the continental US, and used alone may not be useful in establishing recent movements (Keller et al., 2016).

Table 1 Isotope ratios from measured osteological samples.

	Material	**$^{87/86}$Sr**	**δ^{18}O (‰ VPDB)**	**δ^{13}C (‰ VPDB)**	**$\delta\ ^{13}C_{coll}$ (‰)**	**$\delta\ ^{15}$N (‰)**
Identified Mecklenburg John Doe	Bone	0.708307	-----	----	-15.98	10.05
Unidentified Mecklenburg Jane Doe 2011	Tooth enamel	0.706827	-2.01	-7.10	----	----
	Bone	0.708043	----	----	-13.41	10.97
Identified Mecklenburg John Doe 1987	Tooth enamel	0.708905	-4.22	-8.93	----	----

Bone Collagen $\delta^{13}C$, $\delta^{15}N$ for Diet Markers

Carbon ($\delta^{13}C$) and nitrogen ($\delta^{15}N$) values reflect locally available dietary sources (Ambrose & Norr, 1993; Deniro & Epstein, 1981) . The $\delta^{13}C$ from the bone collagen is consistent with a C_4-based diet observed in US populations (-15.98‰) (Bartelink et al., 2014).

Investigative Genetic Genealogy (IGG)

A relative reported a first cousin was missing in January of 2023, whose profile matched the Mecklenburg County John Doe. Using DNA kits from private genealogy databases, familial matches from the first cousin who submitted the missing person's report, and subsequently a biological son of the potential decedent, were used to positively identify the Mecklenburg County John Doe.

Summary

The decedent was positively identified via IGG in March of 2023. He was originally from South Carolina and was known to live on the streets of Charlotte. Anthropological analyses along with isotopic analyses are consistent with the demographic information provided in the missing person's report, and these analyses were used as a road map for IGG.

Unidentified Mecklenburg Jane Doe 2011

Case Background

An incomplete set of skeletal remains was discovered by the Department of Transportation (DOT) workers in a wooded area of Mecklenburg County, North Carolina in March 2011. Forensic anthropological analyses were conducted as part of the cold case initiative at NCSU in March of 2024. The decedent was estimated to be a 23–49-year-old Mesoamerican female using the software 3D-ID and web-based system rASUDAS (González-Colmenares et al., 2007; Lamendin et al., 1992; Scott et al., 2018; Slice & Ross, 2024). Extensive carnivore

scavenging was present throughout the postcranial elements. There are dark gray dental amalgam fillings on the left and right mandibular first molars. A mandibular incisor and a rib were selected for isotopic analyses ($^{87/86}$Sr, δ^{18}O, δ^{13}C, δ^{15}N) in 2022.

Enamel and Bone Apatite Dual Isotopic ($^{87/86}Sr$, $\delta^{18}O$, $\delta^{13}C$) Signatures for Geographic Origin

The strontium ($^{87/86}$Sr) and oxygen (δ^{18}O) data are consistent with geographic origin outside of the US (Table 1) (C. Juarez, 2011; Keller et al., 2016; Laffoon et al., 2013; Lustig, 2013; Regan, 2006; Wright, 2005). Using data from Keller et al. (2016), Laffoon et al. (2012), Juarez (2011), and Wright (2012) of US Cadets, Circum-Caribbean born, modern Mexican-born, and Guatemalan-born individuals, respectively, the measured values from the tooth enamel cluster on a bivariate graph with the Mesoamerican and Caribbean born group for strontium (0.7068), oxygen (-2.01‰), and the Caribbean group for oxygen and carbon (-7.10‰) (Figures 3, 4) (C. Juarez, 2011; Keller et al., 2016; Laffoon et al., 2013; Wright, 2005). Measured strontium values between enamel (0.706827) and bone apatite (0.708043) vary, with the observed bone apatite value trending closer to the normal range of modern Americans (Lustig, 2013). Based on remodeling rates of ribs, these results suggest the decedent relocated to the US within the last 5-10 years of their life (Cox & Sealy, 1997).

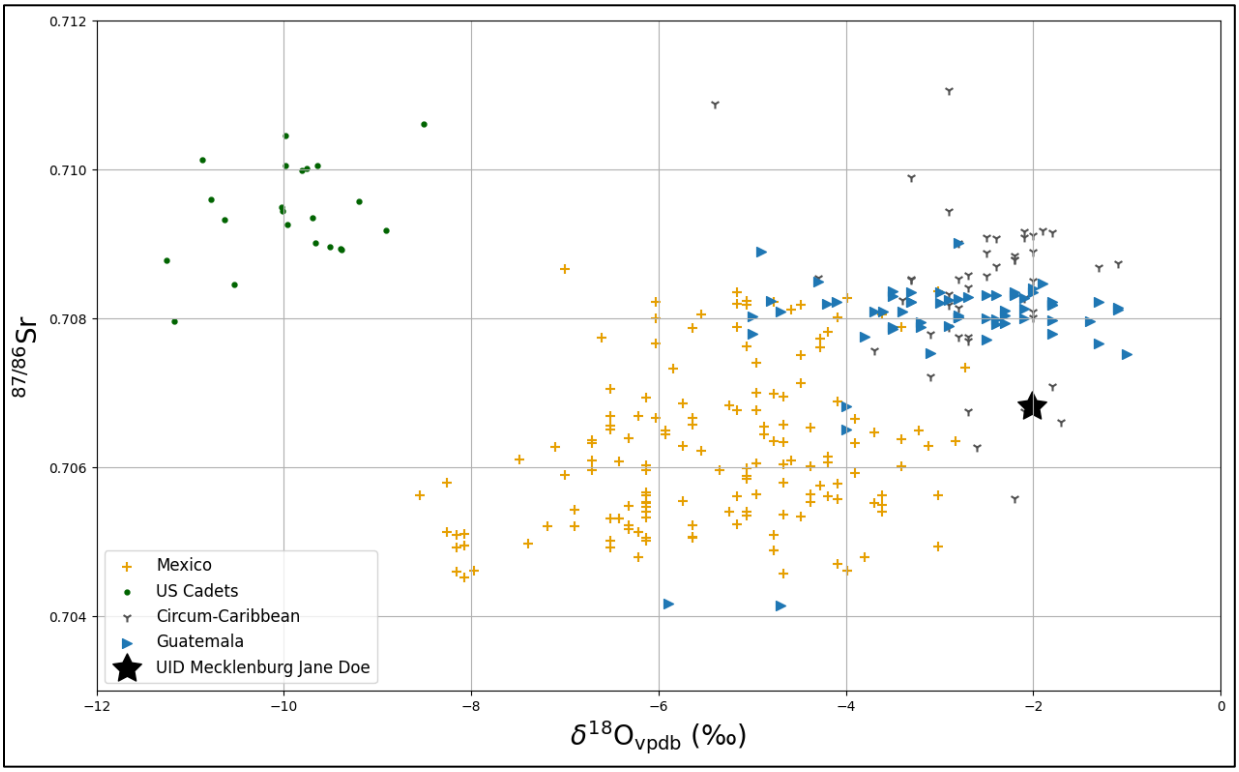

Figure 3 $\delta^{18}O_{vpdb}$ values vs. $^{87/86}Sr$ of Unidentified Mecklenburg Jane Doe plotted against known samples from regions within the US and known samples from Mesoamerica and the Circum-Caribbean (C. Juarez, 2011; Keller et al., 2016; Laffoon et al., 2013; Wright, 2005).

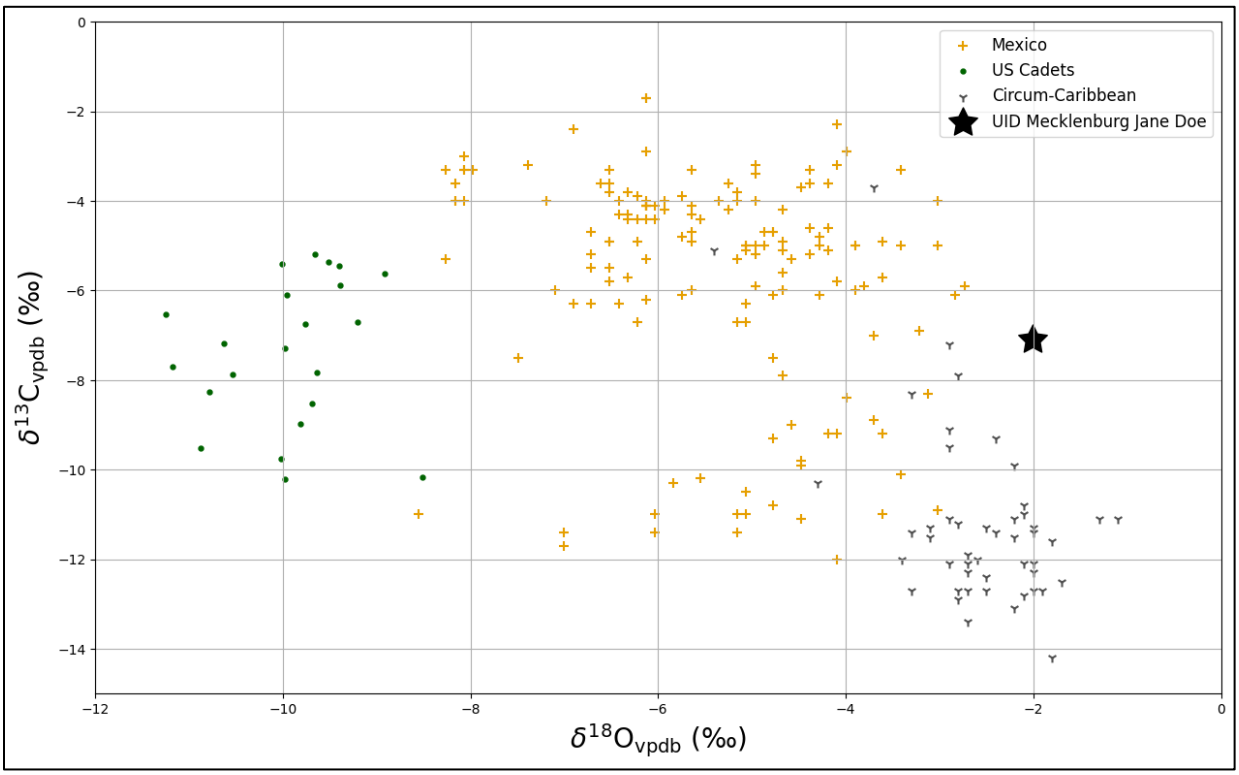

Figure 4 $\delta^{18}O_{vpdb}$ values vs. $\delta^{13}C_{vpdb}$ of Unidentified Mecklenburg Jane Doe plotted against known samples from regions within the US and known samples from Mesoamerica and the Circum-Caribbean (C. Juarez, 2011; Keller et al., 2016; Laffoon et al., 2013; Wright, 2005).

Enamel and Bone Collagen Isotopic Signatures for Diet and Identity ($\delta^{13}C$, $\delta^{15}N$)

Measured $\delta^{13}C$ from both bone collagen (-13.41‰) and tooth enamel (-7.10‰) are more enriched than a typical US diet, consistent with a higher proportion of C4 plants (namely corn and corn products) in the diet during childhood and in recent decades (Bartelink et al., 2018). Marine diets and oceanic environments also affect dietary isotopic values of carbon and nitrogen (Christensen et al., 2014). When plotted on a bivariate graph, the bone sample clusters with Circum-Caribbean samples with oceanic or marine contributions to diet (Figure 5) (Christensen et al., 2014; Keegan & DeNiro, 1988).

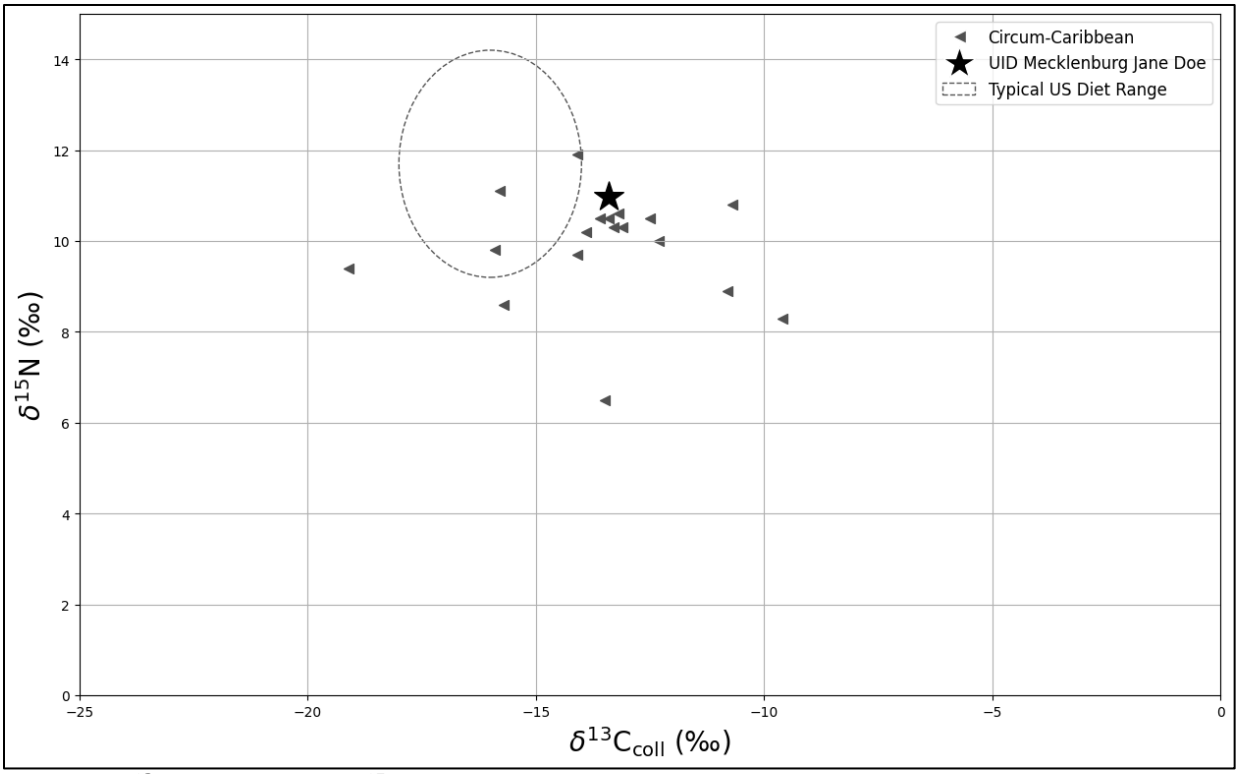

Figure 5 $\delta^{13}C_{coll}$ values vs. $\delta^{15}N$ from bone collagen of Unidentified Mecklenburg Jane Doe plotted against observed range of the US American diet and known samples within the Mesoamerica and the Circum-Caribbean (Christensen et al., 2014; Keegan & DeNiro, 1988).

Summary

The decedent remains unidentified. The enamel isotopic results suggest the decedent was born in the Circum-Caribbean or Mesoamerican regions and bone apatite signatures suggest they had recently relocated to North Carolina within the last 5-10 years. The assessment of population affinity using modern techniques (e.g., 3D-ID and rASUDAS) was consistent with isotopic results. This individual is most likely undocumented and will be triaged for IGG.

Identified Mecklenburg John Doe 1987

Case Background

A cranium was recovered in Mecklenburg County, North Carolina from a creek bed. Forensic anthropological analysis was conducted at NCSU in January of 2024. Population affinity was estimated to be a male of West African/Nigerian origin using 3D-ID software, with a

posterior probability of 0.8364 and a typicality of 0.0422 (Slice & Ross, 2024). The typicality probability is low, meaning that the decedent is not well represented within the reference samples of the software. Bomb pulse dating was applied to confirm the antiquity of the remains and rule out historical origin. The second maxillary premolar was used to estimate the year of birth, which was estimated to be around 1955 and to estimate an age-at-death range of 30-40 years old(Johnstone-Belford & Blau, 2020). No trauma or pathologies were noted on the cranium. A right 1st maxillary premolar was selected for isotopic analyses ($^{87/86}$Sr, δ^{18}O δ^{13}C) in 2022. A maxillary premolar was selected for bomb pulse dating in 2023.

Enamel Dual Isotopic ($^{87/86}$Sr, δ^{18}O) Signatures for Geographic Origin

The strontium ($^{87/86}$Sr) and oxygen (δ^{18}O) data are consistent with geographic origin within North America (Table 1) (Keller et al., 2016; Lustig, 2013; Regan, 2006). Using data from Keller et al. 2016 of US Cadets, the measured oxygen and strontium values from the enamel cluster on the bivariate graph on the edge of the Southeast region of the United States (Figure 6). These values are consistent with the area where the remains were recovered. When considering population affinity estimation, data from Keller et al. (2016) of US cadets, Schroeder et al. (2009) for Barbadian-born and African-born individuals, and Laffoon et al. (2012) for Circum-Caribbean born individuals, the decedent clusters between the US and the Caribbean-born group for strontium (0.708905), oxygen (-4.22‰), and carbon (-8.93‰) (Figures 7, 8) (Keller et al., 2016; Laffoon et al., 2013; Schroeder et al., 2009). However, other regions of origin within North America cannot be ruled out.

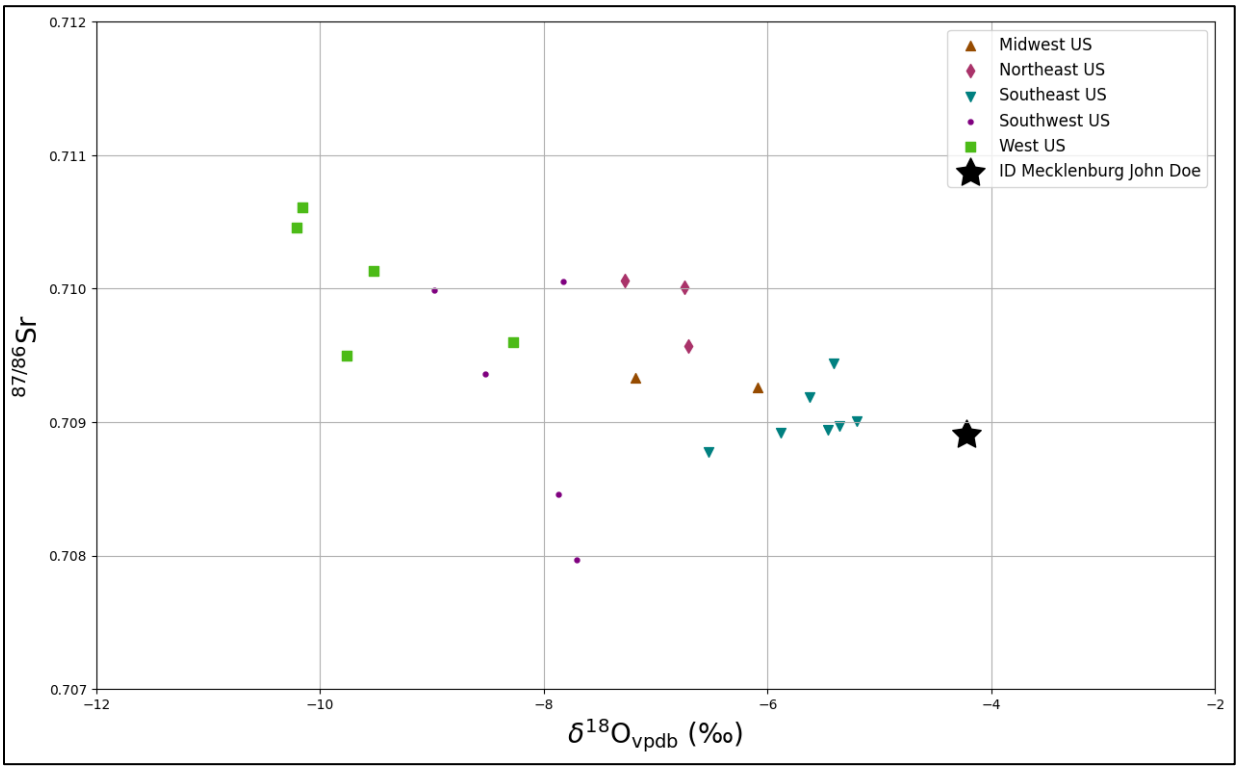

Figure 6 $\delta^{18}O_{vpdb}$ values vs. $^{87/86}Sr$ of Identified Mecklenburg John Doe plotted against known samples from regions within the US (Keller et al., 2016).

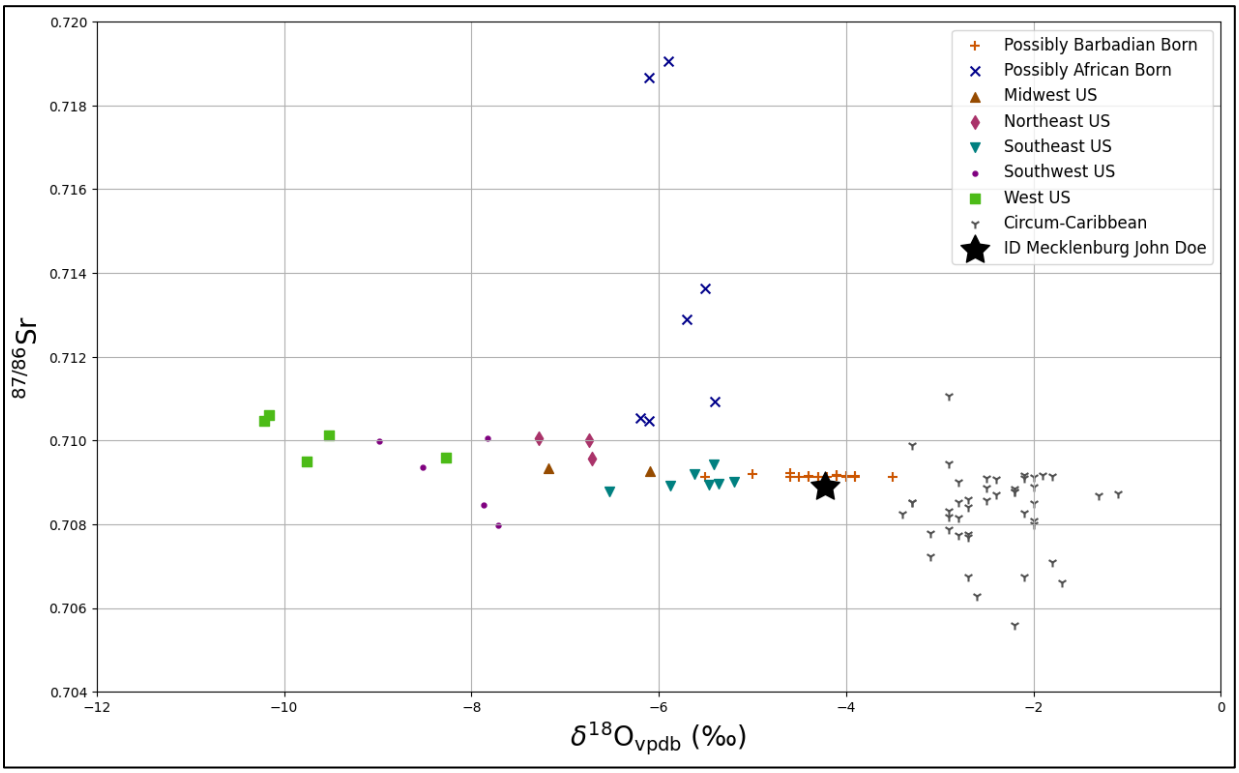

Figure 7 $\delta^{18}O_{vpdb}$ values vs. $^{87/86}Sr$ of Identified Mecklenburg John Doe plotted against known samples from regions within the US, known samples from the Circum-Caribbean and, possibly Barbadian-born and African-born individuals (Keller et al., 2016; Laffoon et al., 2013; Schroeder et al., 2009).

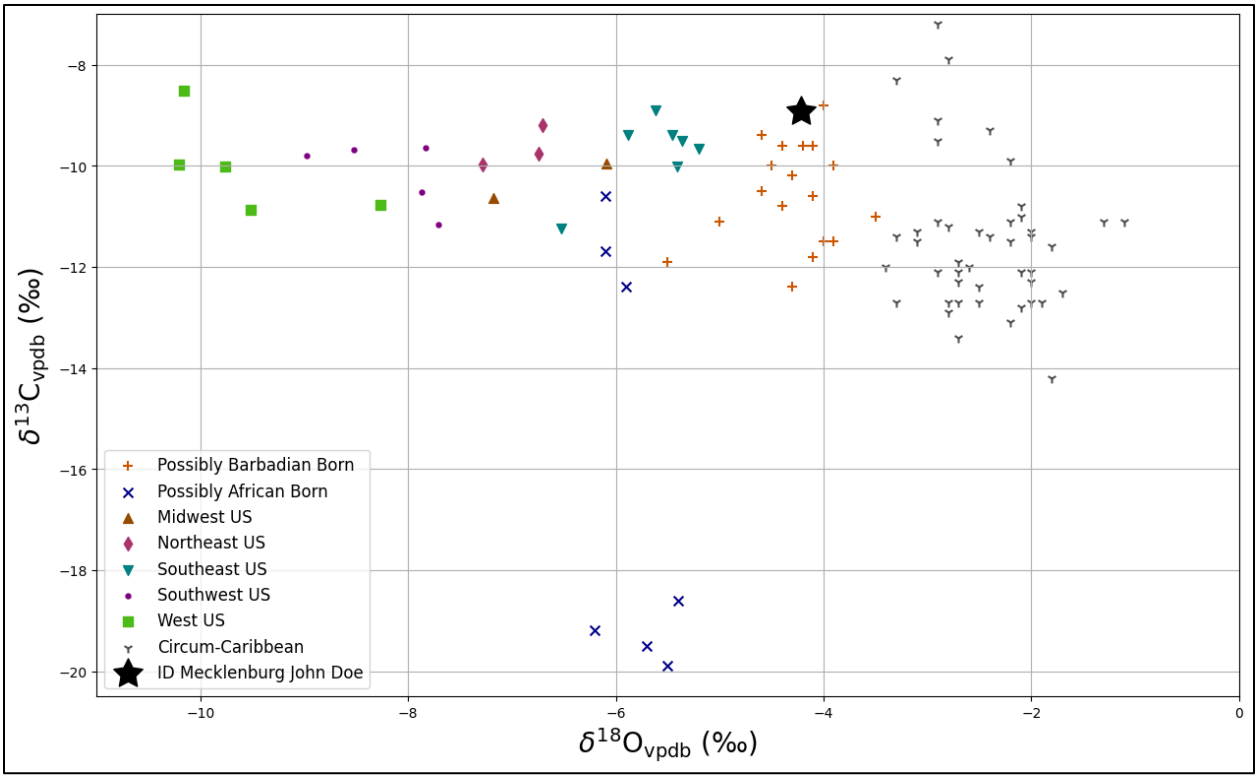

Figure 8 $\delta^{18}O_{vpdb}$ values vs. $\delta^{13}C_{vpdb}$ of Identified Mecklenburg John Doe plotted against known samples from regions within the US, known samples from the Circum-Caribbean and, possibly Barbadian-born and African-born individuals (Keller et al., 2016; Laffoon et al., 2013; Schroeder et al., 2009).

Investigative Genetic Genealogy (IGG)

This individual was identified in May 2024 via IGG. Estimates of year-of-birth and West African origin aided in the direction of the IGG investigation.

Summary

The decedent was positively identified via IGG. The family confirmed the age-at-death when he went missing in 1987, the family's West African origin, and that he was born in the Charlotte, NC area. Anthropological analyses and isotope results are consistent with the information provided by the family. However, the isotope results were broadly consistent with this finding, and could not be used to narrow down a region of origin more specific than North America.

Discussion

The human right to personal identity is internationally recognized through various declarations and conventions (e.g., United Nations Convention on the Rights of the Child, Article 8). According to the FBI's National Crime Information Center (NCIC) statistics, there were 8,415 records of unidentified persons in 2021. NamUs states that our missing and unidentified are the nation's silent mass disaster. NamUs lists 158 unidentified persons in the state of North Carolina with over 100 being skeletonized with national estimates of 4,400 unidentified bodies recovered each year (Hickman et al., 2007). However, this is likely an underestimate as the data in this reference are almost twenty years old (Ross & Passalacqua, 2024). Further complicating identifications, foreign-born and undocumented migrants pose unique challenges as conventional identification tools such as familial DNA reference databases target U.S. citizens (Kramer et al., 2020). While the ability to solve these cases is multifactorial, information regarding the region of origin using modern tools such as 3D-ID (Slice & Ross, 2024) and isotopic analyses (Kimmerle et al., 2010; Kramer et al., 2020) is critical to estimating the place of origin. Anthropological analyses draw on modern population affinity techniques such as rASUDAS and 3D-ID. Historical events, gene flow, and migration have shaped similarities and differences observed in modern populations, and population affinity is a statistical approach to examining skeletal variation without the use of racial and typological axioms (Ross & Pilloud, 2021). When combined with isotopic analyses, such as presented in this multidisciplinary approach, an individual's place of origin can be more confidently estimated. However, both population affinity and isotopic analyses rely on reference populations and reference data with which to compare individual measurements or values. Continued collection and publication of these data is essential to obtain global coverage.

Applying these methods requires a systematic process to determine which method(s) to apply to each case (Figure 9). Initially, skeletonized remains undergo anthropological analyses, utilizing current methods of estimating the biological profile, trauma, and/or pathologies (González-Colmenares et al., 2007; Hartnett, 2010b, 2010a; Jantz & Ousley, 2005; Lamendin et al., 1992; Scott et al., 2018; Slice & Ross, 2024). In cases where taphonomic or postmortem alteration is minimal, there is a higher likelihood that further analyses (i.e., DNA or isotope analyses) will yield viable results. Bone and tooth samples are selected and sent to State and private laboratories for DNA and isotope analyses. When the circumstances of discovery are not straightforward, radiocarbon bomb-pulse dating can be used to establish antiquity and forensic significance. Ultimately, the application of these methods still may not provide an identification. The last method applied is IGG, which draws on all previous analyses in genealogical research. IGG is very costly, relying on grant and law enforcement funding and is used as a last resort with cases being prioritized based on the preservation of remains, circumstances of death, and investigative information.

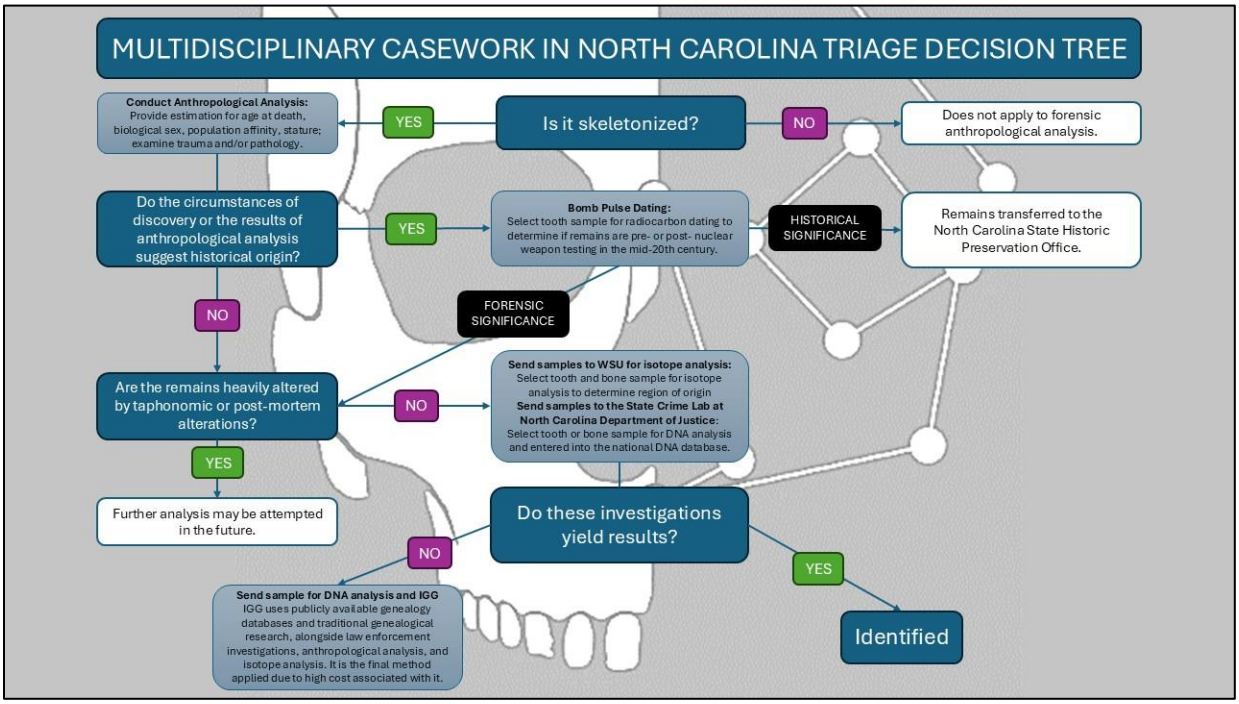

Figure 9 Decision tree demonstrating the process of applying various methods to current cases of unidentified remains and to cold case re-examination. These analyses are completed under grant and law enforcement funding at the North Carolina State University Human Identification and Forensic Analysis Laboratory.

Conclusion

The cases outlined in this report utilize a collaborative approach to casework, leading to the successful identification of several decedents, including the two outlined above. Where investigations are ongoing, input from anthropological and isotopic analyses can now be considered in further evaluations and methods, such as IGG. This multidisciplinary approach to forensic casework in North Carolina continues to inform investigators in cold case reanalysis and is the first step in addressing the cold caseload within the state.

CHAPTER 6

DISCUSSION

The application of isotope analyses to forensic casework in North Carolina must account for the taphonomic effects specific to the region's climate, assess the accuracy of spatial isotopic models for geolocation, and determine the methods of applying stable isotope analysis in prioritizing cases for identification. Unidentified skeletal remains have often been exposed to taphonomic elements for extended periods of time long after decomposition has been completed. This prolonged exposure results in various forms of physical damage to the bones including corrosion, plant root intrusion, postmortem fracturing, carnivore scavenging, and rodent gnawing, among other taphonomic effects (Pokines et al., 2013). The resulting remains present challenges for traditional anthropological techniques, as the skeletal remains may be incomplete, or damaged, and identifying information may be lost. Given these limitations, isotope analysis serves as a valuable alternative by offering a chemical approach to examining bone and teeth. However, to rely confidently on isotopic data in forensic contexts, it is critical to understand how local taphonomic conditions might alter these chemical signatures. Recognizing the conditions in which these values may be affected ensures more accurate interpretation and strengthens the reliability of this method in forensic identification efforts.

In Chapter Three, we examined how taphonomic processes can affect the C:N ratio, and the $\delta^{13}C$ and $\delta^{15}N$ values in juvenile *Sus scrofa domesticus* bone collagen. Postmortem alterations, driven by environmental factors such as temperature, moisture, and microbial activity, can influence the integrity of isotopic signals and potentially bias interpretations. This is especially concerning when such data are used in applied settings, such as reconstructing diet or assessing geographic origin. It is therefore essential to implement preventative measures to

mitigate these effects and ensure analytical reliability. One such measure is the use of established collagen pretreatment protocols (DeNiro & Epstein, 1978; Szpak et al., 2017; van Klinken & Hedges, 1995). These methods are designed to remove humic substances, lipids, and other contaminants that are present in modern bone and have been shown to minimize external influences on $\delta^{13}C$ and $\delta^{15}N$ values in bone collagen. Results from Chapter Three support the continued use of these protocols when interpreting isotopic values from modern bone, particularly under the depositional environments examined. Applying these standardized procedures allows researchers to have greater confidence that the isotopic signals recovered are biologically meaningful rather than taphonomically altered. In addition to confirming the utility of pretreatment methods, the results of Chapter Three also contributed to our broader understanding of how environmental conditions affect preservation.

The taphonomic conclusions drawn from the isotope analyses in Chapter Three were consistent with findings from previous studies that used other techniques to assess bone degradation (Hale & Ross, 2023; Ross & Hale, 2018). Similar conditions found in hot, wet, and humid seasons, characteristic of North Carolina seasons, were associated with more severe taphonomic effects, leading to the degradation of bone collagen early in the postmortem period. These findings are consistent with broader taphonomic research, which has long recognized that warm and moist environments can significantly impact the preservation of organic components in skeletal remains (Jans, 2021; Turner-Walker, 2007; Turner-Walker et al., 2023). Although the sample size in this study was relatively small, the consistency between our findings and those of previous research strengthens the validity of the conclusions. Future research with larger sample sizes and broader environmental sampling could clarify the extent and mechanisms of these

taphonomic effects, offering more refined guidance for isotopic interpretation in forensic contexts.

In Chapter Four, we learned that the theoretical $^{87/86}Sr$ and $\delta^{18}O$ isotopic trends are evident and related to the physiography of North Carolina. The interpretation of isotopic values from tooth and bone for geolocation relies heavily on the accuracy and resolution of existing spatial isotopic models. In North Carolina, the state's topography and underlying geology provide a strong basis for developing predictable isoscapes for both $^{87/86}Sr$ and $\delta^{18}O$ isotopic values. Because $\delta^{18}O$ values become increasingly depleted in the heavier isotope (^{18}O) with rising elevation, the rising elevation from the Atlantic Coastline in the east to the Blue Ridge Mountains in the west allows for a predictable spatial patterning of $\delta^{18}O$ values across the state. Similarly, the geology of North Carolina follows a roughly east-to-west pattern of variation, with distinct geological provinces contributing to predictable regional variation in $^{87/86}Sr$ ratios based on bedrock composition. Despite these natural patterns, the quality and resolution of the resulting isosocape are only as strong as the data used to construct it (de Oliveira Mascarenhas et al., 2022; Laffoon et al., 2013).

Currently, the dual isotopic $^{87/86}Sr$ and $\delta^{18}O$ isoscapes produced in Chapter Four would benefit from additional testing, and possibly additional water samples, particularly from more populous regions within the state. These regions include Charlotte, Raleigh, and Greensboro, which are critical zones of human activity and are in the counties from which most of the forensic casework originates, particularly those of cold cases, or recently recovered unidentified individuals. Furthermore, the incorporation of additional human enamel samples into the model from individuals of known origin would significantly improve the applicability and accuracy of the model in forensic investigations. This added resolution could enhance confidence in isotopic

assignment, particularly in regions where isotopic variation is less distinct or more difficult to interpret. Additionally, temporal relationships between municipal water sources, and an individual's life history, should also be considered. We demonstrated that the tap water input was not appropriate to use in MecklenburgID, whose water source was likely not that of the modern municipal sources which reflect enriched $\delta^{18}O$ values than other sources of drinking water.

In Chapter Four, these patterns generally hold true. Importantly, the results suggest that the isoscape should not be interpreted in isolation or as a definitive exclusionary tool. For instance, although the remains of the individual in one case study were recovered in Mecklenburg County, the isotopic results did not align with that location when tested in our model. However, excluding the region based solely on the model would not have been appropriate without considering additional lines of evidence, such as contextual, biological, or circumstantial information. Once we excluded the tap water values from the model, the prediction interval included the correct region of origin. This highlights the need for a cautious and integrative approach to interpreting isoscape data in forensic settings. The models' current limitations are particularly evident in the densely populated counties that generate the majority of forensic casework in the state. Ongoing refinement and validation will help ensure the model can better support investigative and identification forensic efforts throughout North Carolina.

In Chapter Five, we demonstrated how isotopic analyses can enhance casework by offering additional data points to guide the next steps in the identification process. Isotopic information helps determine whether a case meets certain conditions, such as a likely US origin, that increase the likelihood of successful identification via forensic genetic genealogy (FGG). This method is not intended to create a hierarchy of importance among cases, nor to suggest that those without initial isotopic or anthropological alignment are less deserving of identification.

Rather, it offers a data-informed process to determine which cases may benefit most immediately from high-investment techniques.

The application of stable isotope analysis can significantly contribute to identification efforts, particularly when integrated into a broader multidisciplinary approach (Chesson, 2014; Kramer & Bartelink, 2022). Isotopic data, when used alongside anthropological assessments, can inform a decision-making process aimed at prioritizing cases that are most likely to yield a positive identification using methods outlined in the standard operating procedure of the Human Identification and Forensic Analysis Laboratory at NCSU. This approach supports the efficient use of resources, especially guiding whether a case may benefit from more complex and costly techniques, such as FGG. The importance of triaging cases lies not in limiting analytical scope, but in maximizing the likelihood of success based on information gathered from preliminary analyses. In practice, FGG relies on comparative databases that are primarily composed of genetic data from individuals residing in the United States (Glynn, 2022). These databases have grown largely through commercial testing and advertisement aimed at connecting individuals with their ancestral roots. Therefore, individuals whose anthropological profiles or isotopic signatures suggest a region of origin outside the US may not be well represented in these databases, reducing the chances of a genetic match. In such cases, applying FGG prematurely may exhaust valuable resources with limited results. Instead, alternative investigative methods may be more appropriate. While the ideal scenario would involve unlimited funding and time to analyze every unidentified case to its fullest extent, this is not the reality faced by most medicolegal jurisdictions. The staggering number of unresolved unidentified skeletal remains only continues to rise, creating a backlog that makes strategic triage a practical approach (Ritter et al., 2007).

Since implementing this multidisciplinary approach, eleven out of seventeen cases have yielded positive identifications, six of which had isotopic analyses conducted prior to the application of further methods (Long, 2025). These results support the efficacy of this integrative approach. Forensic anthropology, by nature, is a multidisciplinary field, drawing from biological, anthropological, medical, and chemical sciences to piece together the identity of the unknown. Incorporating stable isotope analysis into this toolkit not only extends the reach of traditional anthropological methods but also enhances the ability to make informed, strategic decisions. Embracing multidisciplinary and strategic approaches will be essential to addressing the growing number of unidentified cases and refining the process for identification of unknown decedents.

Together, the three main chapters of this dissertation demonstrate the value of applying multidisciplinary methods to forensic casework in North Carolina, with a particular focus on stable isotope analysis as a tool for data interpretation and a strategic tool in case management. In Chapter Three, the effects of taphonomic processes on bone collagen were explored, emphasizing the need for the examination of conditions of taphonomic alteration and consideration of environments where pretreatment methods may help to curb this alteration. Chapter Four built upon this foundation by evaluating the effectiveness of spatial isotopic models for strontium and oxygen across the state, revealing the promise and the current limitations of isoscapes for geolocation. This was evident in densely populated areas, and further testing of these models could help to clarify and enhance these issues. Finally, Chapter Five applied these methods into a practical decision-making framework, where isotopic analyses play a critical role in triaging cases for further investigation, including forensic genetic genealogy. Collectively, these chapters demonstrate how isotopic methods, when informed by regional context, environmental conditions, and broader investigative goals, enhance the understanding of

postmortem change, improve region of origin estimations, and improve the efficiency and success of identification efforts in forensic contexts.

CHAPTER 7

CONCLUSION

The current research serves as a starting point for future research exploring the application of isotope analysis to forensic casework in North Carolina. Firstly, one key area for further exploration is the impact of taphonomic processes on isotopic values in bone collagen. Understanding these effects is critical for improving the accuracy of isotopic interpretations in forensic contexts. One way to examine this would be to test the effectiveness of pretreatment protocols. Future studies could apply approved pretreatment methods and compare between treated and untreated samples from Chapter Three. Hypothetically, the treated samples will show less isotopic variation, as the pretreatment would reduce isotopic variability introduced by taphonomic alteration. Confirming this hypothesis would advance the understanding of how early taphonomic processes influence isotopic values in bone collagen, thus addressing a challenge in forensic analysis.

Additionally, comparing measured values between different tissues such as collagen, bone carbonate, and dental enamel, could help clarify how each tissue type is affected by seasonal deposition and burial conditions. This would contribute to a more nuanced and detailed understanding of the specific processes and impacts that taphonomic processes have on isotopic values, highlighting how different tissues respond to postmortem changes across environments. To refine this understanding, future research could focus on more specific environmental variables present in the depositional environment. Physical and temporal variables, such as soil type, humidity, temperature, etc., could be investigated to better characterize the environments and the resulting effects on isotopic values observed between seasons and depositions.

Examining environmental data more closely offers a more accurate depiction of how taphonomic processes alter bone collagen and other tissues.

Future studies could combine isotopic analysis of collagen with other measures of taphonomic alteration, for example, the measures of macro- and microscopic alterations alongside molecular techniques, such as amino acid profiling, could offer a more comprehensive picture of postmortem changes to skeletal remains. Comparing these results between seasons and depositions allows for an investigation into the depositional seasons and environments that affect the preservation of skeletal remains. Understanding these alterations is essential for constructing accurate forensic timelines, as well as reliance upon isotopic data from tissues when deposited in environments linked to skeletal degradation. Continued research will help build upon existing literature and refine methodologies for interpreting isotopic data in forensic anthropology.

On a broader scale, spatial models of isotopic distribution from water sources in North Carolina need to be tested with more known samples from individuals with confirmed regions of origin. This will help assess the accuracy of current models and identify and clarify potential gaps. If the model continues to exclude the true region of origin from certain regions, the model could be further enhanced in these regions with the addition of water samples with Sr and O measurements from drinking water sources, particularly from populous counties. While using enamel-based isoscapes for comparison remains the most reliable method, challenges related to adequate sampling from across the study area exist. Regardless, testing multiple isoscapes constructed with different datasets would offer a more robust understanding of how to spatially model isotopes for forensic purposes. Given the diverse approaches used to construct isoscapes in other regions globally, a unique approach for North Carolina could involve combining both dental enamel and drinking water isotope data in the dual-isotope model.

Furthermore, it would be beneficial to enhance and apply good practice guides for the measurement and interpretation of isotopic values in forensic cases (P. J. H. Dunn & Carter, 2018). This guide should emphasize that isotopic data should be used alongside other laboratory protocols whenever possible to ensure a more complete and accurate analysis. In cases where postmortem alteration has resulted in sparse or damaged remains, isotopic analysis could still be considered, but the interpretation should not exclude other sources of information. The region of recovery should remain a primary consideration when hypothesizing about an individual's origin, as it is often the simplest and most plausible explanation.

Stable isotope analysis has already shown promise in forensic casework in North Carolina, particularly when a part of a multidisciplinary approach. This method has proven effective in triaging cases for forensic genetic genealogy, allowing for the prioritization and classification of cases for further analysis and investigations. Through collaboration with law enforcement agencies and crime labs nationwide, this approach has helped investigators make positive identifications. Furthermore, data from identified individuals with a confirmed region of origin is continually being compiled, which will contribute to refining future spatial isotope models and enhance our understanding of human isotopic tissue composition. Ultimately, the goal of forensic anthropology is to assist in identification, a basic human right, and stable isotope analysis is a tool that can strengthen this process.

REFERENCES

Åberg, G. (1995). The use of natural strontium isotopes as tracers in environmental studies. *Water, Air, and Soil Pollution*, *79*(1), 309–322. https://doi.org/10.1007/BF01100444

Aggarwal, J., Habicht-Mauche, J., & Juarez, C. (2008). Application of heavy stable isotopes in forensic isotope geochemistry: A review. *Applied Geochemistry*, *23*(9), 2658–2666. https://doi.org/10.1016/j.apgeochem.2008.05.016

Allègre, C. J., Manhès, G., & Göpel, C. (1995). The age of the Earth. *Geochimica et Cosmochimica Acta*, *59*(8), 1445–1456. https://doi.org/10.1016/0016-7037(95)00054-4

AlQahtani, S. J., Hector, M. P., & Liversidge, H. M. (2010). Brief communication: The London atlas of human tooth development and eruption. *American Journal of Physical Anthropology*, *142*(3), 481–490. https://doi.org/10.1002/ajpa.21258

Ambrose, S. H. (1986). Stable carbon and nitrogen isotope analysis of human and animal diet in Africa. *Journal of Human Evolution*, *15*(8), 707–731. https://doi.org/10.1016/S0047-2484(86)80006-9

Ambrose, S. H. (1990). Preparation and characterization of bone and tooth collagen for isotopic analysis. *Journal of Archaeological Science*, *17*(4), 431–451. https://doi.org/10.1016/0305-4403(90)90007-R

Ambrose, S. H. (1991). Effects of diet, climate and physiology on nitrogen isotope abundances in terrestrial foodwebs. *Journal of Archaeological Science*, *18*(3), 293–317. https://doi.org/10.1016/0305-4403(91)90067-Y

Ambrose, S. H., & Norr, L. (1993). Experimental Evidence for the Relationship of the Carbon Isotope Ratios of Whole Diet and Dietary Protein to Those of Bone Collagen and Carbonate. In J. B. Lambert & G. Grupe (Eds.), *Prehistoric Human Bone: Archaeology at the Molecular Level* (pp. 1–37). Springer. https://doi.org/10.1007/978-3-662-02894-0_1

Ammer, S. T. M., Bartelink, E. J., Vollner, J. M., Anderson, B. E., & Cunha, E. M. (2020). Spatial Distributions of Oxygen Stable Isotope Ratios in Tap Water From Mexico for Region of Origin Predictions of Unidentified Border Crossers. *Journal of Forensic Sciences*, *65*(4), 1049–1055. https://doi.org/10.1111/1556-4029.14283

ArcGIS Pro [version 3.3] (Version 3.3). (2024). [Computer software]. ESRI.

Balzer, A., Gleixner, G., Grupe, G., Schmidt, H.-L., Schramm, S., & Turban-Just, S. (1997). In Vitro Decomposition of Bone Collagen by Soil Bacteria: The Implications for Stable Isotope Analysis in Archaeometry. *Archaeometry*, *39*(2), 415–429. https://doi.org/10.1111/j.1475-4754.1997.tb00817.x

Bartelink, E. J., Berg, G., Beasley, M., & Chesson, L. (2014). Application of stable isotope forensics for predicting region of origin of human remains from past wars and conflicts. *Annals of Anthropological Practice*, *38*. https://doi.org/10.1111/napa.12047

Bartelink, E. J., Berg, G. E., Chesson, L. A., Tipple, B. J., Beasley, M. M., Prince-Buitenhuys, J. R., MacInnes, H., MacKinnon, A. T., & Latham, K. E. (2018). *Chapter 15—Applications of Stable Isotope Forensics for Geolocating Unidentified Human Remains From Past Conflict Situations and Large-Scale Humanitarian Efforts* (K. E. Latham, E. J. Bartelink,

& M. Finnegan, Eds.; pp. 175–184). Academic Press. https://doi.org/10.1016/B978-0-12-805429-1.00015-6

Bartelink, E. J., & Chesson, L. A. (2019). Recent applications of isotope analysis to forensic anthropology. *Forensic Sciences Research*, *4*(1), 29–44. https://doi.org/10.1080/20961790.2018.1549527

Bartelink, E. J., Chesson, L. A., Tipple, B. J., Hall, S., & Kramer, R. T. (2020). *Multi-isotope approaches for region-of-origin predictions of undocumented border crossers from the US–Mexico border* (pp. 369–384). https://doi.org/10.1002/9781119482062.ch24

Bartelink, E. J., MacKinnon, A., Prince-Buitenhuys, J., Tipple, B., & Chesson, L. (2016). Stable Isotope Forensics as an Investigative Tool in Missing Persons Investigations. In *Handbook of Missing Persons* (pp. 443–462). https://doi.org/10.1007/978-3-319-40199-7_29

Bataille, C. P., & Bowen, G. J. (2012). Mapping 87Sr/86Sr variations in bedrock and water for large scale provenance studies. *Chemical Geology*, *304–305*, 39–52. https://doi.org/10.1016/j.chemgeo.2012.01.028

Bataille, C. P., Crowley, B. E., Wooller, M. J., & Bowen, G. J. (2020). Advances in global bioavailable strontium isoscapes. *Palaeogeography, Palaeoclimatology, Palaeoecology*, *555*, 109849. https://doi.org/10.1016/j.palaeo.2020.109849

Bataille, C. P., von Holstein, I. C. C., Laffoon, J. E., Willmes, M., Liu, X.-M., & Davies, G. R. (2018). A bioavailable strontium isoscape for Western Europe: A machine learning approach. *PloS One*, *13*(5), e0197386. https://doi.org/10.1371/journal.pone.0197386

Bateman, A. S., & Kelly, S. D. (2007). Fertilizer nitrogen isotope signatures. *Isotopes in Environmental and Health Studies*, *43*(3), 237–247. https://doi.org/10.1080/10256010701550732

Beard, B. L., & Johnson, C. M. (2000). Strontium isotope composition of skeletal material can determine the birth place and geographic mobility of humans and animals. *Journal of Forensic Sciences*, *45*(5), 1049–1061.

Beasley, M., Lesnik, J., McKee-Zech, H., & Duncan, A. (2024). Using Stable Nitrogen Isotope Ratios from Human Skeletal Muscle Tissue for Postmortem Interval (PMI) Estimation (Part 1). *Forensic Anthropology*. https://doi.org/10.5744/fa.2023.0001

Becker, J. S. (2005). Recent developments in isotope analysis by advanced mass spectrometric techniques. *Journal of Analytical Atomic Spectrometry*, *20*(11), 1173–1184. https://doi.org/10.1039/B508895J

Bell, L. S., Skinner, M. F., & Jones, S. J. (1996). The speed of post mortem change to the human skeleton and its taphonomic significance. *Forensic Science International*, *82*(2), 129–140. https://doi.org/10.1016/0379-0738(96)01984-6

Benson, S., Lennard, C., Maynard, P., & Roux, C. (2006). Forensic applications of isotope ratio mass spectrometry—A review. *Forensic Science International*, *157*(1), 1–22. https://doi.org/10.1016/j.forsciint.2005.03.012

Bentley, A. R. (2006). Strontium Isotopes from the Earth to the Archaeological Skeleton: A Review. *Journal of Archaeological Method and Theory*, *13*(3), 135–187. https://doi.org/10.1007/s10816-006-9009-x

Berg, G. E., Chesson, L. A., Yuryang, J., Youngsoon, S., & Bartelink, E. J. (2022). A large-scale evaluation of intraperson isotopic variation within human bone collagen and bioapatite. *Forensic Science International*, *336*, 111319. https://doi.org/10.1016/j.forsciint.2022.111319

Bertrand, B., Clauzel, T., Richardin, P., Bécart, A., Morbidelli, P., Hédouin, V., & Marques, C. (2024). Application and implications of radiocarbon dating in forensic case work: When medico-legal significance meets archaeological relevance. *Forensic Sciences Research*, *9*(3), owae046. https://doi.org/10.1093/fsr/owae046

Boecklen, W. J., Yarnes, C. T., Cook, B. A., & James, A. C. (2011). On the Use of Stable Isotopes in Trophic Ecology. *Annual Review of Ecology, Evolution, and Systematics*, *42*(Volume 42, 2011), 411–440. https://doi.org/10.1146/annurev-ecolsys-102209-144726

Boutton, T. W., Lynott, M. J., & Bumsted, M. P. (1991). Stable carbon isotopes and the study of prehistoric human diet. *Critical Reviews in Food Science and Nutrition*, *30*(4), 373–385. https://doi.org/10.1080/10408399109527548

Bowen, G. J. (2010). Isoscapes: Spatial Pattern in Isotopic Biogeochemistry. *Annual Review of Earth and Planetary Sciences*, *38*(1), 161–187. https://doi.org/10.1146/annurev-earth-040809-152429

Bowen, G. J., Ehleringer, J. R., Chesson, L. A., Stange, E., & Cerling, T. E. (2007). Stable isotope ratios of tap water in the contiguous United States. *Water Resources Research*, *43*(3). https://doi.org/10.1029/2006WR005186

Bowen, G. J., Guo, J. S., & Allen, S. T. (2022). A 3-D groundwater isoscape of the contiguous USA for forensic and water resource science. *PloS One*, *17*(1), e0261651. https://doi.org/10.1371/journal.pone.0261651

Bowen, G. J., & Revenaugh, J. (2003). Interpolating the isotopic composition of modern meteoric precipitation. *Water Resources Research*, *39*(10). https://doi.org/10.1029/2003WR002086

Bowen, G. J., & Wilkinson, B. (2002). Spatial distribution of δ18O in meteoric precipitation. *Geology*, *30*(4), 315–318. https://doi.org/10.1130/0091-7613(2002)030<0315:SDOOIM>2.0.CO;2

Bowman, S. (1990). *Radiocarbon Dating*. University of California Press.

Brand, W. A., Coplen, T. B., Vogl, J., Rosner, M., & Prohaska, T. (2014). Assessment of international reference materials for isotope-ratio analysis (IUPAC Technical Report). *Pure and Applied Chemistry*, *86*(3), 425–467. https://doi.org/10.1515/pac-2013-1023

Brennan, S. R., Zimmerman, C. E., Fernandez, D. P., Cerling, T. E., McPhee, M. V., & Wooller, M. J. (2015). Strontium isotopes delineate fine-scale natal origins and migration histories of Pacific salmon. *Science Advances*, *1*(4), e1400124. https://doi.org/10.1126/sciadv.1400124

Britton, K., Crowley, B. E., Bataille, C. P., Miller, J. H., & Wooller, M. J. (2022). Editorial: A Golden Age for Strontium Isotope Research? Current Advances in Paleoecological and Archaeological Research. *Frontiers in Ecology and Evolution*, *9*. https://doi.org/10.3389/fevo.2021.820295

Brock, F., Wood, R., Higham, Ditchfield, P., Bayliss, A., & Ramsey, C. (2012). Reliability of Nitrogen Content (%N) and Carbon:Nitrogen Atomic Ratios (C:N) as Indicators of Collagen Preservation Suitable for Radiocarbon Dating. *Radiocarbon*, *54*, 879–886. https://doi.org/10.1017/S0033822200047524

Brown, P., & Parker, J. (1985). *North Carolina Geologic Map (1985)* [Geologic Map]. North Carolina Geological Survey.

Buikstra, J. E., DeWitte, S. N., Agarwal, S. C., Baker, B. J., Bartelink, E. J., Berger, E., Blevins, K. E., Bolhofner, K., Boutin, A. T., Brickley, M. B., Buzon, M. R., Cova, C. de la, Goldstein, L., Gowland, R., Grauer, A. L., Gregoricka, L. A., Halcrow, S. E., Hall, S. A., Hillson, S., … Zakrzewski, S. R. (2022). Twenty-first century bioarchaeology: Taking stock and moving forward. *American Journal of Biological Anthropology*, *178*, 54–114. https://doi.org/10.1002/ajpa.24494

Capo, R. C., Stewart, B. W., & Chadwick, O. A. (1998). Strontium isotopes as tracers of ecosystem processes: Theory and methods. *Geoderma*, *82*(1), 197–225. https://doi.org/10.1016/S0016-7061(97)00102-X

Caruso, V., Marinoni, N., Diella, V., Possenti, E., Mancini, L., Cantaluppi, M., Berna, F., Cattaneo, C., & Pavese, A. (2021). Diagenesis of juvenile skeletal remains: A multimodal and multiscale approach to examine the post-mortem decay of children's bones. *Journal of Archaeological Science*, *135*, 105477. https://doi.org/10.1016/j.jas.2021.105477

Cerling, T. E., Harris, J. M., MacFadden, B. J., Leakey, M. G., Quade, J., Eisenmann, V., & Ehleringer, J. R. (1997). Global vegetation change through the Miocene/Pliocene boundary. *Nature*, *389*(6647), 153–158. https://doi.org/10.1038/38229

Chenery, C. A., Pashley, V., Lamb, A. L., Sloane, H. J., & Evans, J. A. (2012). The oxygen isotope relationship between the phosphate and structural carbonate fractions of human bioapatite. *Rapid Communications in Mass Spectrometry : RCM*, *26*(3), 309–319. https://doi.org/10.1002/rcm.5331

Chenery, C., Müldner, G., Evans, J., Eckardt, H., & Lewis, M. (2010). Strontium and stable isotope evidence for diet and mobility in Roman Gloucester, UK. *Journal of Archaeological Science*, *37*(1), 150–163. https://doi.org/10.1016/j.jas.2009.09.025

Chesson, L. A. (2014). Stable Isotopes in Forensics Applications. *Treatise on Geochemistry*, *14*, 34.

Chesson, L. A., & Berg, G. E. (2022). The use of stable isotopes in postconflict forensic identification. *WIREs Forensic Science*, *4*(2), e1439. https://doi.org/10.1002/wfs2.1439

Chesson, L. A., Berg, G. E., & Megyesi, M. (2024). Disaster victim identification: Stable isotope analysis and the identification of unknown decedents. *Journal of Forensic Sciences*, *69*(5), 1658–1670. https://doi.org/10.1111/1556-4029.15554

Chesson, L. A., Tipple, B. J., Ehleringer, J. R., Park, T., & Bartelink, E. J. (2018). *Forensic applications of isotope landscapes ("isoscapes")* (pp. 127–148). https://doi.org/10.1002/9781119226529.ch8

Chesson, L. A., Tipple, B., Mackey, G., Hynek, S., Fernandez, D., & Ehleringer, J. (2012). Strontium isotopes in tap water from the coterminous USA. *Ecosphere*, *3*, art67. https://doi.org/10.1890/ES12-00122.1

Chikaraishi, Y., Steffan, S. A., Ogawa, N. O., Ishikawa, N. F., Sasaki, Y., Tsuchiya, M., & Ohkouchi, N. (2014). High-resolution food webs based on nitrogen isotopic composition of amino acids. *Ecology and Evolution*, *4*(12), 2423–2449. https://doi.org/10.1002/ece3.1103

Child, A. M. (1995). Microbial Taphonomy of Archaeological Bone. *Studies in Conservation*, *40*(1), 19–30. https://doi.org/10.2307/1506608

Chisholm, B. S., Nelson, D. E., & Schwarcz, H. P. (1982). Stable-carbon isotope ratios as a measure of marine versus terrestrial protein in ancient diets. *Science (New York, N.Y.)*, *216*(4550), 1131–1132. https://doi.org/10.1126/science.216.4550.1131

Christensen, A. M., Passalacqua, N. V., & Bartelink, E. J. (2014). *Chapter 5—Forensic Taphonomy* (A. M. Christensen, N. V. Passalacqua, & E. J. Bartelink, Eds.; pp. 119–147). Academic Press. https://doi.org/10.1016/B978-0-12-418671-2.00005-7

Coplen, T. B. (1988). Normalization of oxygen and hydrogen isotope data. *Chemical Geology: Isotope Geoscience Section*, *72*(4), 293–297. https://doi.org/10.1016/0168-9622(88)90042-5

Coplen, T. B. (2011). Guidelines and recommended terms for expression of stable-isotope-ratio and gas-ratio measurement results. *Rapid Communications in Mass Spectrometry*, *25*(17), 2538–2560. https://doi.org/10.1002/rcm.5129

Coplen, T. B., Kendall, C., & Hopple, J. A. (1983). Comparison of stable isotope reference samples. *Nature*, *302*, 236–238.

Corr, L. T., Sealy, J. C., Horton, M. C., & Evershed, R. P. (2005). A novel marine dietary indicator utilising compound-specific bone collagen amino acid δ13C values of ancient humans. *Journal of Archaeological Science*, *32*(3), 321–330. https://doi.org/10.1016/j.jas.2004.10.002

Cox, G., & Sealy, J. (1997). Investigating Identity and Life Histories: Isotopic Analysis and Historical Documentation of Slave Skeletons Found on the Cape Town Foreshore, South Africa. *International Journal of Historical Archaeology*, *1*(3), 207–224. https://doi.org/10.1023/A:1027349115474

Craig, H. (1953). The geochemistry of the stable carbon isotopes. *Geochimica et Cosmochimica Acta*, *3*(2), 53–92. https://doi.org/10.1016/0016-7037(53)90001-5

Craig, H. (1961). Isotopic Variations in Meteoric Waters. *Science (New York, N.Y.)*, *133*(3465), 1702–1703. https://doi.org/10.1126/science.133.3465.1702

Crenshaw, A. M. (2020). *Decoupled Strontium and Lead Isotopes in North Carolina Rivers* [M.S., The University of North Carolina at Chapel Hill]. https://www.proquest.com/docview/2421128457/abstract/27D1F472786F4A4DPQ/1

Curtis, M. J., Beaumont, J., Elamin, F., Wilson, A. S., & Koon, H. E. C. (2022). Method of micro-sampling human dentine collagen for stable isotope analysis. *Rapid Communications in Mass Spectrometry*, *36*(13), e9305. https://doi.org/10.1002/rcm.9305

Damann, F. E., & Jans, M. M. E. (2017). Microbes, anthropology, and bones. In D. O. Carter, J. K. Tomberlin, M. E. Benbow, & J. L. Metcalf (Eds.), *Forensic Microbiology* (1st ed., pp. 312–327). John Wiley & Sons, Incorporated. http://ebookcentral.proquest.com/lib/ncsu/detail.action?docID=4830606

Dansgaard, W. (1954). The O18-abundance in fresh water. *Geochimica et Cosmochimica Acta*, *6*(5), 241–260. https://doi.org/10.1016/0016-7037(54)90003-4

Dansgaard, W. (1964). Stable isotopes in precipitation. *Tellus*, *16*(4), 436–468. https://doi.org/10.1111/j.2153-3490.1964.tb00181.x

Daux, V., Lécuyer, C., Héran, M.-A., Amiot, R., Simon, L., Fourel, F., Martineau, F., Lynnerup, N., Reychler, H., & Escarguel, G. (2008). Oxygen isotope fractionation between human phosphate and water revisited. *Journal of Human Evolution*, *55*(6), 1138–1147. https://doi.org/10.1016/j.jhevol.2008.06.006

Dawson, T. E., Mambelli, S., Plamboeck, A. H., Templer, P. H., & Tu, K. P. (2002). Stable Isotopes in Plant Ecology. *Annual Review of Ecology, Evolution, and Systematics*, *33*(Volume 33, 2002), 507–559. https://doi.org/10.1146/annurev.ecolsys.33.020602.095451

de Oliveira Mascarenhas, R., Sena-Souza, J. P., Bernasconi, S. M., McKenzie, J. A., Vasconcelos, C., Muniz, T. R., Nogueira e Silva, M. P., da Silva Salvador, F. A., & Rumbelsperger, A. M. B. (2022). Building an isoscape based on tooth enamel for human provenance estimation in Brazil. *Forensic Science International*, *330*, 111109. https://doi.org/10.1016/j.forsciint.2021.111109

DeNiro, M. J. (1985). Postmortem preservation and alteration of in vivo bone collagen isotope ratios in relation to palaeodietary reconstruction. *Nature*, *317*(6040), 806–809. https://doi.org/10.1038/317806a0

DeNiro, M. J. (1987). Stable Isotopy and Archaeology. *American Scientist*, *75*(2), 182–191.

DeNiro, M. J., & Epstein, S. (1978). Influence of diet on the distribution of carbon isotopes in animals. *Geochimica et Cosmochimica Acta*, *42*(5), 495–506. https://doi.org/10.1016/0016-7037(78)90199-0

Deniro, M. J., & Epstein, S. (1981). Influence of diet on the distribution of nitrogen isotopes in animals. *Geochimica et Cosmochimica Acta*, *45*(3), 341–351. https://doi.org/10.1016/0016-7037(81)90244-1

Dotsika, E. (2020). Correlation between δ18Ow and δ18Oen for estimating human mobility and paleomobility patterns. *Scientific Reports*, *10*(1), 15439. https://doi.org/10.1038/s41598-020-71683-7

Dunn, P., & Carter, J. F. (2018). *Good Practice Guide for Isotope Ratio Mass Spectrometry Second Edition 2018*.

Dunn, P. J. H., & Carter, J. F. (2018). Publication of the second edition of the FIRMS good practice guide for isotope ratio mass spectrometry. *Isotopes in Environmental and Health Studies*, *54*(6), 656–657. https://doi.org/10.1080/10256016.2018.1531495

Eagle, R. A., Enriquez, M., Grellet-Tinner, G., Pérez-Huerta, A., Hu, D., Tütken, T., Montanari, S., Loyd, S. J., Ramirez, P., Tripati, A. K., Kohn, M. J., Cerling, T. E., Chiappe, L. M., & Eiler, J. M. (2015). Isotopic ordering in eggshells reflects body temperatures and suggests differing thermophysiology in two Cretaceous dinosaurs. *Nature Communications*, *6*(1), Article 1. https://doi.org/10.1038/ncomms9296

Eck, C. J., DiGangi, E. A., & Bethard, J. D. (2019). Assessing the efficacy of isotopic provenancing of human remains in Colombia. *Forensic Science International*, *302*, 109919. https://doi.org/10.1016/j.forsciint.2019.109919

Ehleringer, J. R., Thompson, A. H., Podlesak, D. W., Bowen, G. J., Chesson, L. A., Cerling, T. E., Park, T., Dostie, P., & Schwarcz, H. (2010). A Framework for the Incorporation of Isotopes and Isoscapes in Geospatial Forensic Investigations. In J. B. West, G. J. Bowen, T. E. Dawson, & K. P. Tu (Eds.), *Isoscapes: Understanding movement, pattern, and process on Earth through isotope mapping* (pp. 357–387). Springer Netherlands. https://doi.org/10.1007/978-90-481-3354-3_17

Emmons, A. L., Mundorff, A. Z., Hoeland, K. M., Davoren, J., Keenan, S. W., Carter, D. O., Campagna, S. R., & DeBruyn, J. M. (n.d.). Postmortem Skeletal Microbial Community Composition and Function in Buried Human Remains. *mSystems*, *7*(2), e00041-22. https://doi.org/10.1128/msystems.00041-22

Fahy, G. E., Deter, C., Pitfield, R., Miszkiewicz, J. J., & Mahoney, P. (2017). Bone deep: Variation in stable isotope ratios and histomorphometric measurements of bone remodelling within adult humans. *Journal of Archaeological Science*, *87*, 10–16. https://doi.org/10.1016/j.jas.2017.09.009

Fauberteau, A. E., Chartrand, M. M. G., Hu, L., St-Jean, G., & Bataille, C. P. (2021). Investigating a cold case using high-resolution multi-isotope profiles in human hair. *Forensic Chemistry*, *22*, 100300. https://doi.org/10.1016/j.forc.2020.100300

Faure, G. (1977). *Principles of isotope geology*. Wiley. https://catalog.lib.ncsu.edu/catalog/NCSU421779

Faure, G., & Hurley, P. M. (1963). The Isotopic Composition of Strontium in Oceanic and Continental Basalts: Application to the Origin of Igneous Rocks 1. *Journal of Petrology*, *4*(1), 31–50. https://doi.org/10.1093/petrology/4.1.31

Faure, G., & Powell, J. L. (1972). *Strontium Isotope Geology*. Springer. https://doi.org/10.1007/978-3-642-65367-4

Fogel, M., Tuross, N., & DW, O. (1989). Nitrogen Isotope Tracers of Human Lactation in Modern and Archaeological Populations. *Carnegie Inst Wash Yearbook*, *88*.

Fournier, N. A., & Ross, A. H. (2013). Radiocarbon Dating: Implications for Establishing a Forensic Context. *Forensic Science Policy & Management: An International Journal*, *4*(3–4), 96–104. https://doi.org/10.1080/19409044.2013.858801

Fry, B. (2006). *Stable Isotope Ecology*. Springer. https://doi.org/10.1007/0-387-33745-8

Fuller, B. t., Fuller, J. l., Harris, D. a., & Hedges, R. e. m. (2006). Detection of breastfeeding and weaning in modern human infants with carbon and nitrogen stable isotope ratios. *American Journal of Physical Anthropology*, *129*(2), 279–293. https://doi.org/10.1002/ajpa.20249

Fuller, B. T., Fuller, J. L., Sage, N. E., Harris, D. A., O'Connell, T. C., & Hedges, R. E. M. (2005). Nitrogen balance and δ15N: Why you're not what you eat during nutritional stress. *Rapid Communications in Mass Spectrometry*, *19*(18), 2497–2506. https://doi.org/10.1002/rcm.2090

Glynn, C. L. (2022). Bridging Disciplines to Form a New One: The Emergence of Forensic Genetic Genealogy. *Genes*, *13*(8), 1381. https://doi.org/10.3390/genes13081381

González-Colmenares, G., Botella-López, M. C., Moreno-Rueda, G., & Fernández-Cardenete, J. R. (2007). Age estimation by a dental method: A comparison of Lamendin's and Prince & Ubelaker's technique. *Journal of Forensic Sciences*, *52*(5), 1156–1160. https://doi.org/10.1111/j.1556-4029.2007.00508.x

Gordon, G. W., Saul, T. B., Steadman, D., Wescott, D. J., & Knudson, K. (2018). Preservation of hair stable isotope signatures during freezing and law enforcement evidence packaging. *Forensic Chemistry*, *11*, 108–119. https://doi.org/10.1016/j.forc.2018.10.004

Granke, M., Does, M. D., & Nyman, J. S. (2015). The Role of Water Compartments in the Material Properties of Cortical Bone. *Calcified Tissue International*, *97*(3), 292–307. https://doi.org/10.1007/s00223-015-9977-5

Guiry, E. (2019). Complexities of Stable Carbon and Nitrogen Isotope Biogeochemistry in Ancient Freshwater Ecosystems: Implications for the Study of Past Subsistence and Environmental Change. *Frontiers in Ecology and Evolution*, *7*. https://doi.org/10.3389/fevo.2019.00313

Guiry, E. J., & Szpak, P. (2020). Quality control for modern bone collagen stable carbon and nitrogen isotope measurements. *Methods in Ecology and Evolution*, *11*(9), 1049–1060. https://doi.org/10.1111/2041-210X.13433

Guy, H., Masset, C., & Baud, C.-A. (1997). Infant taphonomy. *International Journal of Osteoarchaeology*, *7*(3), 221–229. https://doi.org/10.1002/(SICI)1099-1212(199705)7:3

Hackett, C. J. (1981). Microscopical focal destruction (tunnels) in exhumed human bones. *Medicine, Science, and the Law*, *21*(4), 243–265. https://doi.org/10.1177/002580248102100403

Haglund, W. D., & Sorg, M. H. (1997). *Forensic taphonomy: The postmortem fate of human remains*. Boca Raton : CRC Press, 1997]. https://catalog.lib.ncsu.edu/catalog/NCSU946795

Hale, A. R., & Ross, A. H. (2023). Investigating the Timing and Extent of Juvenile and Fetal Bone Diagenesis in a Temperate Environment. *Biology*, *12*(3). https://doi.org/10.3390/biology12030403

Harbeck, M., & Grupe, G. (2009). Experimental chemical degradation compared to natural diagenetic alteration of collagen: Implications for collagen quality indicators for stable

isotope analysis. *Archaeological and Anthropological Sciences*, *1*(1), 43–57. https://doi.org/10.1007/s12520-009-0004-5

Hartnett, K. M. (2010a). Analysis of age-at-death estimation using data from a new, modern autopsy sample–part I: pubic bone. *Journal of Forensic Sciences*, *55*(5), 1145–1151. https://doi.org/10.1111/j.1556-4029.2010.01399.x

Hartnett, K. M. (2010b). Analysis of age-at-death estimation using data from a new, modern autopsy sample–part II: sternal end of the fourth rib. *Journal of Forensic Sciences*, *55*(5), 1152–1156. https://doi.org/10.1111/j.1556-4029.2010.01415.x

Hedges, R. E. M. (2000). Appraisal of radiocarbon dating of kiore bones (Pacific rat Rattus exulans) in New Zealand. *Journal of the Royal Society of New Zealand*, *30*(4), 385–398. https://doi.org/10.1080/03014223.2000.9517630

Hedges, R. E. M. (2002). Bone diagenesis: An overview of processes. *Archaeometry*, *44*(3), 319–328. https://doi.org/10.1111/1475-4754.00064

Hedges, R. E. M., Clement, J. G., Thomas, C. D., & O'Connell, T. C. (2007). Collagen turnover in the adult femoral mid-shaft: Modeled from anthropogenic radiocarbon tracer measurements. *American Journal of Physical Anthropology*, *133*(2), 808–816. https://doi.org/10.1002/ajpa.20598

Hedges, R. E. M., Millard, A. R., & Pike, A. W. G. (1995). Measurements and Relationships of Diagenetic Alteration of Bone from Three Archaeological Sites. *Journal of Archaeological Science*, *22*(2), 201–209. https://doi.org/10.1006/jasc.1995.0022

Hemer, K. A., & Evans, J. A. (2018). *The Contribution of Stable Isotope Analysis to the Study of Childhood Movement and Migration* (S. Crawford, D. M. Hadley, & G. Shepherd, Eds.; p. 0). Oxford University Press. https://doi.org/10.1093/oxfordhb/9780199670697.013.27

Herring, D. A., Saunders, S. R., & Katzenberg, M. A. (1998). Investigating the weaning process in past populations. *American Journal of Physical Anthropology*, *105*(4), 425–439. https://doi.org/10.1002/(SICI)1096-8644(199804)105:4

Heumann, K. G., Eisenhut, S., Gallus, S., Hebeda, E. H., Nusko, R., Vengosh, A., & Walczyk, T. (1995). Recent developments in thermal ionization mass spectrometric techniques for isotope analysis. A review. *Analyst*, *120*(5), 1291–1299. https://doi.org/10.1039/AN9952001291

Hickman, M. J., Hughes, K. A., Strom, K. J., & Ropero-Miller, J. D. (2007). *Medical Examiners and Coroners' Offices, 2004*. https://bjs.ojp.gov/content/pub/pdf/meco04.pdf

Hill, P. A. (1998). Bone Remodelling. *British Journal of Orthodontics*, *25*(2), 101–107. https://doi.org/10.1093/ortho.25.2.101

Hillson, S. (1996). *Dental Anthropology*. Cambridge University Press. https://doi.org/10.1017/CBO9781139170697

Hillson, S. (2014). *Tooth Development in Human Evolution and Bioarchaeology*. Cambridge University Press. https://doi.org/10.1017/CBO9780511894916

Hobson, K. A., Bowen, G. J., Wassenaar, L. I., Ferrand, Y., & Lormee, H. (2004). Using stable hydrogen and oxygen isotope measurements of feathers to infer geographical origins of

migrating European birds. *Oecologia*, *141*(3), 477–488. https://doi.org/10.1007/s00442-004-1671-7

Hoefs, J. (2015). *Stable Isotope Geochemistry*. Springer International Publishing. https://doi.org/10.1007/978-3-319-19716-6

Holt, E., Evans, J. A., & Madgwick, R. (2021). Strontium (87Sr/86Sr) mapping: A critical review of methods and approaches. *Earth-Science Reviews*, *216*, 103593. https://doi.org/10.1016/j.earscirev.2021.103593

Hood-Nowotny, R., & Knols, B. G. J. (2007). Stable isotope methods in biological and ecological studies of arthropods. *Entomologia Experimentalis et Applicata*, *124*(1), 3–16. https://doi.org/10.1111/j.1570-7458.2007.00572.x

Hopkins, D. W., Wiltshire, P. E. J., & Turner, B. D. (2000). Microbial characteristics of soils from graves: An investigation at the interface of soil microbiology and forensic science. *Applied Soil Ecology*, *14*(3), 283–288. https://doi.org/10.1016/S0929-1393(00)00063-9

Iacumin, P., Rossi, M., Selmo, E., & Venturelli, G. (2022). Oxygen Isotopes in Carbonate and Phosphate of Modern Mammal Bioapatite: New Data and Critical Revision after about 25 Years from the First Recognitions. *Minerals*, *12*(10). https://doi.org/10.3390/min12101204

Jaggers, K. A., & Rogers, T. L. (2009). The Effects of Soil Environment on Postmortem Interval: A Macroscopic Analysis. *Journal of Forensic Sciences*, *54*(6), 1217–1222. https://doi.org/10.1111/j.1556-4029.2009.01160.x

Jans, M. M. E. (2008). Microbial bioerosion of bone – a review. In M. Wisshak & L. Tapanila (Eds.), *Current Developments in Bioerosion* (pp. 397–413). Springer Berlin Heidelberg. https://doi.org/10.1007/978-3-540-77598-0_20

Jans, M. M. E. (2021). Microscopic Destruction of Bone. In J. Pokines & S. A. Symes (Eds.), *Manual of Forensic Taphonomy* (2nd ed., pp. 19–36). CRC Press. https://doi.org/10.1201/b15424-3

Jans, M. M. E., Nielsen-Marsh, C. M., Smith, C. I., Collins, M. J., & Kars, H. (2004). Characterisation of microbial attack on archaeological bone. *Journal of Archaeological Science*, *31*(1), 87–95. https://doi.org/10.1016/j.jas.2003.07.007

Jantz, R. L., & Ousley, S. D. (2005). FORDISC 3: Computerized forensic discriminant functions, Version 3.0. *The University of Tennessee, Knoxville*.

JMP®, Version 17.0. SAS Institute Inc., Cary, NC, 1989–2021. (n.d.).

Johnson, D. L., Chau, T. H., & Chesson, L. A. (2025). The oxygen isotopic composition of tooth enamel carbonate: A review of measurement methods & forensic applications. *TrAC Trends in Analytical Chemistry*, *183*, 118084. https://doi.org/10.1016/j.trac.2024.118084

Johnstone-Belford, E. C., & Blau, S. (2020). A Review of Bomb Pulse Dating and its Use in the Investigation of Unidentified Human Remains. *Journal of Forensic Sciences*, *65*(3), 676–685. https://doi.org/10.1111/1556-4029.14227

Juarez, C. (2011). Geolocation: A pathway to identification for deceased undocumented border crossers [PhD Thesis]. In *ProQuest Dissertations and Theses*.

https://www.proquest.com/dissertations-theses/geolocation-pathway-identification-deceased/docview/865041957/se-2?accountid=12725 http://JS8LB8FT5Y.search.serialssolutions.com/directLink?&atitle=Geolocation%253A+A+pathway+to+identification+for+deceased+undocumented+border+crossers&author=Juarez%252C+Chelsey&issn=&title=Geolocation%253A+A+pathway+to+identification+for+deceased+undocumented+border+crossers&volume=&issue=&date=2011-01-01&spage=&id=doi:&sid=ProQ_ss&genre=article

Juarez, C. A. (2008). Strontium and geolocation, the pathway to identification for deceased undocumented mexican border-crossers: A preliminary report. *Journal of Forensic Sciences*, *53*(1), 46–49. https://doi.org/10.1111/j.1556-4029.2007.00610.x

Kamenov, G. D., Lofaro, E. M., Goad, G., & Krigbaum, J. (2018). Trace elements in modern and archaeological human teeth: Implications for human metal exposure and enamel diagenetic changes. *Journal of Archaeological Science*, *99*, 27–34. https://doi.org/10.1016/j.jas.2018.09.002

Katzenberg, M. A. (2008). Stable Isotope Analysis: A Tool for Studying Past Diet, Demography, and Life History. In *Biological Anthropology of the Human Skeleton* (pp. 411–441). John Wiley & Sons, Ltd. https://doi.org/10.1002/9780470245842.ch13

Katzenberg, M. A., Herring, D. A., & Saunders, S. R. (1996). Weaning and infant mortality: Evaluating the skeletal evidence. *American Journal of Physical Anthropology*, *101*, 177–199. https://doi.org/10.1002/(SICI)1096-8644(1996)23

Katzenberg, M. A., & Lovell, N. C. (1999). Stable isotope variation in pathological bone. *International Journal of Osteoarchaeology*, *9*(5), 316–324. https://doi.org/10.1002/(SICI)1099-1212(199909/10)9:5<316::AID-OA500>3.0.CO;2-D

Keegan, W. F., & DeNiro, M. J. (1988). Stable Carbon- and Nitrogen-Isotope Ratios of Bone Collagen Used to Study Coral-Reef and Terrestrial Components of Prehistoric Bahamian Diet. *American Antiquity*, *53*(2), 320–336. https://doi.org/10.2307/281022

Keller, A. T., Regan, L. A., Lundstrom, C. C., & Bower, N. W. (2016). Evaluation of the efficacy of spatiotemporal Pb isoscapes for provenancing of human remains. *Forensic Science International*, *261*, 83–92. https://doi.org/10.1016/j.forsciint.2016.02.006

Kendall, C., Elliott, E. M., & Wankel, S. D. (2007). *Tracing Anthropogenic Inputs of Nitrogen to Ecosystems* (pp. 375–449). https://doi.org/10.1002/9780470691854.ch12

Kendall, C., Eriksen, A. M. H., Kontopoulos, I., Collins, M. J., & Turner-Walker, G. (2018). Diagenesis of archaeological bone and tooth. *Palaeogeography, Palaeoclimatology, Palaeoecology*, *491*, 21–37. https://doi.org/10.1016/j.palaeo.2017.11.041

Kimmerle, E. H., Falsetti, A., & Ross, A. H. (2010). Immigrants, Undocumented Workers, Runaways, Transients and the Homeless: Towards Contextual Identification Among Unidentified Decedents. *Forensic Science Policy & Management: An International Journal*, *1*(4), 178–186. https://doi.org/10.1080/19409041003636991

Klein, P. D., & Klein, E. R. (1997). Chapter 1 Stable isotopes: Origins and safety. In T. R. Browne (Ed.), *Pharmacochemistry Library* (Vol. 26, pp. 1–11). Elsevier. https://doi.org/10.1016/S0165-7208(97)80148-1

Knudson, K. J., Price, T. D., Buikstra, J. E., & Blom, D. E. (2004). The Use of Strontium Isotope Analysis to Investigate Tiwanaku Migration and Mortuary Ritual in Bolivia and Peru. *Archaeometry*, *46*(1), 5–18. https://doi.org/10.1111/j.1475-4754.2004.00140.x

Koch, P. L. (1998). Isotopic Reconstruction of Past Continental Environments. *Annual Review of Earth and Planetary Sciences*, *26*(1), 573–613. https://doi.org/10.1146/annurev.earth.26.1.573

Koch, P. L., Behrensmeyer, A. K., Stott, A. W., Evershed, R. P., Tuross, N., & Fogel, M. L. (2000). The Effects of Weathering on the Stable Isotope Composition of Bones. *Ancient Biomolecules*, *3*(2), 117.

Koch, P. L., Tuross, N., & Fogel, M. L. (1997). The Effects of Sample Treatment and Diagenesis on the Isotopic Integrity of Carbonate in Biogenic Hydroxylapatite. *Journal of Archaeological Science*, *24*(5), 417–429. https://doi.org/10.1006/jasc.1996.0126

Kootker, L. M., Ammer, S. T. M., Wescott, D. J., Davies, G. R., & Mickleburgh, H. L. (2024). Sr–Pb isotope differences in pre- and post-burial human bone, teeth, and hair keratin: Implications for isotope forensics. *International Journal of Legal Medicine*, *138*(1), 151–164. https://doi.org/10.1007/s00414-023-02976-5

Kootker, L. M., Plomp, E., Ammer, S. T. M., Hoogland, V., & Davies, G. R. (2020). Spatial patterns in 87Sr/86Sr ratios in modern human dental enamel and tap water from the Netherlands: Implications for forensic provenancing. *Science of The Total Environment*, *729*, 138992. https://doi.org/10.1016/j.scitotenv.2020.138992

Kootker, L. M., von Holstein, I. C. C., Broeders, J., Wescott, D. J., Davies, G. R., & Mickleburgh, H. L. (2020). The effects of decomposition and environment on antemortem H-Pb-Sr isotope compositions and degradation of human scalp hair: Actualistic taphonomic observations. *Forensic Science International*, *312*, 110336. https://doi.org/10.1016/j.forsciint.2020.110336

Kramer, R. T., & Bartelink, E. J. (2022). Childhood and Adulthood Residency Prediction Using Strontium (87Sr/86Sr) and Oxygen (δ18O) Isotopes for Unidentified Deceased Migrants Recovered in Southern Texas. *Forensic Anthropology*, *5*(1), 25–45.

Kramer, R. T., Bartelink, E. J., Herrmann, N. P., Bataille, C. P., & Spradley, K. (2020). Application of stable isotopes and geostatistics to infer region of geographical origin for deceased undocumented Latin American migrants. In R. C. Parra, S. C. Zapico, & D. H. Ubelaker (Eds.), *Forensic Science and Humanitarian Action: Interacting with the Dead and the Living: Vol. Volume 1* (1st ed., pp. 425–440). John Wiley & Sons Ltd. https://doi.org/10.1002/9781119482062.ch27

Kramer, R. T., Kinaston, R. L., Holder, P. W., Armstrong, K. F., King, C. L., Sipple, W. D. K., Martin, A. P., Pradel, G., Turnbull, R. E., Rogers, K. M., Reid, M., Barr, D., Wijenayake, K. G., Buckley, H. R., Stirling, C. H., & Bataille, C. P. (2022). A bioavailable strontium (87Sr/86Sr) isoscape for Aotearoa New Zealand: Implications for food forensics and biosecurity. *PloS One*, *17*(3), e0264458. https://doi.org/10.1371/journal.pone.0264458

Krueger, H. W., & Sullivan, C. H. (1984). Models For Carbon Isotope Fractionation Between Diet and Bone. In W. L. Wittry & R. E. Ritzenthaler (Eds.), *Old Copper Complex: An Archaic Manifestation In Wisconsin* (Fayetteville; pp. 205–220).

Laffoon, J. E., Rojas, R. V., & Hofman, C. L. (2013). *Oxygen and Carbon Isotope Analysis of Human Dental Enamel from the Caribbean: Implications for Investigating Individual Origins*. https://doi.org/10.1111/j.1475-4754.2012.00698.x

Laffoon, J. E., Sonnemann, T. F., Shafie, T., Hofman, C. L., Brandes, U., & Davies, G. R. (2017). Investigating human geographic origins using dual-isotope (87Sr/86Sr, δ18O) assignment approaches. *PLOS ONE*, *12*(2), e0172562.

Lambert, J. B., Simpson, S. V., Weiner, S. G., & Buikstra, J. E. (1985). Induced metal-ion exchange in excavated human bone. *Journal of Archaeological Science*, *12*(2), 85–92. https://doi.org/10.1016/0305-4403(85)90053-6

Lamendin, H., Baccino, E., Humbert, J. F., Tavernier, J. C., Nossintchouk, R. M., & Zerilli, A. (1992). A simple technique for age estimation in adult corpses: The two criteria dental method. *Journal of Forensic Sciences*, *37*(5), 1373–1379.

Latham, K. E., & Miller, J. J. (2018). DNA recovery and analysis from skeletal material in modern forensic contexts. *Forensic Sciences Research*, *4*(1), 51–59. https://doi.org/10.1080/20961790.2018.1515594

Laughinghouse, S. (2024). *North Carolina Division of Water Resources Groundwater Management Branch Monitoring Well Network 2024 Annual Report* (p. 70) [Annual Report]. North Carolina Department of Environmental Quality.

Lee-Thorp, J. A. (2008). On Isotopes and Old Bones*. *Archaeometry*, *50*(6), 925–950. https://doi.org/10.1111/j.1475-4754.2008.00441.x

Lee-Thorp, J. A., Sealy, J. C., & van der Merwe, N. J. (1989). Stable carbon isotope ratio differences between bone collagen and bone apatite, and their relationship to diet. *Journal of Archaeological Science*, *16*(6), 585–599. https://doi.org/10.1016/0305-4403(89)90024-1

Lee-Thorp, J. A., & van der Merwe, N. J. (1991). Aspects of the chemistry of modern and fossil biological apatites. *Journal of Archaeological Science*, *18*(3), 343–354. https://doi.org/10.1016/0305-4403(91)90070-6

Lee-Thorp, J., & Sponheimer, M. (2003). Tooth enamel remains a virtually closed system for stable light isotope and trace element archives in fossils. *Am. J. Phys. Anthropol., S36*, 138–138.

Lehn, C., Mützel, E., & Rossmann, A. (2011). Multi-element stable isotope analysis of H, C, N and S in hair and nails of contemporary human remains. *International Journal of Legal Medicine*, *125*(5), 695–706. https://doi.org/10.1007/s00414-011-0595-0

Long, N. (2025). *Applying Multidisciplinary Approach to Forensic Casework in North Carolina* [Poster]. AAFS, Baltimore, MD.

Long, N., Sheets, K., Thornton, E. K., & Ross, A. H. (2024). Applying multidisciplinary methods to forensic casework in North Carolina. *Forensic Sciences Research*, *9*(3), owae038. https://doi.org/10.1093/fsr/owae038

Longinelli, A. (1984). Oxygen isotopes in mammal bone phosphate: A new tool for paleohydrological and paleoclimatological research? *Geochimica et Cosmochimica Acta*, *48*(2), 385–390. https://doi.org/10.1016/0016-7037(84)90259-X

Lustig, A. (2013). *Using strontium isotope analysis on modern populations to determine geolocation reliability in a forensic context*. https://hdl.handle.net/2144/21211

Manifold, B. M. (2012). Intrinsic and extrinsic factors involved in the preservation of non-adult skeletal remains in archaeology and forensic science. *Bull Int Assoc Paleodont*, *6*, 51–69.

Martin, L., & Rackard, F. (2016). IMAGES IN CLINICAL MEDICINE. Hair-on-End Sign. *The New England Journal of Medicine*, *374*(19), e23. https://doi.org/10.1056/NEJMicm1510045

Mascarenhas, R. de O., Sena-Souza, J. P., Bernasconi, S. M., McKenzie, J. A., Vasconcelos, C., Muniz, T. R., Silva, M. P. N. E., Salvador, F. A. da S., & Rumbelsperger, A. M. B. (2022). Building an isoscape based on tooth enamel for human provenance estimation in Brazil. *Forensic Science International*, *330*, 111109. https://doi.org/10.1016/j.forsciint.2021.111109

McNeely, E. (2023, April 3). *The History of Charlotte Water | Charlotte Water Blog*. https://cltwaterblog.org/2023/04/the-history-of-charlotte-water/

Megyesi, M. S., Nawrocki, S. P., & Haskell, N. H. (2005). Using accumulated degree-days to estimate the postmortem interval from decomposed human remains. *Journal of Forensic Sciences*, *50*(3), 618–626.

Meier-Augenstein, W. (2017). *Stable Isotope Forensics—Methods and Applications of Stable Isotope Analysis; 2nd ed.* https://doi.org/10.1002/9781119080190

Meier-Augenstein, W., & Kemp, H. F. (2012). Stable Isotope Analysis: Hair and Nails. In *Wiley Encyclopedia of Forensic Science*. John Wiley & Sons, Ltd. https://doi.org/10.1002/9780470061589.fsa1043

Merwe, N. J. van der. (1982). Carbon Isotopes, Photosynthesis, and Archaeology: Different pathways of photosynthesis cause characteristic changes in carbon isotope ratios that make possible the study of prehistoric human diets. *American Scientist*, *70*(6), 596–606.

Milani, C., Tomassini, L., Gambelunghe, C., Pini, N., Calcagnile, L., Quarta, G., D'Elia, M., Scendoni, R., Fedeli, P., & Lancia, M. (2025). Radiocarbon and bomb pulse dating in the forensic context: A systematic review. *Forensic Science International*, *367*, 112367. https://doi.org/10.1016/j.forsciint.2025.112367

Miller, M. J., Dong, Y., Pechenkina, K., Fan, W., & Halcrow, S. E. (2020). Raising girls and boys in early China: Stable isotope data reveal sex differences in weaning and childhood diets during the eastern Zhou era. *American Journal of Physical Anthropology*, *172*(4), 567–585. https://doi.org/10.1002/ajpa.24033

Muccio, Z., & Jackson, G. P. (2009). Isotope ratio mass spectrometry. *Analyst*, *134*(2), 213–222. https://doi.org/10.1039/B808232D

Nelson, B. K., Deniro, M. J., Schoeninger, M. J., De Paolo, D. J., & Hare, P. E. (1986). Effects of diagenesis on strontium, carbon, nitrogen and oxygen concentration and isotopic composition of bone. *Geochimica et Cosmochimica Acta*, *50*(9), 1941–1949. https://doi.org/10.1016/0016-7037(86)90250-4

Nielsen-Marsh, C. M., & Hedges, R. E. M. (2000). Patterns of Diagenesis in Bone I: The Effects of Site Environments. *Journal of Archaeological Science*, *27*(12), 1139–1150. https://doi.org/10.1006/jasc.1999.0537

Nielsen-Marsh, C. M., Smith, C. I., Jans, M. M. E., Nord, A., Kars, H., & Collins, M. J. (2007). Bone diagenesis in the European Holocene II: Taphonomic and environmental considerations. *Journal of Archaeological Science*, *34*(9), 1523–1531. https://doi.org/10.1016/j.jas.2006.11.012

Obertová, Z., Skrzypek, G., Danišík, M., Rankenburg, K., Cummaudo, M., Olivieri, L., Mazzarelli, D., Cappella, A., Evans, N., Ubelaker, D., & Cattaneo, C. (2023). Stable Isotope Provenance of Unidentified Deceased Migrants—A Pilot Study. *Biology*, *12*(11), 1371. https://doi.org/10.3390/biology12111371

O'Brien, D. M. (2015). Stable Isotope Ratios as Biomarkers of Diet for Health Research. *Annual Review of Nutrition*, *35*, 565–594. https://doi.org/10.1146/annurev-nutr-071714-034511

Ortner, D. J., & Turner-walker, G. (2003). Chapter 2—The Biology of Skeletal Tissues. In D. J. Ortner (Ed.), *Identification of Pathological Conditions in Human Skeletal Remains (Second Edition)* (pp. 11–35). Academic Press. https://doi.org/10.1016/B978-012528628-2/50039-9

Peel, M. C., Finlayson, B. L., & McMahon, T. A. (2007). Updated world map of the Köppen-Geiger climate classification. *Hydrology and Earth System Sciences*, *11*(5), 1633–1644. https://doi.org/10.5194/hess-11-1633-2007

Pellegrini, M., & Snoeck, C. (2016). Comparing bioapatite carbonate pre-treatments for isotopic measurements: Part 2 — Impact on carbon and oxygen isotope compositions. *Chemical Geology*, *420*, 88–96. https://doi.org/10.1016/j.chemgeo.2015.10.038

Pérez-Martínez, C., Pérez-Cárceles, M. D., Legaz, I., Prieto-Bonete, G., & Luna, A. (2017). Quantification of nitrogenous bases, DNA and Collagen type I for the estimation of the postmortem interval in bone remains. *Forensic Science International*, *281*, 106–112. https://doi.org/10.1016/j.forsciint.2017.10.039

Peucker-Ehrenbrink, B., & Fiske, G. J. (2019). A continental perspective of the seawater 87Sr/86Sr record: A review. *Chemical Geology*, *510*, 140–165. https://doi.org/10.1016/j.chemgeo.2019.01.017

Pokines, J., Symes, S. A., & Roper, C. (2013). *Manual of Forensic Taphonomy*. Taylor & Francis Group. http://ebookcentral.proquest.com/lib/ncsu/detail.action?docID=1344839

Pollard, A. M., Pellegrini, M., & Lee-Thorp, J. (2011). Technical note: Some observations on the conversion of dental enamel δ18op values to δ18ow to determine human mobility. *American Journal of Physical Anthropology*, *145*(3), 499–504. https://doi.org/10.1002/ajpa.21524

Post, D. M. (2002). Using Stable Isotopes to Estimate Trophic Position: Models, Methods, and Assumptions. *Ecology*, *83*(3), 703–718. https://doi.org/10.2307/3071875

Quinn, R. L. (2024a). Bomb pulse 14 C evidence for consistent remodeling rates of cortical femur collagen in middle-late adulthood. *American Journal of Biological Anthropology*, *183*(4), e24887. https://doi.org/10.1002/ajpa.24887

Quinn, R. L. (2024b). How much time is recorded with a rib bone isotope? *Journal of Archaeological Science: Reports*, *57*, 104593. https://doi.org/10.1016/j.jasrep.2024.104593

Regan, L. (2006). *Isotopic Determination of Region of Origin in Modern Peoples: Applications for Identification of U.S. War-Dead From the Vietnam Conflict*. 295.

Reid, R. A. G., Jans, M. M. E., Chesson, L. A., Taylor, R. J., & Berg, G. E. (2024). The influence of taphonomy on histological and isotopic analyses of treated and untreated buried modern human bone. *Journal of Archaeological Science*, *161*, 105901. https://doi.org/10.1016/j.jas.2023.105901

Reitsema, L. J. (2013). Beyond diet reconstruction: Stable isotope applications to human physiology, health, and nutrition. *American Journal of Human Biology: The Official Journal of the Human Biology Council*, *25*(4), 445–456. https://doi.org/10.1002/ajhb.22398

Richards, M. P., Mays, S., & Fuller, B. T. (2002). Stable carbon and nitrogen isotope values of bone and teeth reflect weaning age at the Medieval Wharram Percy site, Yorkshire, UK. *American Journal of Physical Anthropology*, *119*(3), 205–210. https://doi.org/10.1002/ajpa.10124

Richards, M. P., & Trinkaus, E. (2009). Isotopic evidence for the diets of European Neanderthals and early modern humans. *Proceedings of the National Academy of Sciences*, *106*(38), 16034–16039. https://doi.org/10.1073/pnas.0903821106

Ritter, N., Schmitt, G. R., Taylor, L. R., Horowitz, J., United States, & National Institute of Justice (U.S.). (2007). *Missing persons and unidentified remains: The nation's silent mass disaster.* U.S. Dept. of Justice, Office of Justice Programs. https://catalog.hathitrust.org/Record/101806486

Ross, A. H., & Hale, A. R. (2018). Decomposition of juvenile-sized remains: A macro- and microscopic perspective. *Forensic Sciences Research*, *3*(4), 310–319. https://doi.org/10.1080/20961790.2018.1489362

Ross, A. H., & Passalacqua, N. V. (2024). *Chapter 8—Unidentified decedent investigation protocols* (A. H. Ross & J. H. Byrd, Eds.; pp. 247–258). Academic Press. https://doi.org/10.1016/B978-0-12-819394-5.00004-3

Ross, A. H., & Pilloud, M. (2021). The need to incorporate human variation and evolutionary theory in forensic anthropology: A call for reform. *American Journal of Physical Anthropology*, *176*(4), 672–683. https://doi.org/10.1002/ajpa.24384

Ross, A. H., & Williams, S. E. (2021). Ancestry Studies in Forensic Anthropology: Back on the Frontier of Racism. *Biology*, *10*(7), Article 7. https://doi.org/10.3390/biology10070602

Saul, T. B., Chesson, L. A., Steadman, D. W., & Gordon, G. W. (2021). Considerations for Stable Isotope Analysis of Human Hair: The Impact of Postmortem Environmental Exposure. *Forensic Anthropology*, *4*(3), 173–184. https://doi.org/10.5744/fa.2020.0052

Scheeres, M., Knipper, C., Hauschild, M., Schönfelder, M., Siebel, W., Pare, C., & Alt, K. W. (2014). "Celtic migrations": Fact or fiction? Strontium and oxygen isotope analysis of the

Czech cemeteries of Radovesice and Kutná Hora in Bohemia. *American Journal of Physical Anthropology*, *155*(4), 496–512. https://doi.org/10.1002/ajpa.22597

Scheuer, L., Black, S., & Schaefer, M. C. (2010). *Juvenile Osteology: A Laboratory and Field Manual*. Academic Press.

Schoeninger, M. J., & DeNiro, M. J. (1984). Nitrogen and carbon isotopic composition of bone collagen from marine and terrestrial animals. *Geochimica et Cosmochimica Acta*, *48*(4), 625–639. https://doi.org/10.1016/0016-7037(84)90091-7

Schoeninger, M. J., DeNiro, M. J., & Tauber, H. (1983). Stable nitrogen isotope ratios of bone collagen reflect marine and terrestrial components of prehistoric human diet. *Science (New York, N.Y.)*, *220*(4604), 1381–1383. https://doi.org/10.1126/science.6344217

Schoeninger, M. J., & Moore, K. (1992). Bone Stable Isotope Studies in Archaeology. *Journal of World Prehistory*, *6*(2), 247–296.

Schroeder, H., O'Connell, T. C., Evans, J. A., Shuler, K. A., & Hedges, R. E. M. (2009). Trans-Atlantic slavery: Isotopic evidence for forced migration to Barbados. *American Journal of Physical Anthropology*, *139*(4), 547–557. https://doi.org/10.1002/ajpa.21019

Schwarcz, H. P., & Nahal, H. (2021). Theoretical and observed C/N ratios in human bone collagen. *Journal of Archaeological Science*, *131*, 105396. https://doi.org/10.1016/j.jas.2021.105396

Schwarcz, H. P., & Schoeninger, M. J. (1991). Stable isotope analyses in human nutritional ecology. *American Journal of Physical Anthropology*, *34*, 283–321. https://doi.org/10.1002/ajpa.1330340613

Scott, G. R., & Irish, J. D. (2017). *Human Tooth Crown and Root Morphology: The Arizona State University Dental Anthropology System*. Cambridge University Press. https://doi.org/10.1017/9781316156629

Scott, G. R., Pilloud, M. A., Navega, D., Coelho, J. d'Oliveira, Cunha, E., & Irish, J. D. (2018). rASUDAS: A New Web-Based Application for Estimating Ancestry from Tooth Morphology. *Forensic Anthropology*, *1*(1). https://doi.org/10.5744/fa.2018.0003

Sealy, J., Armstrong, R., & Schrire, C. (1995). Beyond lifetime averages: Tracing life histories through isotopic analysis of different calcified tissues from archaeological human skeletons. *Antiquity*, *69*(263), 290–300. https://doi.org/10.1017/S0003598X00064693

Sealy, J., Johnson, M., Richards, M., & Nehlich, O. (2014). Comparison of two methods of extracting bone collagen for stable carbon and nitrogen isotope analysis: Comparing whole bone demineralization with gelatinization and ultrafiltration. *Journal of Archaeological Science*, *47*, 64–69. https://doi.org/10.1016/j.jas.2014.04.011

Sharp, Z. (2017). Principles of Stable Isotope Geochemistry, 2nd Edition. *Open Textbooks*. https://doi.org/ https://doi.org/10.25844/h9q1-0p82

Shepherd, T. J., Dirks, W., Roberts, N. M. W., Patel, J. G., Hodgson, S., Pless-Mulloli, T., Walton, P., & Parrish, R. R. (2016). Tracing fetal and childhood exposure to lead using isotope analysis of deciduous teeth. *Environmental Research*, *146*, 145–153. https://doi.org/10.1016/j.envres.2015.12.017

Simmons, T. (2017). Post-Mortem Interval Estimation: An Overview of Techniques. In *Taphonomy of Human Remains: Forensic Analysis of the Dead and the Depositional Environment* (pp. 134–142). John Wiley & Sons, Ltd. https://doi.org/10.1002/9781118953358.ch10

Singh Sehrawat, J., & Rai, N. (2023). Carbon (δ13C) and nitrogen (δ15N) isotope ratios reveal geographic affinity and dietary status of Ajnala skeletal remains: A forensic anthropological study. *Medicine, Science, and the Law*, *63*(4), 298–308. https://doi.org/10.1177/00258024231159591

Slice, D., & Ross, A. (2024). *3D-ID: geometric morphometric classification of crania for forensic scientists*. http://www.3d-id.org

Smith, C. I., Nielsen-Marsh, C. M., Jans, M. M. E., & Collins, M. J. (2007). Bone diagenesis in the European Holocene I: Patterns and mechanisms. *Journal of Archaeological Science*, *34*(9), 1485–1493. https://doi.org/10.1016/j.jas.2006.11.006

Snoeck, C., & Pellegrini, M. (2015). Comparing bioapatite carbonate pre-treatments for isotopic measurements: Part 1—Impact on structure and chemical composition. *Chemical Geology*, *417*, 394–403. https://doi.org/10.1016/j.chemgeo.2015.10.004

Standard for Population Affinity Estimation in Forensic Anthropology (132; Version 1st Edition). (2023).

Stenhouse, M. J., & Baxter, M. S. (2020). 3. The Uptake of Bomb 14C in Humans. In *Radiocarbon Dating* (pp. 324–341). University of California Press. https://www.degruyter.com/document/doi/10.1525/9780520312876-033/pdf

Stewart, K. G. (Kevin G., & Roberson, M.-R. (2007). *Exploring the geology of the Carolinas: A field guide to favorite places from Chimney Rock to Charleston*. University of North Carolina Press. https://catalog.lib.ncsu.edu/catalog/NCSU1963937

Stokes, K. L., Forbes, S. L., Benninger, L. A., Carter, D. O., & Tibbett, M. (2009). *Decomposition Studies Using Animal Models in Contrasting Environments: Evidence from Temporal Changes in Soil Chemistry and Microbial Activity* (K. Ritz, L. Dawson, & D. Miller, Eds.; pp. 357–377). Springer Netherlands. https://doi.org/10.1007/978-1-4020-9204-6_23

Symes, S. A., Williams, J. A., Murray, E. A., Hoffman, J. M., Holland, T. D., Saul, J. M., Saul, F. P., & Pope, E. J. (2002). Taphonomic Context of Sharp-Force Trauma in Suspected Cases of Human Mutilation and Dismemberment. In *Advances in Forensic Taphonomy*. CRC Press.

Szpak, P. (2011). Fish bone chemistry and ultrastructure: Implications for taphonomy and stable isotope analysis. *Journal of Archaeological Science*, *38*(12), 3358–3372. https://doi.org/10.1016/j.jas.2011.07.022

Szpak, P., Krippner, K., & Richards, M. P. (2017). Effects of Sodium Hydroxide Treatment and Ultrafiltration on the Removal of Humic Contaminants from Archaeological Bone. *International Journal of Osteoarchaeology*, *27*(6), 1070–1077. https://doi.org/10.1002/oa.2630

Tarrant, D., Yazedjian, L., Hepburn, J., Fonseca, S., Talamo, S., & Richards, M. (2025). The use of dietary isotopes as a preliminary step in the death investigation of unidentified skeletal human remains in British Columbia, Canada. *Journal of Forensic Sciences*, *70*(1), 28–37. https://doi.org/10.1111/1556-4029.15653

Tea, I., De Luca, A., Schiphorst, A.-M., Grand, M., Barillé-Nion, S., Mirallié, E., Drui, D., Krempf, M., Hankard, R., & Tcherkez, G. (2021). Stable Isotope Abundance and Fractionation in Human Diseases. *Metabolites*, *11*(6), 370. https://doi.org/10.3390/metabo11060370

Tipple, B. J., & Pagani, M. (2007). The Early Origins of Terrestrial C4 Photosynthesis. *Annual Review of Earth and Planetary Sciences*, *35*(Volume 35, 2007), 435–461. https://doi.org/10.1146/annurev.earth.35.031306.140150

Trueman, C. N., & Martill, D. M. (2002). The long–term survival of bone: The role of bioerosion. *Archaeometry*, *44*(3), 371–382. https://doi.org/10.1111/1475-4754.t01-1-00070

Turner-Walker, G. (2007). The Chemical and Microbial Degradation of Bones and Teeth. In R. Pinhasi & S. Mays (Eds.), *Advances in Human Palaeopathology* (Vol. 1, pp. 3–29). John Wiley & Sons, Ltd. https://doi.org/10.1002/9780470724187.ch1

Turner-Walker, G., Galiacho, A. G., Armentano, N., & Hsu, C.-Q. (2023). Bacterial bioerosion of bones is a post-skeletonisation phenomenon and appears contingent on soil burial. *Quaternary International*, *660*, 75–83. https://doi.org/10.1016/j.quaint.2022.12.009

Tuross, N., Behrensmeyer, A. K., & Eanes, E. D. (1989). Strontium increases and crystallinity changes in taphonomic and archaeological bone. *Journal of Archaeological Science*, *16*(6), 661–672. https://doi.org/10.1016/0305-4403(89)90030-7

Tykot, R. (2016). Isotope Analysis and the Histories of Maize. In J. Staller, R. Tykot, & B. Benz (Eds.), *Histories of Maize in Mesoamerica: Multidisciplinary Approaches* (1st ed., pp. 130–142). Routledge. https://doi.org/10.4324/9781315427294

Ubelaker, D. H., & Khosrowshahi, H. (2019). Estimation of Age in Forensic Anthropology: Historical Perspective and Recent Methodological Advances. *Forensic Sciences Research*, *4*(1), 1–9. https://doi.org/10.1080/20961790.2018.1549711

Ueda, M., & Bell, L. S. (2021). Assessing the predictability of existing water-to-enamel geolocation models against known human teeth. *Scientific Reports*, *11*, 15645. https://doi.org/10.1038/s41598-021-95153-w

van Klinken, G. J. (1999). Bone Collagen Quality Indicators for Palaeodietary and Radiocarbon Measurements. *Journal of Archaeological Science*, *26*(6), 687–695. https://doi.org/10.1006/jasc.1998.0385

van Klinken, G. J., Richards, M. P., & Hedges, B. E. M. (2002). An Overview of Causes for Stable Isotopic Variations in Past European Human Populations: Environmental, Ecophysiological, and Cultural Effects. In S. H. Ambrose & M. A. Katzenberg (Eds.), *Biogeochemical Approaches to Paleodietary Analysis* (pp. 39–63). Springer US. https://doi.org/10.1007/0-306-47194-9_3

van Klinken, G. J. van, & Hedges, R. E. M. (1995). Experiments on Collagen-Humic Interactions: Speed of Humic Uptake, and Effects of Diverse Chemical Treatments. *Journal of Archaeological Science*, *22*(2), 263–270. https://doi.org/10.1006/jasc.1995.0028

Vogel, J. C., & Merwe, N. J. van der. (1977). Isotopic Evidence for Early Maize Cultivation in New York State. *American Antiquity*, *42*(2), 238–242. https://doi.org/10.2307/278984

Warner, M., Plemons, A., Herrmann, N., & Regan, L. (2017). Refining Stable Oxygen and Hydrogen Isoscapes for the Identification of Human Remains in Mississippi. *Journal of Forensic Sciences*, *63*. https://doi.org/10.1111/1556-4029.13575

WaterIsotopes.org. (n.d.). Retrieved May 25, 2022, from https://wateriso.utah.edu/waterisotopes/index.html

Watts, E., Coleman, D., Colon-Ramirez, A., & Walsh, A. (2019). Unexpected Sources of Strontium to the Neuse and Cape Fear River Basins, North Carolina: Implications for the Global Strontium Isotope Budget in Seawater. *Journal of Geophysical Research: Earth Surface*, *124*. https://doi.org/10.1029/2018JF004797

Weiner, S., & Wagner, H. D. (1998). THE MATERIAL BONE: Structure-Mechanical Function Relations. *Annual Review of Materials Science*, *28*(1), 271–298. https://doi.org/10.1146/annurev.matsci.28.1.271

Wescott, D. J. (2018). Recent Advances in Forensic Anthropology: Decomposition Research. *Forensic Sciences Research*, *3*(4), 278–293. https://doi.org/10.1080/20961790.2018.1488571

West, J. B., Bowen, G. J., Cerling, T. E., & Ehleringer, J. R. (2006). Stable isotopes as one of nature's ecological recorders. *Trends in Ecology & Evolution*, *21*(7), 408–414. https://doi.org/10.1016/j.tree.2006.04.002

White, L., & Booth, T. J. (2014). The origin of bacteria responsible for bioerosion to the internal bone microstructure: Results from experimentally-deposited pig carcasses. *Forensic Science International*, *239*, 92–102. https://doi.org/10.1016/j.forsciint.2014.03.024

White, T. D., Black, M. T., & Folkens, P. A. (2011). *Human Osteology*. Academic Press.

White, T. D., Black, M. T., & Folkens, P. A. (2012). Chapter 5—Teeth. In T. D. White, M. T. Black, & P. A. Folkens (Eds.), *Human Osteology (Third Edition)* (pp. 101–128). Academic Press. https://doi.org/10.1016/B978-0-12-374134-9.50005-2

Wright, L. E. (2005). Identifying immigrants to Tikal, Guatemala: Defining local variability in strontium isotope ratios of human tooth enamel. *Journal of Archaeological Science*, *32*(4), 555–566. https://doi.org/10.1016/j.jas.2004.11.011

Wright, L. E. (2012). Immigration to Tikal, Guatemala: Evidence from stable strontium and oxygen isotopes. *Journal of Anthropological Archaeology*, *31*(3), 334–352. https://doi.org/10.1016/j.jaa.2012.02.001

Wright, L. E., & Schwarcz, H. P. (1998). Stable carbon and oxygen isotopes in human tooth enamel: Identifying breastfeeding and weaning in prehistory. *American Journal of Physical Anthropology*, *106*(1), 1–18. https://doi.org/10.1002/(SICI)1096-8644(199805)106:1<1::AID-AJPA1>3.0.CO;2-W

Yoshino, M., Kimijima, T., Miyasaka, S., Sato, H., & Seta, S. (1991). Microscopical study on estimation of time since death in skeletal remains. *Forensic Science International*, *49*(2), 143–158. https://doi.org/10.1016/0379-0738(91)90074-S

APPENDICES

Appendix A

Chapter 3 Supplementary File

Sample ID	Season	Deposition	mg C	δ13C (‰)	δ15N (‰)	C:N
F1	Summer	Blanket	0.02	-11.46	-0.4	5
F3	Fall	Blanket	0.18	-8.98	1.4	3.4
F5	Winter	Blanket	0.12	-9.90	1.9	3.5
F8	Spring	Blanket	0.12	-9.50	1.6	3.4
F9	Spring	Bag	0.09	-10.83	2.1	3.8
F10	Summer	Blanket	0.59	-9.85	2.0	3.6
F12	Summer	Control	0.19	-10.47	2.6	3.7
F13	Fall	Blanket	0.11	-9.45	1.2	3.3
F14	Fall	Bag	0.06	-9.62	0.9	3.6
F15	Fall	Control	0.03	-7.94	-0.3	4
F16	Winter	Blanket	0.08	-9.12	1.9	3.4
F17	Winter	Bag	0.07	-10.94	2.1	3.6
F18	Winter	Control	0.03	-9.00	0.8	4.1
F19	Spring	Blanket	0.07	-10.72	1.2	3.5
F20	Spring	Bag	0.1	-9.98	2.0	3.4
F21	Spring	Control	0.03	-11.80	0.5	4.2
J1	Summer	Surface	1.04	-15.65	3.8	4.1
J3	Fall	Surface	0.32	-15.03	2.2	3.6
J4	Fall	Buried	0.43	-15.29	3.3	3.6
J5	Winter	Surface	0.33	-14.61	3.4	3.6
J6	Winter	Buried	0.38	-15.10	3.3	3.4
J7	Spring	Surface	0.71	-13.98	3.5	3.6
J8	Spring	Buried	0.19	-14.53	2.5	3.5
J9	Summer	Surface	0.14	-15.62	2.9	4.1
J10	Summer	Buried	0.36	-17.28	3.5	4.3
J12	Fall	Buried	0.16	-14.29	2.9	4.2
J14	Winter	Buried	0.17	-13.84	3.1	3.3
J15	Spring	Surface	0.02	-13.53	1.2	5
J16	Spring	Buried	0.08	-14.13	2.4	3.4

Appendix B

Chapter 4 Supplementary File 1

Project ID	Contact Name	Contact Email	Citation	URL	Project Name	License	Proprietary
00099	Gabriel Bowen	gabe.bowen@utah.edu	unpublished		Courses and misc		0
00225	Gabriel Bowen	gabe.bowen@utah.edu			2019 Groundwater		0
00140	J. Renee Brooks	Brooks.Reneej@epa.gov	Brooks, J. R. (2024) Water Stable Isotope data from NARS (NRSA and NLA). U.S. EPA Office of Research and Development.	https://doi.org/10.23719/1531017	NARS 2013-2014	https://pasteur.epa.gov/license/sciencehub-license.html	0
00048	Carol Kendall		Deacon, J.R., Lee, C.J., Toccalino, P.L., Warren, M.P., Baker, N.T., Crawford, C.G., Gilliom, R.G., and Woodside, M.D., 2015, Tracking water-quality of the Nationâ€™s rivers and streams, U.S. Geological Survey Web page	https://10.5066/F70G3H51	NASQAN/HBN, C. Kendall Thesis (1993)		0
00287	Phoebe Aron	paron@umich.edu	Aron, P.G., Levin, N.E., Beverly, E.J., Huth, T.E., Passey, B.H., Pelletier, E.M., Poulsen, C.J., Winkelstern, I.Z., Yarian, D.A., 2020. Triple oxygen isotopes in the water cycle. Chemical Geology 120026.	https://doi.org/10.1016/j.chemgeo.2020.120026	UM crowdsourced triple oxygen isotope dataset		0

Chapter 4 Supplementary File 1 (continued).

00275	Isoforensics Inc	howaconsulting.llc@gmail.com	unpublished	https://www.isoforensics.com/	Isoforensic Global DB	NA	0
00165	J. Renee Brooks	Brooks.Reneej@epa.gov	Brooks, J. R. (2024) Water Stable Isotope data from NARS (NRSA and NLA). U.S. EPA Office of Research and Development.	https://doi.org/10.23719/1531017	NARS 2008-2009	https://pasteur.epa.gov/license/sciencehub-license.html	0
00210	USGS Water Data Support Team		United States Geological Survey (2019) Water quality samples for the nation.	https://nwis.waterdata.usgs.gov/nwis/	US Water Quality Field/Lab Samples		0
00077	Gabriel Bowen	gabe.bowen@utah.edu	Bowen, G. J., et al (2007)Stable isotope ratios of tap water in the contiguous United States, Water Resour. Res., 43, W03419 doi: 10.1029/2006WR005186		USTap		0
00090	Tyler Coplen		Coplen, T.B., Landwehr, J.M., Qi, Haiping, and Lorenz, J.M. (2013) The d2H and d18O of tap water from 349 sites in the United States and selected territories: U.S. Geological Survey Data Series 703, 113 p., at https://pubs.usgs.gov/ds/703.	http://pubs.usgs.gov/ds/703	Tap water at 349 sites		0

Chapter 4 Supplementary File 2 Compiled $^{87/86}Sr$ data from Watts et al. 2018 and Crenshaw 2020.

Sample	Date	Type	Latitude (°N)	Longitude (°E)	Downstream distance (km)	$^{87/86}Sr$	[Sr] (ppb)	Pub
WEH-02F			36.21	-79.19		0.704456		Crenshaw
WEH-02U			36.21	-79.19		0.704463		Crenshaw
NCSW-33A			35.427	-80.411		0.704873		Crenshaw
EW-EEH			36.19	-79.15		0.704975		Crenshaw
EEH-02F			36.19	-79.15		0.705091		Crenshaw
EEH-02U			36.19	-79.15		0.705094		Crenshaw
EW-WEH			36.21	-79.19		0.705269		Crenshaw
EC04			36.06	-78.98		0.705365		Crenshaw
EC05F			36.06	-78.98		0.70537		Crenshaw
EC02			36.06	-78.98		0.705371		Crenshaw
EC03			36.06	-78.98		0.705375		Crenshaw
NCSW-07			36.033	-79.944		0.705379		Crenshaw
NCSW-04			36.386	-79.108		0.705396		Crenshaw
EC05U			36.06	-78.98		0.705403		Crenshaw
NCSW-Q19			36.386	-79.107		0.705461		Crenshaw
WFL-03U			36.09	-78.82		0.705642		Crenshaw
WFL-03F			36.09	-78.82		0.705647		Crenshaw
EW-WFL			36.09	-78.82		0.706099		Crenshaw
NCSW-44			35.548	-79.025		0.706258		Crenshaw
EW-WFL02			36.09	-78.82		0.70627		Crenshaw
NCSW-01A			35.776	-79.147		0.706321		Crenshaw
NCSW-01B			35.776	-79.147		0.706331		Crenshaw
NCSW-08			35.776	-79.147		0.706413		Crenshaw
NCSW-45			35.396	-78.774		0.706437		Crenshaw
NCSW-43.d			36.089	-79.37		0.706581		Crenshaw

Chapter 4 Supplementary File 2 (continued).

NCSW-43			36.089	-79.37		0.706608		Crenshaw
NCSW-Q20			36.334	-78.768		0.706633		Crenshaw
NCSW-03			36.334	-78.768		0.706694		Crenshaw
EW-CRB			36.05	-78.75		0.706837		Crenshaw
NCSW-02			36.348	-78.414		0.706849		Crenshaw
RCC-83			34.4	-78.29		0.707054		Crenshaw
NCSW-39B			34.75	-78.78		0.707433		Crenshaw
NCSW-39A			34.75	-78.78		0.707462		Crenshaw
EW-LRB			36.05	-78.72		0.707489		Crenshaw
EW-NLB			36	-78.67		0.707518		Crenshaw
EW-EFL			35.94	-78.58		0.707895		Crenshaw
EW-EFL02			35.94	-78.58		0.707923		Crenshaw
EFL-03U			35.94	-78.58		0.707963		Crenshaw
NCSW-32			35.822	-78.352		0.707989		Crenshaw
EW-GC			35.18	-77.13		0.708146		Crenshaw
EW-RGS			35.65	-78.41		0.708306		Crenshaw
EW-LRNM			35.35	-78.03		0.708422		Crenshaw
EW-LROM			35.37	-78.02		0.708597		Crenshaw
EW-LRGS			35.59	-78.19		0.708628		Crenshaw
EW-PL			35.31	-77.94		0.70864		Crenshaw
EW-SS			35.23	-77.85		0.708801		Crenshaw
70-2017 RCC			34.83	-80.67		0.708821		Crenshaw
NCSW-Q48			35.697	-76.11		0.708911		Crenshaw
NCSW-35A			35.441	-79.589		0.708938		Crenshaw
EW-TR			35.1	-77.05		0.709114		Crenshaw
NCSW-Q77			34.919	-77.263		0.709189		Crenshaw

Chapter 4 Supplementary File 2 (continued).

MFL-03U			36.056	-78.676		0.709221		Crenshaw
EW-FB			34.99	-76.95		0.709222		Crenshaw
EW-FR			35.07	-76.97		0.709223		Crenshaw
NCSW-36B			34.94	-79.88		0.70924		Crenshaw
NCSW-Q67			35.585	-76.518		0.709255		Crenshaw
NCSW-36A			34.94	-79.88		0.709265		Crenshaw
EW-SCM			35.14	-77.06		0.709301		Crenshaw
NCSW-46.d			35.348	-78.024		0.709318		Crenshaw
NCSW-46			35.348	-78.024		0.709346		Crenshaw
NCSW-47			35.312	-77.945		0.709362		Crenshaw
NCSW-Q78			34.779	-76.859		0.709411		Crenshaw
EW-SCNM			35.22	-77.15		0.709467		Crenshaw
NCSW-31			35.96	-77.795		0.709523		Crenshaw
NCSW-Q48.2			35.72	-76.194		0.709709		Crenshaw
RCC-84			34.36	-77.9		0.709819		Crenshaw
RCC-86			34.01	-78.63		0.709844		Crenshaw
EW-SCOM			35.23	-77.11		0.709887		Crenshaw
NCSW-Q26			36.35	-76.073		0.709906		Crenshaw
NCSW-Q47			35.862	-76.384		0.709919		Crenshaw
EW-MFL02			36.06	-78.68		0.70995		Crenshaw
NCSW-48.d			35.312	-77.303		0.710058		Crenshaw
NCSW-48			35.312	-77.303		0.710079		Crenshaw
71-2017 RCC			34.92	-80.52		0.710174		Crenshaw
NCSW-Q66			35.231	-77.114		0.71021		Crenshaw
EW-MFL			36.06	-78.68		0.710311		Crenshaw

Chapter 4 Supplementary File 2 (continued).

NCSW-34A			35.306	-80.074		0.710372		Crenshaw
NCSW-16			35.836	-80.831		0.710483		Crenshaw
NCSW-41B			34.98	-77.86		0.710489		Crenshaw
NCSW-41A			34.98	-77.86		0.710526		Crenshaw
NCSW-30			35.895	-77.529		0.710537		Crenshaw
NCSW-Q25			36.268	-76.545		0.710603		Crenshaw
NCSW-27			36.209	-77.383		0.710623		Crenshaw
NCSW-42.d			34.54	-79.04		0.710758		Crenshaw
NCSW-42			34.54	-79.04		0.710795		Crenshaw
NCSW-29			35.86	-77.041		0.711012		Crenshaw
NCSW-28			36.401	-76.93		0.711031		Crenshaw
NCSW-26			36.427	-77.591		0.711051		Crenshaw
RCC-Q81B			34.624	-79.057		0.711488		Crenshaw
EW-GFT2			35.37	-77.45		0.711562		Crenshaw
RCC-Q81A			34.901	-79.349		0.711669		Crenshaw
NCSW-40A			34.76	-78.41		0.71192		Crenshaw
RCC-82			34.48	-78.88		0.712102		Crenshaw
NCSW-22			35.285	-82.027		0.71215		Crenshaw
NCSW-06			36.375	-79.993		0.712194		Crenshaw
NCSW-38			34.77	-79.09		0.712295		Crenshaw
NCSW-05			36.473	-79.736		0.712553		Crenshaw
74-2017 RCC			34.77	-79.09		0.712611		Crenshaw
NCSW-25			35.299	-81.004		0.712712		Crenshaw
NCSW-37B			34.82	-79.53		0.712719		Crenshaw
NCSW-Q18			36.474	-79.737		0.712757		Crenshaw
NCSW-37A			34.82	-79.53		0.712919		Crenshaw

Chapter 4 Supplementary File 2 (continued).

73-2017 RCC			34.82	-79.53		0.713135		Crenshaw
NCSW-15			36.014	-80.416		0.714381		Crenshaw
NCSW-10			36.448	-81.603		0.714891		Crenshaw
NCSW-Q15			35.926	-79.054		0.715016		Crenshaw
NCSW-Q16			36.216	-80.434		0.715071		Crenshaw
NCSW-09			36.239	-81.822		0.715783		Crenshaw
NCSW-24			35.252	-81.255		0.715946		Crenshaw
NCSW-17			35.797	-82.686		0.716407		Crenshaw
NCSW-12			36.086	-81.366		0.717342		Crenshaw
NCSW-19			35.202	-83.841		0.717491		Crenshaw
NCSW-18			35.332	-83.594		0.717829		Crenshaw
NCSW-20			35.367	-83.255		0.718226		Crenshaw
NCSW-13			35.992	-81.539		0.718234		Crenshaw
NCSW-23			35.304	-81.567		0.718539		Crenshaw
NCSW-21			35.502	-82.593		0.718835		Crenshaw
NCSW-11			36.474	-81.337		0.719094		Crenshaw
NCSW-14			35.793	-81.677		0.720729		Crenshaw
32-2017 RCC			35.746	-82.209		0.726745		Crenshaw
W-11	22-May-17	Groundwater	36.069	-79	23.1	0.703835	100	Watts
W-09	22-May-17	Groundwater	36.158	-78.959	21.7	0.704045	230	Watts
W-02	22-May-17	Groundwater	36.056	-78.994	24.4	0.704218	120	Watts
WEH-02F	9-Apr-17	Water(F)	36.205	-79.19	0	0.704456	52	Watts
WEH-02U	9-Apr-17	Water(U)	36.205	-79.19	0	0.704463	53	Watts
W-07	22-May-17	Groundwater	36.071	-78.956	26	0.704537	100	Watts
SR-05	3-Feb-17	Diabase rock	36.107	-78.761	39	0.704711		Watts

Chapter 4 Supplementary File 2 (continued).

SR-03	3-Feb-17	Diabase rock	36.107	-78.761	38.9	0.70475		Watts
W-06	22-May-17	Groundwater	36.096	-78.93	26.6	0.704842	270	Watts
SR-01	3-Feb-17	Diabase rock	36.107	-78.761	40.3	0.704845	85,000	Watts
W-01	22-May-17	Groundwater	36.068	-78.996	23.4	0.704929	730	Watts
EW-EEH	1-Jun-16	Water(F)	36.191	-79.15	4.08	0.704975	59	Watts
EEH-02F	9-Apr-17	Water(F)	36.191	-79.15	4.08	0.705091	48	Watts
EEH-02U	9-Apr-17	Water(U)	36.191	-79.15	4.08	0.705094	49	Watts
ACR16	16-Jun-17	Water(F)	36.128	-79.406	51.2	0.705152	68	Watts
BQ-06	17-Feb-17	Dioritic rock	36.105	-79.012	19.7	0.705233		Watts
BQ-07	17-Feb-17	Water(F)	36.106	-79.005	20.2	0.705256	68	Watts
EW-WEH	1-Jun-16	Water(F)	36.205	-79.19	0.25	0.705269	69	Watts
EC04	17-Jun-16	Water(F)	36.056	-78.978	25.5	0.705365	77	Watts
EC05F	9-Apr-17	Water(F)	36.056	-78.978	25.5	0.70537	50	Watts
EC02	17-Jun-16	Water(F)	36.056	-78.978	25.5	0.705371	78	Watts
EC03	17-Jun-16	Water(F)	36.056	-78.978	25.5	0.705375	77	Watts
EC05U	9-Apr-17	Water(U)	36.056	-78.978	25.5	0.705403	52	Watts
W-04	22-May-17	Groundwater	36.116	-79.041	16.9	0.705559	100	Watts
ACR15	16-Jun-17	Water(F)	35.996	-79.951	0	0.705561	85	Watts
WFL-03U	9-Apr-17	Water(U)	36.088	-78.824	35.7	0.705642	51	Watts
WFL-03F	9-Apr-17	Water(F)	36.088	-78.824	35.7	0.705647	52	Watts
ACR14	16-Jun-17	Water(F)	35.751	-79.732	33.5	0.705679	68	Watts
ACR13	16-Jun-17	Water(F)	35.641	-79.62	49.4	0.705691	69	Watts
W-05	22-May-17	Groundwater	35.999	-78.992	29.2	0.705739	140	Watts
W-08	22-May-17	Groundwater	36.251	-78.963	21.2	0.705751	50	Watts
ACR18	16-Jun-17	Water(F)	35.772	-79.144	90.7	0.705798	59	Watts
ACR12	16-Jun-17	Water(F)	35.544	-79.587	59.9	0.70583	70	Watts
W-03	22-May-17	Groundwater	36.025	-79.01	25.9	0.705887	84	Watts

Chapter 4 Supplementary File 2 (continued).

EW-WFL	1-Jun-16	Water(F)	36.088	-78.823	35.5	0.706099	60	Watts
ACR11	16-Jun-17	Water(F)	35.458	-79.382	71.1	0.706218	68	Watts
EW-WFL02	7-Jul-16	Water(F)	36.088	-78.824	35.5	0.70627	39	Watts
BQ-03A	17-Feb-17	Granitic softrock	36.106	-79.012	19.7	0.706323		Watts
BQ-05	17-Feb-17	Granitic rock	36.105	-79.012	19.7	0.70662	600,000	Watts
ACR10	16-Jun-17	Water(F)	35.55	-79.025	97.2	0.706746	68	Watts
ACR17	16-Jun-17	Water(F)	36.091	-79.37	53.4	0.706787	67	Watts
ACR09	16-Jun-17	Water(F)	35.398	-78.774	125	0.706801	67	Watts
EW-CRB	7-Jul-16	Water(F)	36.05	-78.751	43.4	0.706837	45	Watts
W-12	22-May-17	Groundwater	35.994	-78.986	30	0.706958	190	Watts
ACR08	16-Jun-17	Water(F)	35.047	-78.859	144	0.70702	58	Watts
ACR07	16-Jun-17	Water(F)	34.997	-78.851	149	0.707033	56	Watts
BQ-02	17-Feb-17	Granitic softrock	36.106	-79.011	19.7	0.707261	2,300,000	Watts
ACR06	16-Jun-17	Water(F)	34.834	-78.824	165	0.707314	50	Watts
ACR03	16-Jun-17	Water(F)	34.403	-78.293	232	0.707408	45	Watts
EW-LRB	7-Jul-16	Water(F)	36.053	-78.722	45.6	0.707489	50	Watts
EW-NLB	7-Jul-16	Water(F)	36.002	-78.665	52.6	0.707518	50	Watts
ACR05	16-Jun-17	Water(F)	34.626	-78.575	197	0.707671	38	Watts
EW-EFL	1-Jun-16	Water(F)	35.94	-78.58	62.6	0.707895	44	Watts
EW-EFL02	7-Jul-16	Water(F)	35.94	-78.58	62.6	0.707923	44	Watts
EFL-03F	9-Apr-17	Water(F)	35.94	-78.58	62.5	0.707958		Watts
EFL-03U	9-Apr-17	Water(U)	35.94	-78.58	62.5	0.707963	41	Watts
EW-GC	26-May-16	Water(F)	35.179	-77.132	220	0.708146	700	Watts
EW-RGS	1-Jun-16	Water(F)	35.646	-78.406	94.4	0.708306	55	Watts
EW-LRNM	1-Jun-16	Water(F)	35.35	-78.032	142	0.708422	47	Watts

Chapter 4 Supplementary File 2 (continued).

EW-LRO	1-Jun-16	Water(F)	35.371	-78.018	141	0.708597	48	Watts
EW-LRGS	1-Jun-16	Water(F)	35.589	-78.188	114	0.708628	56	Watts
EW-PL	1-Jun-16	Water(F)	35.314	-77.945	150	0.70864	48	Watts
SS-1916	9-Jan-16	Water(F)	35.229	-77.846	163	0.708726	39	Watts
SS-81215	12-Aug-15	Water(F)	35.229	-77.846	163	0.708736	73	Watts
EW-SS	26-May-16	Water(F)	35.229	-77.846	163	0.708801	49	Watts
SS-91315	13-Sep-15	Water(F)	35.229	-77.846	163	0.708868	66	Watts
SS-112215	22-Nov-15	Water(F)	35.229	-77.846	163	0.708956	27	Watts
NB-112215	22-Nov-15	Water(F)	35.104	-77.035	232	0.709031	35	Watts
EW-TR	26-May-16	Water(F)	35.099	-77.048	231	0.709114	180	Watts
ACR02	16-Jun-17	Water(F)	34.235	-77.952	262	0.70912	470	Watts
NB-91315	13-Sep-15	Water(F)	35.104	-77.035	232	0.709173	870	Watts
NB-81215	12-Aug-15	Water(F)	35.104	-77.035	232	0.709174	810	Watts
ACR01	16-Jun-17	Water(F)	34.049	-77.92	279	0.709177	2,800	Watts
PC-91315	13-Sep-15	Water(F)	34.936	-76.841	257	0.709181	2700	Watts
FB-91315	13-Sep-15	Water(F)	34.985	-76.95	245	0.709187	2,300	Watts
PC-101615	16-Oct-15	Water(F)	34.936	-76.841	257	0.709191	1,000	Watts
O-81215	12-Aug-15	Water(F)	35.018	-76.705	263	0.709191	3,600	Watts
PC-101515	15-Oct-15	Water(F)	34.936	-76.841	257	0.709195	1,100	Watts
NB-101515	15-Oct-15	Water(F)	35.104	-77.035	232	0.709198	290	Watts
NB-1916	9-Jan-16	Water(F)	35.104	-77.035	232	0.709198	60	Watts
O-112215	22-Nov-15	Water(F)	35.018	-76.705	263	0.709202	1,200	Watts
O-1916	9-Jan-16	Water(F)	35.018	-76.705	263	0.709203	950	Watts
O-101515	15-Oct-15	Water(F)	35.018	-76.705	263	0.709211	1,700	Watts
CR110FB	9-Oct-15	Water(F)	34.984	-76.948	246	0.709213		Watts
MFL-03U	9-Apr-17	Water(U)	36.056	-78.676	49	0.709221	36	Watts
EW-FB	26-May-16	Water(F)	34.985	-76.95	245	0.709222	760	Watts

Chapter 4 Supplementary File 2 (continued).

MFL-03F	9-Apr-17	Water(F)	36.056	-78.676	49	0.709223	35	Watts
EW-FR	26-May-16	Water(F)	35.067	-76.97	239	0.709223	390	Watts
FB-101515	15-Oct-15	Water(F)	34.985	-76.95	245	0.709227	400	Watts
FB-1916	9-Jan-16	Water(F)	34.985	-76.95	245	0.709232	100	Watts
FB-112215	22-Nov-15	Water(F)	34.985	-76.95	245	0.709251	110	Watts
EW-SCM	26-May-16	Water(F)	35.141	-77.062	228	0.709301	54	Watts
SS-101515	15-Oct-15	Water(F)	35.229	-77.846	163	0.70938	58	Watts
EW-SCOM	26-May-16	Water(F)	35.231	-77.114	219	0.709887	62	Watts
EW-MFL02	7-Jul-16	Water(F)	36.056	-78.676	49.3	0.70995	35	Watts
WS-B01	16-Dec-16	Granitic rock	35.808	-78.496	76.8	0.709991		Watts
W-10	22-May-17	Groundwater	36.243	-79.115	7.97	0.710005	31	Watts
EW-MFL	1-Jun-16	Water(F)	36.056	-78.676	49.3	0.710311	39	Watts
WS-S01	16-Dec-16	Weathered granite	35.813	-78.498	76.3	0.710392		Watts
G-81215	12-Aug-15	Water(F)	35.37	-77.446	185	0.71075	55	Watts
EW-GFT2	26-May-16	Water(F)	35.37	-77.446	185	0.711562	32	Watts
WS-S02	16-Dec-16	Weathered granite	35.813	-78.498	76.3	0.71314		Watts
WS-I02	16-Dec-16	Granitic softrock	35.809	-78.498	76.5	0.713644		Watts
BQ-04	17-Feb-17	Saprolite	36.106	-79.012	19.7	0.714365	34,000	Watts
WS-B02	16-Dec-16	Granitic rock	35.808	-78.496	76.8	0.71474		Watts
WS-I01	16-Dec-16	Granitic softrock	35.809	-78.498	76.5	0.71526		Watts
BQ-01	17-Feb-17	Saprolite	36.106	-79.011	19.7	0.719074	15,000	Watts

Chapter 4 Supplementary File 3 Oxygen water data from waterisotopes.org.

Site Name	Latitude	Longitude	Sample ID	Type	Collection Date	d18O	Project ID	Elevation (ft)
Yadkin River At Yadkin College	35.85666	-80.3861	CK_476	River_or_stream	3/2/1987 0:00	-8.99	00048	639.83
Cataloochee Creek Near Cataloochee	35.66721	-83.0728	CK_1172	River_or_stream	6/28/1985 0:00	-7.71	00048	2459.89
Cataloochee Creek Near Cataloochee	35.66721	-83.0728	CK_1170	River_or_stream	12/3/1984 0:00	-7.70	00048	2459.89
Cataloochee Creek Near Cataloochee	35.66721	-83.0728	CK_1175	River_or_stream	2/11/1986 0:00	-7.65	00048	2459.89
Cataloochee Creek Near Cataloochee	35.66721	-83.0728	CK_1171	River_or_stream	2/4/1985 0:00	-7.55	00048	2459.89
Yadkin River At Yadkin College	35.85666	-80.3861	CK_475	River_or_stream	2/3/1987 0:00	-7.54	00048	639.83
Cataloochee Creek Near Cataloochee	35.66721	-83.0728	CK_1180	River_or_stream	6/8/1987 0:00	-7.53	00048	2459.89
Cataloochee Creek Near Cataloochee	35.66721	-83.0728	CK_1173	River_or_stream	9/17/1985 0:00	-7.50	00048	2459.89
Cataloochee Creek Near Cataloochee	35.66721	-83.0728	CK_1179	River_or_stream	3/10/1987 0:00	-7.50	00048	2459.89
Cataloochee Creek Near Cataloochee	35.66721	-83.0728	CK_1174	River_or_stream	11/18/1985 0:00	-7.49	00048	2459.89

Chapter 4 Supplementary File 3 (continued).

Cataloochee Creek Near Cataloochee	35.66721	-83.0728	CK_1181	River_or_stream	9/14/1987 0:00	-7.42	00048	2459.89
Cataloochee Creek Near Cataloochee	35.66721	-83.0728	CK_1177	River_or_stream	9/22/1986 0:00	-7.40	00048	2459.89
French Broad River At Marshall	35.78611	-82.6608	CK_1167	River_or_stream	3/3/1987 0:00	-7.27	00048	1649.05
Tar River At Tarboro	35.89388	-77.5333	CK_441	River_or_stream	1/29/1987 0:00	-7.15	00048	24.14
Cataloochee Creek Near Cataloochee	35.66721	-83.0728	CK_1178	River_or_stream	11/17/1986 0:00	-7.09	00048	2459.89
Rock Creek Near Norwood	35.1483	-80.1758	CK_482	River_or_stream	3/2/1987 0:00	-6.83	00048	213.20
Cataloochee Creek Near Cataloochee	35.66721	-83.0728	CK_1176	River_or_stream	5/12/1986 0:00	-6.76	00048	2459.89
French Broad River At Marshall	35.78611	-82.6608	CK_1163	River_or_stream	1/29/1986 0:00	-6.73	00048	1649.05
Rock Creek Near Norwood	35.1483	-80.1758	CK_481	River_or_stream	2/2/1987 0:00	-6.55	00048	213.20
French Broad River At Marshall	35.78611	-82.6608	CK_1168	River_or_stream	6/8/1987 0:00	-6.51	00048	1649.05
French Broad River At Marshall	35.78611	-82.6608	CK_1160	River_or_stream	5/22/1985 0:00	-6.49	00048	1649.05

Chapter 4 Supplementary File 3 (continued).

French Broad River At Marshall	35.78611	-82.6608	CK_1159	River_or_stream	2/6/1985 0:00	-6.44	00048	664.42
French Broad River At Marshall	35.78611	-82.6608	CK_1164	River_or_stream	5/13/1986 0:00	-6.39	00048	1649.05
French Broad River At Marshall	35.78611	-82.6608	CK_1158	River_or_stream	12/4/1984 0:00	-6.37	00048	1649.05
Yadkin River At Yadkin College	35.85666	-80.3861	CK_478	River_or_stream	7/7/1987 0:00	-6.33	00048	639.83
Yadkin River At Yadkin College	35.85666	-80.3861	CK_469	River_or_stream	2/3/1986 0:00	-6.29	00048	639.83
French Broad River At Marshall	35.78611	-82.6608	CK_1162	River_or_stream	11/19/1985 0:00	-6.25	00048	1649.05
French Broad River At Marshall	35.78611	-82.6608	CK_1161	River_or_stream	9/16/1985 0:00	-6.24	00048	639.83
Yadkin River At Yadkin College	35.85666	-80.3861	CK_470	River_or_stream	3/12/1986 0:00	-6.24	00048	1649.05
Yadkin River At Yadkin College	35.85666	-80.3861	CK_477	River_or_stream	6/2/1987 0:00	-6.23	00048	639.83
Contentnea Creek At Hookerton	35.42777	-77.5861	CK_458	River_or_stream	1/29/1987 0:00	-6.22	00048	27.31
Yadkin River At Yadkin College	35.85666	-80.3861	CK_474	River_or_stream	11/25/1986 0:00	-6.22	00048	639.83
Yadkin River At Yadkin College	35.85666	-80.3861	CK_463	River_or_stream	2/11/1985 0:00	-6.20	00048	639.83

Chapter 4 Supplementary File 3 (continued).

Yadkin River At Yadkin College	35.85666	-80.3861	CK_465	River_or_stream	5/15/1985 0:00	-6.18	00048	639.83
French Broad River At Marshall	35.78611	-82.6608	CK_1169	River_or_stream	9/14/1987 0:00	-6.17	00048	1649.05
French Broad River At Marshall	35.78611	-82.6608	CK_1166	River_or_stream	11/17/1986 0:00	-6.11	00048	1649.05
Yadkin River At Yadkin College	35.85666	-80.3861	CK_468	River_or_stream	11/26/1985 0:00	-6.06	00048	639.83
Yadkin River At Yadkin College	35.85666	-80.3861	CK_464	River_or_stream	4/1/1985 0:00	-6.00	00048	639.83
Pee Dee River Near Rockingham	34.9461	-79.8697	CK_495	River_or_stream	6/19/1987 0:00	-5.99	00048	123.19
Rock Creek Near Norwood	35.1483	-80.1758	CK_483	River_or_stream	4/20/1987 0:00	-5.96	00048	213.20
Tar River At Tarboro	35.89388	-77.5333	CK_442	River_or_stream	4/27/1987 0:00	-5.93	00048	24.14
Yadkin River At Yadkin College	35.85666	-80.3861	CK_479	River_or_stream	9/2/1987 0:00	-5.88	00048	639.83
Yadkin River At Yadkin College	35.85666	-80.3861	CK_471	River_or_stream	5/20/1986 0:00	-5.86	00048	639.83
Yadkin River At Yadkin College	35.85666	-80.3861	CK_462	River_or_stream	11/20/1984 0:00	-5.85	00048	639.83
French Broad River At Marshall	35.78611	-82.6608	CK_1165	River_or_stream	9/22/1986 0:00	-5.84	00048	1649.05
Pee Dee River Near Rockingham	34.9461	-79.8697	CK_487	River_or_stream	4/2/1985 0:00	-5.70	00048	123.19

Chapter 4 Supplementary File 3 (continued).

Pee Dee River Near Rockingham	34.9461	-79.8697	CK_491	River_or_stream	2/19/1986 0:00	-5.69	00048	123.19
Tar River At Tarboro	35.89388	-77.5333	CK_434	River_or_stream	1/31/1985 0:00	-5.65	00048	30.24
Pee Dee River Near Rockingham	34.9461	-79.8697	CK_490	River_or_stream	12/17/1985 0:00	-5.64	00048	123.19
Pee Dee River Near Rockingham	34.9461	-79.8697	CK_494	River_or_stream	1/13/1987 0:00	-5.64	00048	123.19
Pee Dee River Near Rockingham	34.9461	-79.8697	CK_488	River_or_stream	5/14/1985 0:00	-5.52	00048	5.42
Yadkin River At Yadkin College	35.85666	-80.3861	CK_473	River_or_stream	9/2/1986 0:00	-5.49	00048	639.83
Tar River At Tarboro	35.89388	-77.5333	CK_436	River_or_stream	11/13/1985 0:00	-5.45	00048	24.14
Tar River At Tarboro	35.89388	-77.5333	CK_438	River_or_stream	2/10/1986 0:00	-5.39	00048	24.14
Contentnea Creek At Hookerton	35.42777	-77.5861	CK_459	River_or_stream	5/12/1987 0:00	-5.35	00048	5.42
Yadkin River At Yadkin College	35.85666	-80.3861	CK_466	River_or_stream	7/24/1985 0:00	-5.33	00048	639.83
Yadkin River At Yadkin College	35.85666	-80.3861	CK_467	River_or_stream	8/19/1985 0:00	-5.31	00048	639.83
Contentnea Creek At Hookerton	35.42777	-77.5861	CK_445	River_or_stream	1/7/1985 0:00	-5.15	00048	27.31

Chapter 4 Supplementary File 3 (continued).

Tar River At Tarboro	35.89388	-77.5333	CK_433	River_or_stream	11/8/1984 0:00	-5.10	00048	221.41
Yadkin River At Yadkin College	35.85666	-80.3861	CK_472	River_or_stream	7/23/1986 0:00	-5.09	00048	639.83
Pee Dee River Near Rockingham	34.9461	-79.8697	CK_486	River_or_stream	11/19/1984 0:00	-5.00	00048	5.69
Pee Dee River Near Rockingham	34.9461	-79.8697	CK_492	River_or_stream	5/19/1986 0:00	-5.00	00048	42.58
Rock Creek Near Norwood	35.1483	-80.1758	CK_480	River_or_stream	11/25/1986 0:00	-4.99	00048	213.20
Contentnea Creek At Hookerton	35.42777	-77.5861	CK_457	River_or_stream	1/8/1987 0:00	-4.93	00048	27.31
Tar River At Tarboro	35.89388	-77.5333	CK_435	River_or_stream	5/29/1985 0:00	-4.90	00048	63.09
Contentnea Creek At Hookerton	35.42777	-77.5861	CK_452	River_or_stream	3/11/1986 0:00	-4.89	00048	27.31
Contentnea Creek At Hookerton	35.42777	-77.5861	CK_444	River_or_stream	11/7/1984 0:00	-4.85	00048	27.31
Contentnea Creek At Hookerton	35.42777	-77.5861	CK_446	River_or_stream	3/20/1985 0:00	-4.80	00048	98.87
Tar River At Tarboro	35.89388	-77.5333	CK_437	River_or_stream	11/26/1985 0:00	-4.79	00048	24.14
Contentnea Creek At Hookerton	35.42777	-77.5861	CK_447	River_or_stream	5/13/1985 0:00	-4.76	00048	121.86

Chapter 4 Supplementary File 3 (continued).

Pee Dee River Near Rockingham	34.9461	-79.8697	CK_493	River_or_stream	9/3/1986 0:00	-4.71	00048	44.94
Contentnea Creek At Hookerton	35.42777	-77.5861	CK_451	River_or_stream	1/7/1986 0:00	-4.64	00048	26.73
Pee Dee River Near Rockingham	34.9461	-79.8697	CK_489	River_or_stream	9/17/1985 0:00	-4.61	00048	123.19
Tar River At Tarboro	35.89388	-77.5333	CK_439	River_or_stream	5/21/1986 0:00	-4.59	00048	39.68
Tar River At Tarboro	35.89388	-77.5333	CK_440	River_or_stream	11/13/1986 0:00	-4.49	00048	24.14
Contentnea Creek At Hookerton	35.42777	-77.5861	CK_455	River_or_stream	9/9/1986 0:00	-4.39	00048	73.70
Contentnea Creek At Hookerton	35.42777	-77.5861	CK_450	River_or_stream	11/18/1985 0:00	-4.37	00048	16.88
Contentnea Creek At Hookerton	35.42777	-77.5861	CK_449	River_or_stream	9/5/1985 0:00	-4.29	00048	49.04
Rock Creek Near Norwood	35.1483	-80.1758	CK_484	River_or_stream	6/11/1987 0:00	-4.19	00048	38.38
Contentnea Creek At Hookerton	35.42777	-77.5861	CK_453	River_or_stream	5/6/1986 0:00	-3.88	00048	0.76
Contentnea Creek At Hookerton	35.42777	-77.5861	CK_456	River_or_stream	11/5/1986 0:00	-3.83	00048	46.15

Chapter 4 Supplementary File 3 (continued).

Tar River At Tarboro	35.89388	-77.5333	CK_443	River_or_stream	9/1/1987 0:00	-3.66	00048	28.26
Contentnea Creek At Hookerton	35.42777	-77.5861	CK_448	River_or_stream	7/10/1985 0:00	-3.48	00048	27.31
Rock Creek Near Norwood	35.1483	-80.1758	CK_485	River_or_stream	8/4/1987 0:00	-3.42	00048	213.20
Contentnea Creek At Hookerton	35.42777	-77.5861	CK_461	River_or_stream	9/1/1987 0:00	-3.31	00048	27.31
Contentnea Creek At Hookerton	35.42777	-77.5861	CK_460	River_or_stream	7/23/1987 0:00	-3.13	00048	27.31
Contentnea Creek At Hookerton	35.42777	-77.5861	CK_454	River_or_stream	7/9/1986 0:00	-2.20	00048	27.31
Durham	35.9	-78.8	USTap_238	Tap	12/15/2002 0:00	-3.62	00077	375.18
Charlotte	35.2	-80.9	USTap_239	Tap	12/9/2002 0:00	-0.71	00077	
Arden, NC	35.46	-82.516	W-94320	Tap	8/15/2007 12:15	-5.81	00090	2268.51
Arden, NC	35.46	-82.516	W-98843	Tap	2/20/2008 16:30	-5.80	00090	2268.51
Whiteville, NC	34.392	-78.805	W-98844	Tap	2/21/2008 10:02	-4.15	00090	24.47
Whiteville, NC	34.392	-78.805	W-94318	Tap	8/20/2007 16:30	-4.10	00090	145.57
Charlotte, NC	35.165	-80.882	W-94319	Tap	8/15/2007 11:30	-3.36	00090	686.70

Chapter 4 Supplementary File 3 (continued).

Charlotte, NC	35.165	-80.882	W-98842	Tap	2/20/2008 12:58	-2.86	00090	686.70
Raleigh, NC	35.81	-78.724	W-94538	Tap	8/15/2007 11:00	-2.64	00090	370.72
Raleigh, NC	35.813	-78.706	W-94316	Tap	8/15/2007 7:45	-2.62	00090	481.14
Raleigh, NC	35.81	-78.724	W-98841	Tap	2/21/2008 9:00	-1.74	00090	370.72
Raleigh, NC	35.813	-78.706	W-98840	Tap	2/20/2008 10:30	-1.64	00090	481.14
Hampton Inn	35.91068445	-79.06753709	19-089_GJB MISC18-085	Tap	2/7/2019 17:26	-6.29	00099	473.01
RDU airport	35.87671633	-78.79435425	19-089_GJB MISC18-086	Tap	2/8/2019 6:06	-4.86	00099	380.16
UNC Geology	35.90748334	-79.0520871	19-089_GJB MISC18-084	Tap	2/7/2019 15:07	-3.18	00099	468.38
	36.2739	-81.87096	BrooksStreams_727300	River_or_stream	9/16/2013 0:00	-7.43	00140	2541.25
	35.35514	-83.02467	BrooksStreams_719460	River_or_stream	9/10/2013 0:00	-6.83	00140	3755.16
	35.8788	-82.0796	BrooksStreams_727320	River_or_stream	9/17/2013 0:00	-6.50	00140	2745.21

Chapter 4 Supplementary File 3 (continued).

	35.64379988	-81.74478177	BrooksStreams_719440	River_or_stream	9/9/2013 0:00	-6.14	00140	1262.25
	35.06057	-84.02452	BrooksStreams_727240	River_or_stream	9/13/2013 0:00	-5.95	00140	1587.57
	36.41318284	-80.26479615	BrooksStreams_720800	River_or_stream	7/23/2013 0:00	-5.93	00140	1042.09
	36.25938461	-77.88205316	BrooksStreams_727060	River_or_stream	8/11/2013 0:00	-5.79	00140	150.54
	36.21492	-80.96029	BrooksStreams_712540	River_or_stream	7/24/2013 0:00	-5.77	00140	911.68
	35.71572	-81.84522	BrooksStreams_727260	River_or_stream	9/15/2013 0:00	-5.64	00140	1068.92
	35.3187	-82.01725	BrooksStreams_727220	River_or_stream	9/12/2013 0:00	-5.50	00140	755.99
	36.48171	-77.65994	BrooksStreams_727080	River_or_stream	8/12/2013 0:00	-5.45	00140	64.25
	35.4757	-81.40958	BrooksStreams_720820	River_or_stream	7/22/2013 0:00	-5.44	00140	870.22
	35.39708	-80.7245	BrooksStreams_720700	River_or_stream	7/18/2013 0:00	-5.41	00140	600.07

Chapter 4 Supplementary File 3 (continued).

	35.3521	-81.32958	BrooksStreams_727420	River_or_stream	9/25/2013 0:00	-5.15	00140	885.36
	35.82241	-81.18403	BrooksStreams_719520	River_or_stream	7/19/2013 0:00	-5.11	00140	838.44
	35.93954	-78.57553	BrooksStreams_709200	River_or_stream	8/7/2013 0:00	-4.80	00140	193.87
	36.4717	-76.94345	BrooksStreams_727100	River_or_stream	8/14/2013 0:00	-4.78	00140	-0.01
	35.08239309	-79.58954269	BrooksStreams_731360	River_or_stream	9/18/2013 0:00	-4.61	00140	311.37
	34.58249	-77.96322	BrooksStreams_727360	River_or_stream	9/22/2013 0:00	-4.60	00140	38.89
	36.15021	-76.73789	BrooksStreams_727140	River_or_stream	8/22/2013 0:00	-4.45	00140	0.00
	35.43982	-78.02565	BrooksStreams_709220	River_or_stream	8/8/2013 0:00	-4.37	00140	79.35
	35.63323	-79.53602	BrooksStreams_725040	River_or_stream	8/5/2013 0:00	-4.24	00140	453.74
	36.54382	-76.89025	BrooksStreams_727120	River_or_stream	8/15/2013 0:00	-4.08	00140	0.00

Chapter 4 Supplementary File 3 (continued).

	35.458	-77.675	BrooksStreams_727040	River_or_stream	8/9/2013 0:00	-4.05	00140	31.67
	36.15021	-76.73789	BrooksStreams_731320	River_or_stream	9/27/2013 0:00	-4.02	00140	0.00
	36.4717	-76.94345	BrooksStreams_731340	River_or_stream	9/26/2013 0:00	-3.94	00140	-0.01
	34.32929	-79.03643	BrooksStreams_737040	River_or_stream	6/9/2014 0:00	-3.87	00140	62.10
	34.53497	-78.82338	BrooksStreams_727380	River_or_stream	9/23/2013 0:00	-3.86	00140	92.15
	35.79718	-76.63771	BrooksStreams_727180	River_or_stream	8/23/2013 0:00	-3.82	00140	14.25
	34.74249011	-77.02223998	BrooksStreams_729000	River_or_stream	9/27/2013 0:00	-3.79	00140	8.15
	35.04365	-80.46558	BrooksStreams_727400	River_or_stream	9/24/2013 0:00	-3.65	00140	441.14
	35.17608	-78.80974	BrooksStreams_731540	River_or_stream	9/19/2013 0:00	-3.49	00140	47.94
	34.58249	-77.96322	BrooksStreams_727160	River_or_stream	8/18/2013 0:00	-3.34	00140	38.89

Chapter 4 Supplementary File 3 (continued).

	35.04365	-80.46558	BrooksStreams_727200	River_or_stream	9/8/2013 0:00	-3.09	00140	441.14
	34.3619	-77.93378	BrooksStreams_719500	River_or_stream	7/16/2013 0:00	-2.90	00140	1.29
	35.73299	-78.97088	BrooksStreams_709180	River_or_stream	8/4/2013 0:00	-0.95	00140	245.33
Elk Hollow Branch	36.09917138	-82.04496954	NRSA080 9-2167	River_or_stream	6/28/2009 0:00	-7.94	00165	3770.08
Elk Hollow Branch	36.09917138	-82.04496954	NRSA080 9-0912	River_or_stream	6/14/2009 0:00	-7.66	00165	3770.08
North Fork New River	36.54957105	-81.37325538	NRSA080 9-0940	River_or_stream	6/20/2009 0:00	-7.23	00165	2488.96
Sandymush Creek	35.68219607	-82.77898224	NRSA080 9-0913	River_or_stream	6/16/2009 0:00	-6.65	00165	2113.48
Rockhouse Creek	35.87880485	-82.07959934	NRSA080 9-0944	River_or_stream	6/24/2009 0:00	-6.20	00165	2745.11
Unnamed Creek	36.1118797	-81.51025083	NRSA080 9-2166	River_or_stream	6/27/2009 0:00	-6.01	00165	1357.23
Unnamed Creek	35.64379261	-81.74472009	NRSA080 9-0917	River_or_stream	6/13/2009 0:00	-5.94	00165	1258.42
Unnamed Creek	36.1118797	-81.51025083	NRSA080 9-0911	River_or_stream	6/11/2009 0:00	-5.88	00165	1357.23
Yadkin River	36.21491717	-80.96029352	NRSA080 9-0923	River_or_stream	6/14/2009 0:00	-5.85	00165	912.73
Ammons Branch	35.83760486	-82.65973335	NRSA080 9-0946	River_or_stream	6/25/2009 0:00	-5.85	00165	2077.41
Unnamed Creek	35.02466855	-83.696776	NRSA080 9-0914	River_or_stream	6/20/2009 0:00	-5.83	00165	1974.61

Chapter 4 Supplementary File 3 (continued).

Little Tennessee River	35.35125826	-83.50721925	NRSA0809-0935	River_or_stream	6/12/2009 0:00	-5.82	00165	1720.73
Yadkin River	35.99756325	-80.41812604	NRSA0809-0927	River_or_stream	6/15/2009 0:00	-5.78	00165	671.75
Unnamed Creek	35.97524365	-80.34289834	NRSA0809-0945	River_or_stream	7/11/2009 0:00	-5.77	00165	675.70
Dunkers Creek	35.87615762	-80.35988698	NRSA0809-0916	River_or_stream	6/3/2009 0:00	-5.72	00165	683.36
Martin Creek	35.06056646	-84.0245236	NRSA0809-0925	River_or_stream	6/20/2009 0:00	-5.64	00165	1587.62
Dan River	36.53075226	-79.3282469	NRSA0809-0924	River_or_stream	6/21/2009 0:00	-5.60	00165	358.86
Little Creek	35.47569844	-81.40958389	NRSA0809-0933	River_or_stream	6/14/2009 0:00	-5.52	00165	870.13
Chowan River	36.47169936	-76.94344925	NRSA0809-2169	River_or_stream	6/24/2009 0:00	-5.14	00165	-0.01
Isinglass Creek	36.22364287	-78.14354525	NRSA0809-0949	River_or_stream	7/15/2009 0:00	-5.02	00165	210.54
Roanoke River	36.48170984	-77.65993982	NRSA0809-0920	River_or_stream	6/1/2009 0:00	-5.01	00165	64.25
Little Creek	35.6772782	-78.15344211	NRSA0809-0941	River_or_stream	6/13/2009 0:00	-5.01	00165	154.08
Unnamed Creek	35.52101673	-80.82677006	NRSA0809-0947	River_or_stream	7/14/2009 0:00	-4.98	00165	705.41
Rocky River	35.39707947	-80.72450223	NRSA0809-0930	River_or_stream	6/4/2009 0:00	-4.95	00165	600.01
Unnamed Creek	35.16118924	-80.65668257	NRSA0809-0918	River_or_stream	6/4/2009 0:00	-4.85	00165	690.38
Tar River	35.94535286	-77.53263252	NRSA0809-0936	River_or_stream	6/21/2009 0:00	-4.66	00165	29.53

Chapter 4 Supplementary File 3 (continued).

Cape Fear River	35.17607633	-78.80973674	NRSA0809-0931	River_or_stream	6/22/2009 0:00	-4.60	00165	47.94
South Prong Stinking Quarter Creek	35.99602428	-79.48811819	NRSA0809-0951	River_or_stream	7/15/2009 0:00	-4.41	00165	519.22
Gum Swamp Creek	34.92970407	-79.57290173	NRSA0809-1497	River_or_stream	6/10/2009 0:00	-4.37	00165	260.29
North Prong Stinking Quarter Creek	35.95160632	-79.59086722	NRSA0809-0950	River_or_stream	7/13/2009 0:00	-4.35	00165	622.44
Colly Creek	34.71077157	-78.45665667	NRSA0809-1496	River_or_stream	6/25/2009 0:00	-4.32	00165	67.01
Cape Fear River	35.40008016	-78.77839795	NRSA0809-2168	River_or_stream	6/22/2009 0:00	-4.31	00165	104.46
Cape Fear	35.59448257	-79.05209553	NRSA0809-0938	River_or_stream	6/17/2009 0:00	-4.21	00165	160.69
Cape Fear River	34.92336993	-78.79819948	NRSA0809-0929	River_or_stream	6/23/2009 0:00	-4.20	00165	39.65
Chowan River	36.47169936	-76.94344925	NRSA0809-0939	River_or_stream	6/4/2009 0:00	-4.17	00165	-0.01
Neuse River	35.939543	-78.57552909	NRSA0809-0934	River_or_stream	6/23/2009 0:00	-4.12	00165	193.00
Cape Fear River	35.40008016	-78.77839795	NRSA0809-0921	River_or_stream	6/2/2009 0:00	-3.94	00165	104.46
Unnamed Creek	35.9453853	-78.84513345	NRSA0809-0948	River_or_stream	7/16/2009 0:00	-3.90	00165	366.23
Richardson Creek	35.0436515	-80.46557952	NRSA0809-0919	River_or_stream	6/16/2009 0:00	-3.87	00165	441.24
Island Creek	35.02681061	-77.13455165	NRSA0809-1498	River_or_stream	6/9/2009 0:00	-3.84	00165	8.62

Chapter 4 Supplementary File 3 (continued).

Chowan River	36.15021169	-76.73789	NRSA0809-0928	River_or_stream	6/9/2009 0:00	-3.81	00165	0.00
Grindle Creek	35.59595339	-77.18278205	NRSA0809-0952	River_or_stream	7/15/2009 0:00	-3.73	00165	2.44
Contentnea Creek	35.45800111	-77.67500301	NRSA0809-0926	River_or_stream	6/5/2009 0:00	-3.72	00165	31.67
Long Creek	34.58249492	-77.96322004	NRSA0809-0922	River_or_stream	6/6/2009 0:00	-3.50	00165	38.85
Bryant Swamp	34.53496749	-78.82337584	NRSA0809-0943	River_or_stream	7/14/2009 0:00	-3.50	00165	92.09
Black River	34.51978137	-78.25694366	NRSA0809-0932	River_or_stream	6/7/2009 0:00	-3.46	00165	10.18
Unnamed	35.32025045	-77.02918692	NRSA0809-0937	River_or_stream	6/8/2009 0:00	-3.21	00165	34.67
Falling Creek	35.38552971	-77.7538446	NRSA0809-0915	River_or_stream	6/7/2009 0:00	-3.15	00165	110.38
WT-127 NR SEVEN DEVILS NC (PHYLLITE)	36.1538306	-81.8027611	nwisnc.01.01401462	Ground	8/20/2014 9:00	-7.36	00210	3820.24
MD-062 NR MARSHALL NC (FELSIC GNEISS)	35.8559861	-82.670175	nwisnc.01.01401400	Ground	8/5/2014 10:00	-6.92	00210	2145.87
BU-112 NR BLACK MOUNTAIN NC (QUARTZITE)	35.6148694	-82.2891917	nwisnc.01.01401396	Ground	8/4/2014 14:00	-6.48	00210	2524.03

Chapter 4 Supplementary File 3 (continued).

CS-148 NR YANCEYVILLE NC (MAFIC GNEISS)	36.3932917	-79.4499778	nwisnc.01.01401474	Ground	8/26/2014 12:00	-6.44	00210	1649.05
SW-048 NR CHEROKEE NC (QUARTZITE)	35.5680056	-83.3391472	nwisnc.01.01401427	Ground	8/12/2014 12:00	-6.36	00210	2502.80
BK-128 NR NEBO NC (MAFIC GNEISS)	35.7603778	-81.9068306	nwisnc.01.01401392	Ground	8/4/2014 9:00	-6.32	00210	1294.25
RA-175 NR SOPHIA NC (ARGILLITE)	35.7697222	-79.8913889	nwisnc.01.01401412	Ground	7/28/2014 15:10	-6.27	00210	714.46
YD-203 NR BOONVILLE NC (MAFIC GNEISS)	36.230225	-80.6995306	nwisnc.01.01401466	Ground	8/20/2014 12:00	-6.12	00210	1040.11
GM-023 NR SANTEETLAH NC (QUARTZITE)	35.3676528	-83.8539167	nwisnc.01.01401431	Ground	8/13/2014 11:30	-6.05	00210	1997.29
IR-190 NR STATESVILLE NC (MAFIC GNEISS)	35.8738167	-80.9249833	nwisnc.01.01401404	Ground	8/6/2014 9:00	-6.00	00210	899.39
ED-160 TEMP-5B	35.7954358	-77.4908035	nwisnc.01.99401586	Ground	5/18/1994 13:45	-5.87	00210	40.98

Chapter 4 Supplementary File 3 (continued).

GV-155 NR STEM NC (FELSIC METAIGNEOUS)	36.1784139	-78.797275	nwisnc.01.01401321	Ground	7/24/2014 12:00	-5.81	00210	36.10
PI-590 PM-3	35.7673805	-77.4924701	nwisnc.01.99900208	Ground	2/9/1999 16:00	-5.81	00210	493.53
AM-222 NR OSSIPEE NC (FELSIC METAIGNEOUS)	36.1672472	-79.51095	nwisnc.01.01401450	Ground	8/18/2014 12:30	-5.80	00210	644.43
TR-067 NR ROSMAN NC (FELSIC GNEISS)	35.1454528	-82.8253	nwisnc.01.01401439	Ground	8/14/2014 14:00	-5.78	00210	2192.07
WR-155 NR LITTLETON NC (SCHIST)	36.4885972	-77.9421194	nwisnc.01.01401446	Ground	8/21/2014 13:30	-5.74	00210	243.76
PI-606 PM-4	35.7673805	-77.4924701	nwisnc.01.99900209	Ground	2/9/1999 14:00	-5.73	00210	36.10
PI-594 PM-2S	35.7671027	-77.4930257	nwisnc.01.99900262	Ground	2/25/1999 16:15	-5.72	00210	30.24
ED-156 TEMP-5A	35.7954358	-77.4908035	nwisnc.01.99401587	Ground	5/18/1994 12:45	-5.67	00210	43.78
GR-103 L11D	35.5303004	-77.5556091	nwisnc.01.99901247	Ground	6/2/1999 17:45	-5.67	00210	40.98
GR-097 L8S	35.5286337	-77.557137	nwisnc.01.99901180	Ground	5/21/1999 19:30	-5.66	00210	59.81
PI-592 PM-1S	35.7671027	-77.4930257	nwisnc.01.99900211	Ground	2/11/1999 14:00	-5.65	00210	857.67

Chapter 4 Supplementary File 3 (continued).

NA-218 NR SPRING HOPE NC (FELSIC METAVOLCANIC)	35.9522833	-78.109575	nwisnc.01.01401470	Ground	8/25/2014 12:30	-5.64	00210	290.81
59A 66	36.55525	-76.4405278	nwisva.01.01000062	Ground	12/8/2009 13:30	-5.63	00210	5.42
LE-225 NR SANFORD NC (TRIASSIC BASIN)	35.4832028	-79.2529278	nwisnc.01.01200526	Ground	5/16/2012 14:00	-5.62	00210	433.45
LE-125 NR SANFORD NC (TRIASSIC BASIN)	35.4227139	-79.2943056	nwisnc.01.01200537	Ground	6/7/2012 14:00	-5.62	00210	359.55
CH-251 NR PITTSBORO NC (FELSIC METAVOLCANIC)	35.6853667	-79.1552611	nwisnc.01.01401420	Ground	7/31/2014 12:00	-5.60	00210	49.84
ED-153 BFP-1	35.801547	-77.4744141	nwisnc.01.99500293	Ground	1/23/1995 16:00	-5.60	00210	459.36
MO-254 PINEHURST 25 AT PINEHURST NC (BLACK CREEK)	35.17125	-79.5086111	nwisnc.01.01200810	Ground	9/20/2012 15:15	-5.59	00210	505.78
59A 69	36.5553611	-76.4453611	nwisva.01.01000056	Ground	12/8/2009 17:00	-5.58	00210	5.44

Chapter 4 Supplementary File 3 (continued).

GR-095 L7	35.5286226	-77.5571342	nwisnc.01.99901178	Ground	5/21/1999 18:00	-5.56	00210	59.96
PI-593 PM-1I	35.7671027	-77.4930257	nwisnc.01.99900265	Ground	2/22/1999 16:00	-5.55	00210	30.24
GR-098 L8D NEAR LIZZIE NC (YORKTOWN)	35.5286337	-77.557137	nwisnc.01.99901179	Ground	5/21/1999 17:00	-5.53	00210	5.44
59A 69	36.5553611	-76.4453611	nwisva.01.01000059	Ground	12/10/2009 13:30	-5.53	00210	59.81
ED-149 BFP-3B	35.7954358	-77.4908035	nwisnc.01.99500292	Ground	1/25/1995 16:00	-5.52	00210	40.98
59A 66	36.55525	-76.4405278	nwisva.01.01000064	Ground	12/9/2009 17:15	-5.52	00210	123.19
LE-219 NR SANFORD NC (TRIASSIC BASIN)	35.4600583	-79.2482722	nwisnc.01.01200525	Ground	5/17/2012 12:00	-5.51	00210	367.04
LE-256 NR SANFORD NC (TRIASSIC BASIN)	35.47265	-79.2265417	nwisnc.01.01200522	Ground	5/16/2012 10:15	-5.50	00210	388.94
LE-178 NR SANFORD NC (TRIASSIC BASIN)	35.5031944	-79.2891194	nwisnc.01.01200515	Ground	5/24/2012 15:00	-5.48	00210	600.53
CB-156 NR HARRISBURG NC (FELSIC INTRUSIVE IGNEOUS	35.3177778	-80.6019444	nwisnc.01.01401454	Ground	8/19/2014 9:00	-5.48	00210	302.57

Chapter 4 Supplementary File 3 (continued).

PO-025 NR COLUMBUS NC (FELSIC GNEISS)	35.2619083	-82.2139222	nwisnc.01.01401435	Ground	8/14/2014 10:30	-5.46	00210	40.98
ED-146 BFP-3A	35.7954358	-77.4908035	nwisnc.01.99500288	Ground	1/19/1995 14:30	-5.46	00210	1184.98
LE-279 NR SANFORD NC (TRIASSIC BASIN)	35.4600583	-79.2482722	nwisnc.01.01200544	Spring	5/18/2012 11:00	-5.44	00210	367.04
UN-149 NR WAXHAW NC (FELSIC METAVOLCANIC)	34.8693306	-80.7481889	nwisnc.01.01401416	Ground	7/29/2014 10:30	-5.42	00210	541.68
LE-052 NR SANFORD NC (TRIASSIC BASIN)	35.4737528	-79.3518	nwisnc.01.01200519	Ground	5/14/2012 16:00	-5.39	00210	280.28
59A 39	36.5555	-76.4362778	nwisva.01.01000065	Ground	12/8/2009 15:00	-5.36	00210	5.30
HF-101 NR WINTON NC (UPPER CAPE FEAR)	36.3788333	-77.0318694	nwisnc.01.01301260	Ground	9/24/2013 13:30	-5.35	00210	27.31
59A 66	36.55525	-76.4405278	nwisva.01.01000063	Ground	12/9/2009 17:00	-5.35	00210	41.12
GR-151 LBW-SR-RB-3.0	35.5315503	-77.5585815	nwisnc.01.99901255	Ground	9/13/1999 10:00	-5.34	00210	41.04
59A 69	36.5553611	-76.4453611	nwisva.01.01000058	Ground	12/10/2009 12:00	-5.27	00210	5.44

Chapter 4 Supplementary File 3 (continued).

JH-147 JC-3	35.4768274	-78.303611	nwisnc.01.99900198	Ground	1/28/1999 17:30	-5.22	00210	143.65
GR-102 L11S NEAR LIZZIE NC (SURFICIAL)	35.5301389	-77.5559167	nwisnc.01.99901183	Ground	6/2/1999 16:45	-5.20	00210	47.45
59A 70	36.5553611	-76.4453611	nwisva.01.01000060	Ground	12/10/2009 12:15	-5.18	00210	5.44
GR-084 L5 LIZZIE N26q5	35.5199338	-77.5619982	nwisnc.01.99500399	Ground	3/20/1995 18:00	-5.16	00210	72.76
GR-090 L3	35.5176505	-77.559073	nwisnc.01.99901236	Ground	5/20/1999 19:00	-5.14	00210	76.28
ST-253 NR OAKBORO NC (ARGILLITE)	35.2352611	-80.3277806	nwisnc.01.01401458	Ground	8/19/2014 12:00	-5.13	00210	72.00
GR-106 L14	35.5242368	-77.5599154	nwisnc.01.99901184	Ground	5/27/1999 10:00	-5.13	00210	44.63
GR-089 LBW-DITCH-5.1	35.5271059	-77.5624705	nwisnc.01.99902196	Ground	7/9/1999 14:30	-5.13	00210	520.17
GR-109 L15D	35.5243282	-77.5596926	nwisnc.01.99901195	Ground	5/26/1999 18:00	-5.11	00210	70.99
GR-100 L10	35.5302998	-77.5556227	nwisnc.01.99901250	Ground	6/2/1999 19:45	-5.11	00210	43.78
LE-233 NR SANFORD NC (TRIASSIC BASIN)	35.4950167	-79.2584167	nwisnc.01.01200538	Ground	6/7/2012 11:30	-5.10	00210	72.77
SC-018 LAURINBURG MUN	34.7840496	-79.4414347	nwisnc.01.98100453	Ground	8/12/1981 16:00	-5.10	00210	24.14

Chapter 4 Supplementary File 3 (continued).

GR-094 L6D	35.5199394	-77.5619704	nwisnc.01.99901176	Ground	5/18/1999 19:00	-5.10	00210	315.90
GR-088 L2D	35.5179394	-77.5588592	nwisnc.01.99901151	Ground	5/20/1999 18:00	-5.08	00210	76.17
CH-241 NR SANFORD NC (TRIASSIC BASIN)	35.5279111	-79.3348167	nwisnc.01.01200521	Ground	5/15/2012 16:00	-5.06	00210	258.06
PI-652 BELL ARTHUR CORPORATION 5	35.5491667	-77.4813889	nwisnc.01.01301267	Ground	9/24/2013 10:00	-5.05	00210	76.03
ED-176 D-3	35.8173801	-77.4969148	nwisnc.01.99500336	Ground	1/18/1995 15:30	-5.03	00210	45.58
ED-145 BFP-2B	35.8015469	-77.4827477	nwisnc.01.99500291	Ground	1/25/1995 13:00	-5.00	00210	123.19
59A 76	36.5553889	-76.4466667	nwisva.01.01000184	Ground	12/9/2009 13:45	-5.00	00210	123.19
GR-152 LBW-SR-C-2.0	35.5315503	-77.5585815	nwisnc.01.99901253	Ground	9/13/1999 17:00	-4.98	00210	5.69
59A 75	36.5553889	-76.4466667	nwisva.01.01000185	Ground	12/9/2009 14:00	-4.98	00210	41.04
GR-082 L2 N26q2 NR LIZZIE NC (SURFICIAL)	35.5177778	-77.5591667	nwisnc.01.99500318	Ground	2/1/1995 14:00	-4.97	00210	5.69
59A 77	36.5553889	-76.4466667	nwisva.01.01000182	Ground	12/9/2009 13:00	-4.97	00210	75.41
GR-147 L55 NR LIZZIE NC (YORKTOWN)	35.5177778	-77.5591667	nwisnc.01.99901185	Ground	5/27/1999 16:45	-4.96	00210	75.41

Chapter 4 Supplementary File 3 (continued).

63A 4	36.5528111	-75.9945778	nwisva.01.01000754	Ground	7/13/2010 12:10	-4.94	00210	0.75
ST-252 NR ALBEMARLE NC (METAVOLCANIC)	35.3765917	-80.0738222	nwisnc.01.01401408	Ground	7/29/2014 14:30	-4.92	00210	77.57
GR-115 L20 NEAR LIZZIE NC (SURFICIAL)	35.5077778	-77.5666667	nwisnc.01.99901249	Ground	6/3/1999 10:00	-4.92	00210	415.16
ED-144 BFP-2A	35.8015469	-77.4827477	nwisnc.01.99500294	Ground	1/24/1995 14:00	-4.91	00210	62.96
GR-091 L4S	35.5228976	-77.5633038	nwisnc.01.99901238	Ground	6/11/1999 15:00	-4.91	00210	42.58
GR-083 L4 LIZZIE N26q4	35.5228949	-77.5633069	nwisnc.01.99500400	Ground	3/22/1995 10:00	-4.90	00210	24.14
GR-148 LBW-TRIB-4.0	35.5271059	-77.5624705	nwisnc.01.99901967	Ground	6/18/1999 13:30	-4.89	00210	44.63
WA-300 JP-BEDWELL	35.409606	-77.8810938	nwisnc.01.99900266	Ground	2/26/1999 15:30	-4.88	00210	99.78
PE-099 MAS 12B NR ANNANDALE NC	34.4097222	-77.615	nwisnc.01.01301066	Ground	8/27/2013 16:00	-4.87	00210	24.67
GR-081 L16 LIZZIE N26q15	35.5229001	-77.5632799	nwisnc.01.99901248	Ground	6/11/1999 12:00	-4.87	00210	62.35
BE-117 NR AULANDER NC (UPPER CAPE FEAR)	36.2144111	-77.1292806	nwisnc.01.01301261	Ground	9/24/2013 15:15	-4.86	00210	44.63

Chapter 4 Supplementary File 3 (continued).

GR-149 LBW-TRIB-1.5	35.5271059	-77.5624705	nwisnc.01.99902197	Ground	6/18/1999 19:30	-4.86	00210	69.54
GR-114 L19	35.5077653	-77.5665622	nwisnc.01.99901186	Ground	6/3/1999 10:00	-4.84	00210	77.29
GR-092 L4D	35.5229393	-77.563026	nwisnc.01.99901237	Ground	6/11/1999 11:00	-4.84	00210	61.85
BO-419 WASHINGTON RS M21k2 (CASTLE HAYNE)	35.6297222	-77.0888889	nwisnc.01.01300954	Ground	7/9/2013 14:00	-4.83	00210	0.75
ED-125 CITY OF PINETOPS (NEW WELL 4)	35.7646022	-77.6394187	nwisnc.01.01301228	Ground	9/18/2013 12:45	-4.83	00210	74.31
GR-085 L6 LIZZIE N26q6	35.5202778	-77.5616667	nwisnc.01.99500408	Ground	3/23/1995 13:30	-4.83	00210	36.33
63A 4	36.5528111	-75.9945778	nwisva.01.00900666	Ground	8/13/2009 16:10	-4.83	00210	74.42
PE-097 MAS 10 NR HOLLY SHELTER NR WALKERS NC	34.5522222	-77.8125	nwisnc.01.01300967	Ground	8/7/2013 16:30	-4.82	00210	32.82
GR-081 L16 LIZZIE N26q15	35.5229001	-77.5632799	nwisnc.01.99500401	Ground	3/22/1995 14:30	-4.82	00210	62.35
GR-110 L17 (YORKTOWN)	35.5266667	-77.5572222	nwisnc.01.99901188	Ground	6/4/1999 8:30	-4.81	00210	72.29
WA-292 JP-4	35.4101615	-77.8816494	nwisnc.01.99900224	Ground	2/24/1999 16:15	-4.80	00210	27.31

Chapter 4 Supplementary File 3 (continued).

BO-448 BEAUFORT CO. DISTRICTS VI & VII-64	35.4775	-77.0686111	nwisnc.01.01301154	Ground	9/12/2013 10:30	-4.77	00210	30.96
BE-115 NR WINDSOR NC (UPPER CAPE FEAR)	36.2065778	-76.8625056	nwisnc.01.01301259	Ground	9/24/2013 11:00	-4.77	00210	52.01
BO-464 CITY OF WASHINGTON -6	35.5286111	-76.9658333	nwisnc.01.01301226	Ground	9/17/2013 15:45	-4.76	00210	27.31
WA-290 JP-2	35.4109949	-77.8858162	nwisnc.01.99900223	Ground	2/24/1999 12:00	-4.76	00210	29.04
MO-252 PINEHURST 14 AT PINEHURST NC (BLACK CREEK)	35.1883056	-79.4693611	nwisnc.01.01200811	Ground	9/19/2012 15:30	-4.75	00210	506.70
PE-112 NR HAMPSTEAD NC (CASTLE HAYNE)	34.4063889	-77.6144444	nwisnc.01.01201093	Ground	8/30/2012 18:05	-4.73	00210	40.27
PI-613 CHICOD RS O23L6 NR AYDEN NC	35.4633333	-77.2752778	nwisnc.01.01300862	Ground	6/11/2013 15:30	-4.73	00210	22.77
NH-895 AT WILMINGTON NC (SURFICIAL)	34.2294444	-77.8741944	nwisnc.01.01700314	Ground	5/11/2017 12:00	-4.73	00210	39.97

Chapter 4 Supplementary File 3 (continued).

JO-080 OLIVERS CRSRD T23X1 NR POLLOCKSVIL LENC (CH	35.0065556	-77.3024444	nwisnc.01. 01300965	Ground	7/30/2013 11:00	-4.71	00210	123.19
CR-624 MAS 30 NR VANCEBORO NC	35.3758333	-77.1552778	nwisnc.01. 01300958	Ground	7/25/2013 10:30	-4.67	00210	42.61
BR-083 (NC-199) SOUTHPORT RS (SURFICIAL)	33.9419444	-78.0097222	nwisnc.01. 01201000	Ground	8/30/2012 10:15	-4.66	00210	26.91
GR-120 L25	35.5141684	-77.5591797	nwisnc.01. 99901187	Ground	6/4/1999 15:30	-4.65	00210	75.81
LE-262 NR SANFORD NC (TRIASSIC BASIN)	35.5314833	-79.2149667	nwisnc.01. 01200520	Ground	5/15/2012 11:00	-4.64	00210	27.31
JO-076 MAS 21 AT POLLOCKSVIL LE NC	35.0033333	-77.2197222	nwisnc.01. 01300956	Ground	7/24/2013 14:00	-4.64	00210	293.81
WL-419 TOWN OF STANTONSBU RG 2	35.6013889	-77.8108333	nwisnc.01. 01301264	Ground	9/26/2013 10:45	-4.63	00210	82.94
PI-653 BELL ARTHUR 6	35.7125	-77.5213889	nwisnc.01. 01301270	Ground	9/26/2013 12:00	-4.63	00210	81.77

Chapter 4 Supplementary File 3 (continued).

NH-864 NR CASTLE HAYNE NC (PEEDEE)	34.3005556	-77.9294444	nwisnc.01.01201066	Ground	8/31/2012 11:10	-4.60	00210	32.62
WA-167 WALNUT CREEK 3	35.3012738	-77.8666484	nwisnc.01.01301073	Ground	9/4/2013 14:45	-4.60	00210	96.45
CR-626 PURSER RS P21N1 NR WILMAR NC	35.3738889	-77.1352778	nwisnc.01.01300860	Ground	6/10/2013 15:00	-4.59	00210	155.91
NH-989 (MAS 4) NR WILMINGTON NC (CASTLE HAYNE)	34.2294444	-77.8738889	nwisnc.01.01301006	Ground	8/15/2013 11:00	-4.59	00210	43.49
SA-134 NR CLINTON NC	34.9908333	-78.2841667	nwisnc.01.01301075	Ground	9/5/2013 14:15	-4.59	00210	24.14
BO-358 WILMAR RS P21k6 (CASTLE HAYNE)	35.3812735	-77.0849509	nwisnc.01.01300960	Ground	7/25/2013 14:00	-4.58	00210	37.58
MR-462 NR JAMESVILLE NC (CASTLE HAYNE)	35.8106167	-76.9033611	nwisnc.01.01301229	Ground	9/19/2013 10:00	-4.58	00210	39.63
BE-116 NR WINDSOR NC (UPPER CAPE FEAR)	35.9778972	-76.9526583	nwisnc.01.01301263	Ground	9/25/2013 14:00	-4.58	00210	31.63

Chapter 4 Supplementary File 3 (continued).

NH-989 (MAS 4) NR WILMINGTON NC (CASTLE HAYNE)	34.2294444	-77.8738889	nwisnc.01.01201014	Ground	9/5/2012 9:40	-4.57	00210	26.63
NH-1004 NR WILMINGTON NC (CASTLE HAYNE)	34.1969444	-77.9288889	nwisnc.01.01700271	Ground	5/18/2017 9:30	-4.57	00210	39.68
NH-1008 NR WILMINGTON NC (CASTLE HAYNE)	34.2616667	-77.9430556	nwisnc.01.01700275	Ground	5/19/2017 11:00	-4.56	00210	-1.57
GR-093 L6S	35.5199394	-77.5619704	nwisnc.01.99901177	Ground	5/18/1999 15:45	-4.56	00210	72.77
JO-064 COMFORT RS U26j1 (CASTLE HAYNE)	34.9701618	-77.5030205	nwisnc.01.01300961	Ground	7/29/2013 13:30	-4.54	00210	61.93
MR-463 NR JAMESVILLE NC (CASTLE HAYNE)	35.8313472	-76.8113694	nwisnc.01.01301258	Ground	9/23/2013 14:15	-4.53	00210	44.19
PI-612 O22L1 VOICE OF AMERICA NR BLACK JACK NC	35.4594444	-77.1869444	nwisnc.01.01300861	Ground	6/11/2013 11:00	-4.52	00210	39.68

Chapter 4 Supplementary File 3 (continued).

CR-543 COVE CITY RS R23x2 (CASTLE HAYNE)	35.1721056	-77.311069	nwisnc.01.01300966	Ground	7/30/2013 15:00	-4.52	00210	45.63
NH-989 (MAS 4) NR WILMINGTON NC (CASTLE HAYNE)	34.2294444	-77.8738889	nwisnc.01.01700315	Ground	5/11/2017 14:30	-4.52	00210	45.66
NH-928 NR WILMINGTON NC (CASTLE HAYNE)	34.2320833	-77.9463972	nwisnc.01.01700276	Ground	5/17/2017 16:00	-4.51	00210	35.21
BO-446 BEAUFORT CO. DISTRICTS VI & VII-62	35.4488889	-77.0552778	nwisnc.01.01301155	Ground	9/12/2013 12:00	-4.50	00210	30.00
NH-862 NR WILMINGTON NC (PEEDEE)	34.3125	-77.9452778	nwisnc.01.01201102	Ground	9/7/2012 9:40	-4.47	00210	24.84
PE-106 TOPSAIL BEACH RS BB28J5 (SURFICIAL)	34.3999722	-77.6781667	nwisnc.01.01201089	Ground	9/5/2012 14:10	-4.46	00210	20.78
SA-142 IN TURKEY NC	34.9946944	-78.1805556	nwisnc.01.01301151	Ground	9/10/2013 16:30	-4.46	00210	57.98
NH-1012 NR WILMINGTON NC (PEEDEE)	34.3227778	-77.9919444	nwisnc.01.01700279	Ground	5/25/2017 11:30	-4.46	00210	148.28

Chapter 4 Supplementary File 3 (continued).

DU-134 (NC-224) ROSE HILL RS V32v3 (CASTLE HAYNE)	34.8476677	-78.0222085	nwisnc.01.01300969	Ground	8/7/2013 12:30	-4.43	00210	24.84
NH-862 NR WILMINGTON NC (PEEDEE)	34.3125	-77.9452778	nwisnc.01.01700303	Ground	5/12/2017 12:30	-4.43	00210	81.64
LN-216 NORTH LENOIR 11	35.3016667	-77.7291667	nwisnc.01.01301265	Ground	9/23/2013 11:00	-4.42	00210	44.30
NH-1005 NR WILMINGTON NC (SURFICIAL)	34.2155556	-77.9141667	nwisnc.01.01700272	Ground	5/18/2017 17:00	-4.42	00210	93.58
DU-128 CHINQUAPIN RS W29D5 (CASTLE HAYNE)	34.8229443	-77.8127571	nwisnc.01.01300971	Ground	8/8/2013 11:30	-4.41	00210	40.54
BR-082 (NC-198) SOUTHPORT RS (CASTLE HAYNE)	33.9419444	-78.0097222	nwisnc.01.01301005	Ground	8/14/2013 15:00	-4.40	00210	26.91
LN-222 NORTH LENOIR 17	35.3836111	-77.5019444	nwisnc.01.01301266	Ground	9/23/2013 13:00	-4.39	00210	27.31
NH-1001 NR WILMINGTON NC (SURFICIAL)	34.1130556	-77.9166667	nwisnc.01.01700268	Ground	5/18/2017 14:00	-4.37	00210	27.31

Chapter 4 Supplementary File 3 (continued).

CR-708 FIRST CRAVEN SANITARY DISTRICT-1	35.1213889	-77.0055556	nwisnc.01.01301223	Ground	9/17/2013 8:30	-4.36	00210	8.86
BR-146 (MACO FT O-2) SANDY CREEK NC (PEEDEE)	34.2886722	-78.1566583	nwisnc.01.01700262	Ground	5/8/2017 12:00	-4.35	00210	60.07
BR-148 (MACO FT O-5) SANDY CREEK NC (SURFICIAL)	34.2886722	-78.1566583	nwisnc.01.01700263	Ground	5/8/2017 14:00	-4.34	00210	60.07
NH-871 NR WILMINGTON NC (CASTLE HAYNE)	34.0796167	-77.921825	nwisnc.01.01700306	Ground	5/9/2017 18:40	-4.33	00210	5.56
NH-853 NR WILMINGTON NC (CASTLE HAYNE)	34.2033333	-77.8569444	nwisnc.01.01201059	Ground	8/28/2012 14:00	-4.30	00210	11.75
BR-146 (MACO FT O-2) SANDY CREEK NC (PEEDEE)	34.2886722	-78.1566583	nwisnc.01.01201003	Ground	8/27/2012 18:45	-4.29	00210	18.76
PI-705 NR GRIFTON NC (CASTLE HAYNE)	35.3677889	-77.3851222	nwisnc.01.01301153	Ground	9/11/2013 15:15	-4.29	00210	60.07

Chapter 4 Supplementary File 3 (continued).

NH-1002 NR WILMINGTON NC (SURFICIAL)	34.1786111	-77.9030556	nwisnc.01.01700269	Ground	5/18/2017 16:00	-4.29	00210	29.84
NH-854 NR WILMINGTON NC (SURFICIAL)	34.2322222	-77.8547222	nwisnc.01.01700298	Ground	5/16/2017 15:00	-4.29	00210	27.31
NH-847 NR WILMINGTON NC (PEEDEE)	34.3122222	-77.9263889	nwisnc.01.01201053	Ground	9/7/2012 9:50	-4.28	00210	33.98
NH-1011 NR WILMINGTON NC (PEEDEE)	34.2913889	-77.9161111	nwisnc.01.01700278	Ground	5/25/2017 9:30	-4.28	00210	33.66
ED-175 DEM K-25 O-01	35.7926581	-77.4908034	nwisnc.01.99500337	Ground	1/12/1995 15:00	-4.26	00210	39.95
NH-871 NR WILMINGTON NC (CASTLE HAYNE)	34.0796167	-77.921825	nwisnc.01.01201072	Ground	8/29/2012 11:15	-4.25	00210	5.56
SA-144 IN ROSEBORO NC	34.9586111	-78.5047222	nwisnc.01.01301074	Ground	9/5/2013 11:15	-4.25	00210	116.53
NH-870 NR CASTLE HAYNE NC (CASTLE HAYNE)	34.3516667	-77.8658333	nwisnc.01.01201071	Ground	8/29/2012 15:25	-4.24	00210	37.33
PE-095 MAS 13 NR HAMPSTEAD NC	34.4362778	-77.6209167	nwisnc.01.01301063	Ground	8/20/2013 14:30	-4.24	00210	20.61

Chapter 4 Supplementary File 3 (continued).

BO-443 BEAUFORT CO. DISTRICTS VI & VII-1	35.2919444	-76.8613889	nwisnc.01.01301269	Ground	9/24/2013 16:00	-4.24	00210	28.48
NH-1013 NR CASTLE HAYNE NC (PEEDEE)	34.3294444	-77.8633333	nwisnc.01.01700280	Ground	5/25/2017 13:30	-4.24	00210	54.59
PE-125 NR SURF CITY NC (CASTLE HAYNE)	34.4577528	-77.5658417	nwisnc.01.01301231	Ground	9/19/2013 15:00	-4.23	00210	33.66
NH-847 NR WILMINGTON NC (PEEDEE)	34.3122222	-77.9263889	nwisnc.01.01700296	Ground	5/12/2017 11:30	-4.23	00210	30.89
PE-123 NR TOPSAIL NC (CASTLE HAYNE)	34.3832694	-77.715125	nwisnc.01.01301150	Ground	9/10/2013 13:00	-4.22	00210	48.91
BR-082 (NC-198) SOUTHPORT RS (CASTLE HAYNE)	33.9419444	-78.0097222	nwisnc.01.01200999	Ground	8/30/2012 13:30	-4.21	00210	26.91
NH-869 NR WILMINGTON NC (CASTLE HAYNE)	34.2094444	-77.8725	nwisnc.01.01201070	Ground	9/7/2012 10:45	-4.21	00210	30.01

Chapter 4 Supplementary File 3 (continued).

ON-460 ONSLOW QUARRY RS W26C3 NR RICHLANDSNC (CH)	34.8319444	-77.5438611	nwisnc.01.01301070	Ground	9/3/2013 14:00	-4.21	00210	28.88
NH-1010 NR WILMINGTON NC (SURFICIAL)	34.2780556	-77.8836111	nwisnc.01.01700277	Ground	5/15/2017 14:30	-4.21	00210	52.78
NH-840 NR WILMINGTON NC (CASTLE HAYNE)	34.3022222	-77.7630556	nwisnc.01.01201046	Ground	8/29/2012 14:55	-4.20	00210	27.21
CR-715 TOWN OF RIVER BEND-1	35.0722222	-77.1469444	nwisnc.01.01301268	Ground	9/24/2013 12:00	-4.20	00210	14.60
NH-1007 NR WILMINGTON NC (SURFICIAL)	34.29	-77.7675	nwisnc.01.01700274	Ground	5/16/2017 13:00	-4.20	00210	18.95
NH-830 NR WILMINGTON NC (CASTLE HAYNE)	34.3022222	-77.7655556	nwisnc.01.01700294	Ground	5/9/2017 11:50	-4.20	00210	9.44
NH-883 NR WILMINGTON NC (PEEDEE)	34.2508333	-77.8677778	nwisnc.01.01201082	Ground	9/6/2012 8:15	-4.19	00210	213.20

Chapter 4 Supplementary File 3 (continued).

BR-100 WELL 15A (CASTLE HAYNE/PEEDEE)	33.9802778	-78.0952778	nwisnc.01.01201001	Ground	8/31/2012 14:45	-4.18	00210	54.50
WS-108 K17A8 AT PLYMOUTH NC	35.8238889	-76.7580556	nwisnc.01.01300953	Ground	7/8/2013 14:30	-4.18	00210	41.04
GR-150 LBW-SR-RB-1.5	35.5315503	-77.5585815	nwisnc.01.99901254	Ground	9/13/1999 13:00	-4.18	00210	32.00
PA-176 PAMLICO COUNTY Grantsboro #1	35.0869444	-76.8375	nwisnc.01.01301224	Ground	9/17/2013 10:30	-4.16	00210	38.38
NH-883 NR WILMINGTON NC (PEEDEE)	34.2508333	-77.8677778	nwisnc.01.01700309	Ground	5/8/2017 11:15	-4.16	00210	39.84
CR-685 CITY OF HAVELOCK-5	34.8569444	-76.8908333	nwisnc.01.01301222	Ground	9/16/2013 15:15	-4.15	00210	104.35
PE-111 NR HAMPSTEAD NC (UNKNOWN)	34.365	-77.6813889	nwisnc.01.01201092	Ground	8/30/2012 13:10	-4.13	00210	12.62
NH-857 NR WILMINGTON NC (CASTLE HAYNE)	34.3438889	-77.8113889	nwisnc.01.01201061	Ground	8/30/2012 15:20	-4.12	00210	17.91
BO-384 BATH RS O17I2 NEAR BATH NC	35.4757209	-76.7832695	nwisnc.01.01300955	Ground	7/9/2013 10:00	-4.12	00210	113.16

Chapter 4 Supplementary File 3 (continued).

BL-121 IN ELIZABETHTOWN NC	34.6240594	-78.6002897	nwisnc.01.01301148	Ground	9/9/2013 15:00	-4.12	00210	7.52
PE-100 MAS 5B NR ROCKY POINT NC	34.4197222	-77.8686111	nwisnc.01.01301002	Ground	8/13/2013 14:00	-4.10	00210	104.35
RB-041 ROWLAND MUN	34.5440518	-79.2950418	nwisnc.01.98100452	Ground	8/12/1981 8:30	-4.10	00210	27.03
NH-830 NR WILMINGTON NC (CASTLE HAYNE)	34.3022222	-77.7655556	nwisnc.01.01201036	Ground	8/29/2012 10:15	-4.08	00210	14.60
ON-309 MAS-25 AT HUBERT NC	34.7122222	-77.2327778	nwisnc.01.01301068	Ground	8/28/2013 11:45	-4.08	00210	57.98
ON-527 Deppe V23X6 nr Deppe NC (Castle Hayne)	34.8370417	-77.3032778	nwisnc.01.01301103	Ground	8/27/2013 13:30	-4.08	00210	35.69
PE-106 TOPSAIL BEACH RS BB28J5 (SURFICIAL)	34.3999722	-77.6781667	nwisnc.01.01700321	Ground	5/9/2017 9:30	-4.08	00210	43.43
NH-558 NR WILMINGTON NC (CASTLE HAYNE)	34.2994472	-77.8023333	nwisnc.01.01700288	Ground	5/10/2017 12:00	-4.05	00210	46.30

Chapter 4 Supplementary File 3 (continued).

NH-857 NR WILMINGTON NC (CASTLE HAYNE)	34.3438889	-77.8113889	nwisnc.01.01700299	Ground	5/9/2017 11:30	-4.05	00210	17.91
NH-558 NR WILMINGTON NC (CASTLE HAYNE)	34.2994472	-77.8023333	nwisnc.01.01301149	Ground	9/10/2013 10:45	-4.04	00210	46.30
NH-574 NR WILMINGTON NC (PEEDEE)	34.2995306	-77.8023167	nwisnc.01.01700291	Ground	5/10/2017 11:30	-4.03	00210	46.26
NH-996 NR CASTLE HAYNE NC (PEEDEE)	34.3202778	-77.9186111	nwisnc.01.01700316	Ground	5/10/2017 14:00	-4.03	00210	33.57
NH-558 NR WILMINGTON NC (CASTLE HAYNE)	34.2994472	-77.8023333	nwisnc.01.01201018	Ground	9/5/2012 14:40	-4.02	00210	46.30
BR-279 (SPMT 44-A) SOUTHPORT NC (CASTLE HAYNE)	34.0062417	-77.9858111	nwisnc.01.01301003	Ground	8/14/2013 11:00	-4.01	00210	24.65
BR-279 (SPMT 44-A) SOUTHPORT NC (CASTLE HAYNE)	34.0062417	-77.9858111	nwisnc.01.01700264	Ground	5/17/2017 11:00	-4.01	00210	24.65

Chapter 4 Supplementary File 3 (continued).

NH-997 NR CASTLE HAYNE NC (SURFICIAL)	34.3202778	-77.92	nwisnc.01.01700317	Ground	5/10/2017 12:30	-4.00	00210	32.30
BR-279 (SPMT 44-A) SOUTHPORT NC (CASTLE HAYNE)	34.0062417	-77.9858111	nwisnc.01.01201006	Ground	8/28/2012 15:30	-3.99	00210	24.65
NH-852 NR WILMINGTON NC (CASTLE HAYNE/PEEDEE)	34.1647222	-77.8847222	nwisnc.01.01201058	Ground	8/28/2012 15:00	-3.99	00210	28.44
NH-882 NR WILMINGTON NC (PEEDEE)	34.3013889	-77.7666667	nwisnc.01.01700308	Ground	5/10/2017 17:30	-3.99	00210	12.50
NH-1000 NR CASTLE HAYNE NC (SURFICIAL)	34.3302778	-77.9047222	nwisnc.01.01700267	Ground	5/9/2017 15:00	-3.97	00210	26.79
PA-184 PAMLICO COUNTY Vandemere #1	35.1886111	-76.68	nwisnc.01.01301225	Ground	9/17/2013 13:00	-3.95	00210	7.51
NH-572 NR WILMINGTON NC (PEEDEE)	34.3025333	-77.8132306	nwisnc.01.01700290	Ground	5/10/2017 12:50	-3.94	00210	43.39

Chapter 4 Supplementary File 3 (continued).

NH-854 NR WILMINGTON NC (SURFICIAL)	34.2322222	-77.8547222	nwisnc.01.01201060	Ground	8/29/2012 8:30	-3.93	00210	18.76
NH-881 NR WILMINGTON NC (PEEDEE)	34.2891667	-77.7941667	nwisnc.01.01201080	Ground	9/5/2012 18:15	-3.93	00210	46.15
NH-582 NR WILMINGTON NC (PEEDEE)	34.2709	-77.8264667	nwisnc.01.01700292	Ground	5/10/2017 14:55	-3.93	00210	18.54
NH-564 NR WILMINGTON NC (PEEDEE)	34.2881694	-77.8225861	nwisnc.01.01700289	Ground	5/10/2017 10:05	-3.92	00210	42.84
BR-148 (MACO FT O-5) SANDY CREEK NC (SURFICIAL)	34.2886722	-78.1566583	nwisnc.01.01201004	Ground	8/27/2012 19:55	-3.91	00210	42.88
NH-574 NR WILMINGTON NC (PEEDEE)	34.2995306	-77.8023167	nwisnc.01.01201021	Ground	9/5/2012 14:55	-3.91	00210	60.07
PE-116 NR HAMPSTEAD NC (CASTLE HAYNE)	34.3666667	-77.6913889	nwisnc.01.01201096	Ground	8/30/2012 11:30	-3.91	00210	46.26
NH-548 NR WILMINGTON NC (CASTLE HAYNE)	34.2882444	-77.8225278	nwisnc.01.01700286	Ground	5/10/2017 10:35	-3.91	00210	21.00
63A 3	36.5528	-75.9945667	nwisva.01.01000752	Ground	7/13/2010 10:35	-3.90	00210	0.76

Chapter 4 Supplementary File 3 (continued).

NH-548 NR WILMINGTON NC (CASTLE HAYNE)	34.2882444	-77.8225278	nwisnc.01.01201016	Ground	9/5/2012 14:00	-3.89	00210	42.88
WS-143 NR PLYMOUTH NC (CASTLE HAYNE)	35.8496806	-76.7417278	nwisnc.01.01301257	Ground	9/23/2013 12:30	-3.89	00210	10.21
NH-882 NR WILMINGTON NC (PEEDEE)	34.3013889	-77.7666667	nwisnc.01.01201081	Ground	9/5/2012 17:25	-3.88	00210	12.50
PE-117 NR HAMPSTEAD NC (CASTLE HAYNE)	34.3597222	-77.6791667	nwisnc.01.01301064	Ground	8/21/2013 10:00	-3.88	00210	43.49
NH-556 NR WILMINGTON NC (CASTLE HAYNE)	34.3026222	-77.8132333	nwisnc.01.01700287	Ground	5/10/2017 13:45	-3.88	00210	26.79
NH-999 NR CASTLE HAYNE NC (PEEDEE)	34.3302778	-77.9047222	nwisnc.01.01700319	Ground	5/9/2017 16:00	-3.88	00210	3.70
63A 3	36.5528	-75.9945667	nwisva.01.00900665	Ground	8/13/2009 15:10	-3.88	00210	27.31
NH-564 NR WILMINGTON NC (PEEDEE)	34.2881694	-77.8225861	nwisnc.01.01201019	Ground	9/5/2012 13:45	-3.87	00210	42.84
NH-572 NR WILMINGTON NC (PEEDEE)	34.3025333	-77.8132306	nwisnc.01.01201020	Ground	9/5/2012 15:25	-3.87	00210	43.39

Chapter 4 Supplementary File 3 (continued).

ON-418 CITY OF JACKSONVILLE BP2	34.7926944	-77.4293333	nwisnc.01.01301071	Ground	9/3/2013 16:15	-3.84	00210	44.73
NH-582 NR WILMINGTON NC (PEEDEE)	34.2709	-77.8264667	nwisnc.01.01201022	Ground	9/5/2012 19:00	-3.83	00210	3.70
PE-117 NR HAMPSTEAD NC (CASTLE HAYNE)	34.3597222	-77.6791667	nwisnc.01.01201097	Ground	8/30/2012 12:15	-3.83	00210	27.31
NH-876 NR WILMINGTON NC (PEEDEE)	34.2738889	-77.7905556	nwisnc.01.01201076	Ground	8/27/2012 18:00	-3.82	00210	17.04
ON-308 MAS 14 NR DIXON NC	34.5666667	-77.4894444	nwisnc.01.01301067	Ground	8/28/2013 9:30	-3.82	00210	59.08
PE-110 NR ROCKY POINT NC (PEEDEE)	34.3722222	-77.8038889	nwisnc.01.01201091	Ground	8/29/2012 14:30	-3.80	00210	8.47
BL-094	34.6515583	-78.7241846	nwisnc.01.01301152	Ground	9/11/2013 10:00	-3.80	00210	144.12
NH-827 NR WILMINGTON NC (PEEDEE)	34.2741667	-77.7975	nwisnc.01.01700293	Ground	5/9/2017 16:00	-3.79	00210	10.53
NH-556 NR WILMINGTON NC (CASTLE HAYNE)	34.3026222	-77.8132333	nwisnc.01.01201017	Ground	9/5/2012 15:35	-3.78	00210	43.49
NH-845 NR WILMINGTON NC (PEEDEE)	34.2738889	-77.8077778	nwisnc.01.01201051	Ground	8/28/2012 16:05	-3.77	00210	23.33

Chapter 4 Supplementary File 3 (continued).

NH-827 NR WILMINGTON NC (PEEDEE)	34.2741667	-77.7975	nwisnc.01.01201033	Ground	9/6/2012 16:20	-3.74	00210	10.53
BL-227 NR WHITE LAKE	34.6486389	-78.5325278	nwisnc.01.01301230	Ground	9/19/2013 10:00	-3.72	00210	63.25
ON-227 DIXON RS Y25q3 (CASTLE HAYNE)	34.6113889	-77.4827778	nwisnc.01.01301049	Ground	8/21/2013 15:00	-3.71	00210	66.38
NH-1006 NR WILMINGTON NC (CASTLE HAYNE)	34.29	-77.7675	nwisnc.01.01700273	Ground	5/16/2017 12:30	-3.70	00210	27.21
WS-140 WASHINGTON COUNTY 1	35.8722222	-76.6208333	nwisnc.01.01301227	Ground	9/18/2013 9:15	-3.69	00210	9.67
BR-081 (NC-197) SOUTHPORT RS (PEEDEE)	33.9419444	-78.0097222	nwisnc.01.01200998	Ground	8/30/2012 17:50	-3.67	00210	26.91
NH-834 NR CASTLE HAYNE NC (PEEDEE)	34.3552778	-77.8588889	nwisnc.01.01201040	Ground	9/7/2012 11:00	-3.66	00210	24.14
BR-111 (RS1 FF33 T-1) BOILING SPRINGS NC (CSLHYN)	34.0249194	-78.1017861	nwisnc.01.01201002	Ground	8/28/2012 18:45	-3.63	00210	52.26

Chapter 4 Supplementary File 3 (continued).

NH-834 NR CASTLE HAYNE NC (PEEDEE)	34.3552778	-77.8588889	nwisnc.01.01700295	Ground	5/15/2017 12:00	-3.61	00210	28.26
NH-998 NR WILMINGTON NC (SURFICIAL)	34.265	-77.9233333	nwisnc.01.01700318	Ground	5/10/2017 9:30	-3.60	00210	21.38
BR-372 NR WINNABOW NC (PEEDEE)	34.1430556	-77.9911111	nwisnc.01.01201010	Ground	8/27/2012 16:30	-3.56	00210	18.80
NH-844 NR CASTLE HAYNE NC (PEEDEE)	34.3538889	-77.8780556	nwisnc.01.01201050	Ground	9/7/2012 11:15	-3.55	00210	25.19
CT-206 NR MERRIMON NC (CASTLE HAYNE)	34.9436361	-76.6430056	nwisnc.01.01301221	Ground	9/16/2013 12:45	-3.54	00210	5.30
CT-153 (NC-139) CAMP GLENN RS X17j5 (CASTLE HAYNE)	34.7233333	-76.7533333	nwisnc.01.01301069	Ground	8/29/2013 10:30	-3.50	00210	14.10
BL-072	34.8348888	-78.8255786	nwisnc.01.01301147	Ground	9/9/2013 12:15	-3.36	00210	71.19
HY-192 NR SWANQUARTER NC (CASTLE HAYNE)	35.630175	-76.5597389	nwisnc.01.01301262	Ground	9/25/2013 10:15	-3.26	00210	6.73

Chapter 4 Supplementary File 3 (continued).

RB-039 ROWLAND MUN	34.5393296	-79.2836525	nwisnc.01.98100451	Ground	8/12/1981 12:00	-3.20	00210	148.10
BR-371 NR SOUTHPORT NC (CASTLE HAYNE/PEEDEE)	34.0416667	-78.0380556	nwisnc.01.01201009	Ground	8/28/2012 9:00	-2.74	00210	44.28
NH-859 NR CASTLE HAYNE NC (PEEDEE)	34.3455556	-77.9102778	nwisnc.01.01700301	Ground	5/15/2017 19:00	-1.90	00210	13.78
NH-859 NR CASTLE HAYNE NC (PEEDEE)	34.3455556	-77.9102778	nwisnc.01.01201063	Ground	8/31/2012 10:15	-1.72	00210	13.78
EXX airport	35.77940186	-80.30224259	19-089_USGW-19-029	Tap	3/12/2019 9:53	-6.23	00225	699.14
RHP airport	35.19652559	-83.8629575	19-089_USGW-19-027	Tap	3/12/2019 7:51	-5.85	00225	1697.76
5W4 airport	35.01924509	-79.18910165	19-089_USGW-19-030	Ground	3/12/2019 11:42	-5.43	00225	292.42
USANCDurham	36	-78.9	Isoforensics_2019_sample_0216	Tap	1/14/2003 0:00	-6.90	00275	370.41
USANCBurlington	36.1	-79.4	Isoforensics_2019_sample_0218	Tap	1/14/2003 0:00	-6.60	00275	583.02

Chapter 4 Supplementary File 3 (continued).

	35.9132	-79.0558	Isoforensics_2019_sample_4358	Tap	10/3/2010 0:00	-6.58	00275	488.64
USANCGreensboro	36.0725	-79.7922	Isoforensics_2019_sample_0741	Tap	2/11/2004 0:00	-6.50	00275	832.14
USANCPelham	36.4702	-79.46	Isoforensics_2019_sample_0217	Tap	1/13/2003 0:00	-6.45	00275	494.95
	36.2594	-80.1417	Isoforensics_2019_sample_4731	Tap	8/3/2011 0:00	-6.39	00275	772.96
USANCRaleigh	35.8	-78.6	Isoforensics_2019_sample_0213	Tap	1/15/2003 0:00	-5.75	00275	187.78
USANCWinston-Salem	36.1	-80.2	Isoforensics_2019_sample_0214	Tap	1/13/2003 0:00	-5.65	00275	24.14
USANCNewton	35.6319	-81.1719	Isoforensics_2019_sample_0219	Tap	1/11/2003 0:00	-5.65	00275	964.31
	35.6008	-82.5542	Isoforensics_2019_sample_4249	Tap	10/27/2009 0:00	-5.16	00275	2122.92
	34.2257	-77.9447	Isoforensics_2019_sample_4407	Tap	6/11/2010 0:00	-4.39	00275	34.71
USANCDurham	35.9	-78.8	Isoforensics_2019_sample_0146	Tap	12/15/2002 0:00	-3.62	00275	375.18

Chapter 4 Supplementary File 3 (continued).

USANCCharlotte	35.2	-80.8	Isoforensics_2019_sample_0215	Tap	1/16/2003 0:00	-2.90	00275	706.74
USANCCharlotte	35.2	-80.9	Isoforensics_2019_sample_0147	Tap	12/9/2002 0:00	-0.71	00275	606.36
	36.0474115	-79.0111657	IPL-17O-IPL-18W-688	River_or_stream	12/16/2018 0:00	-6.40	00287	389.48

Appendix C

Chapter 5 Supplementary File 1

Laboratory Methods

Osteological remains were subsampled and cleaned in the WSU Department of Anthropology Stable Isotope Lab. Subsamples of cortical bone and tooth enamel were collected and mechanically cleaned using a dental drill. To prevent contamination across samples, a new drill bit was used for each sample, and the cutting wheels and drill handle were cleaned with ethanol.

Strontium Isotopes ($^{87/86}Sr$)

Mechanically cleaned sub-samples were soaked in a 5% acetic acid solution for 30 minutes to remove non-biogenic strontium (1-3). Following pretreatment, samples were brought to the WSU Radiogenic Isotope and Geochronology Laboratory (RIGL) for column chemistry and mass spectrometry in a class 1000 clean lab to prevent sample contamination. Samples were digested in 8M HNO_3 and loaded into columns containing Eichrom Sr resin to isolate strontium from other ions. Sample $^{87/86}Sr$ was measured on a ThermoFinnigan Neptune Plus MC-ICP-MS. Multiple samples of the strontium standard NBS-987 were run concurrently with the study samples to monitor instrument accuracy.

Enamel $\delta^{13}C$ and $\delta^{18}O$

Enamel samples were treated for residual organics and diagenetic contamination with 2% NaOCL (<24 hours) and 0.1M acetic acid (4 hours) (1,4,5). Samples were rinsed to neutral after each treatment and prior to freezedrying. Sample $\delta^{18}O$ was analyzed in the WSU Stable Isotope Core facility using a ThermoFinnigan Gasbench II coupled to a DeltaPlus XP Isotope Ratio Mass Spectrometer in the WSU Stable Isotope Core Laboratory.

Bone Collagen $\delta^{13}C$ and $\delta^{15}N$

Approximately 0.25 to 0.5g of clean cortical bone was sonicated for 20 minutes in a 2:1:0.8 (v/v) solution of methanol:chloroform: deionized water to remove lipids. Samples were rinsed and the sonication procedure was repeated until the sample solution was clear. Lipid extraction was necessary since lipids within modern bone can skew $\delta^{13}C_{collagen}$ (6,7). After lipid treatment, samples were demineralized in 0.5M HCl, and then treated with 0.125M NaOH to remove organic contaminants. Samples were solubilized in 10^{-3} M hydrochloric acid at 90°C and centrifuged to remove particulates. The resulting collagen was freezedried and analyzed on a Thermo Finnigan Delta-plus XP isotope ratio mass spectrometer coupled to a Carl Erba NC2500 elemental analyzer in the WSU Stable Isotope Core Laboratory.